High-frequency oscillations in hippocampus and amygdala: modulation by ascending systems

Inaugural-Dissertation
zur
Erlangung des Doktorgrades der
Mathematisch-Naturwissenschaftlichen Fakultät
der Heinrich-Heine Universität Düsseldorf

vorgelegt von

Alexei Ponomarenko
aus Petropavlovsk-Kamchatsky

Düsseldorf
2003

Gedruckt mit der Genehmigung der Mathematisch-Naturwissenschaftlichen Fakultät der Heinrich-Heine-Universität Düsseldorf

Referent: Prof. Dr. H.L. Haas

Korreferent: Prof. Dr. J.P. Huston

Tage der mündlichen Prüfung: 18.07, 21.07, 22.07.2003.

CONTENTS

SUMMARY

Long-term potentiation (LTP), a cellular and network-module for the engram-formation, is mostly elicited by high-frequency stimulation of hippocampal fiber-bundles. High-frequency oscillations (200 Hz, „ripples") are naturally induced by synchronous discharge of a large number of CA3 pyramidal neurons and the subsequent excitation of many CA1 pyramidal cells and interneurons. These oscillatory patterns are believed to represent an intrinsic network mechanism of the hippocampus and the physiological LTP stimulus. Ripples were recorded in freely behaving rats by microwire electrode arrays. The atypical waking-promoting agent modafinil, amphetamine and natural sleep deprivation evoked a profound (>200%) increase of ripple occurrence in comparison with the pre-drug slow-wave sleep episode. The duration of waking but not the type of treatment determined the sleep-related increase of ripple numbers. The number of ripples decreased within individual slow wave sleep (SWS) episodes, the duration of a SWS episode predicted the ripple occurrence decay dynamics during the following episode. Paradoxical sleep (PS) or waking episodes (W) acted to reduce elevated ripple numbers but evoked an increase of ripple occurrence when this had been low at the beginning of PS.

Benzodiazepines are known to potentiate GABAergic transmission, they diminished ripple oscillations. The benzodiazepine antagonist flumazenil also reduced the number of ripples. The modulation of $GABA_A$-transmission by benzodiazepines, zolpidem and diazepam, reduced amplitude and frequency of ripples; zoplidem elevated ripple duration.

The histaminergic system exerted divergent effects upon ripple oscillations: systemic administration of an antagonist of H_1-receptors elevated the number of ripples, whilst an antagonist of H_2-receptors produced a transient suppression.

In the basolateral amygdaloid (BL) and endopiriform nuclei (EPN) local field potentials and single-unit activities were recorded in parallel with the hippocampal EEG. Units from both EPN and BL exhibited similar irregular firing patterns with bursts and mean firing rates <1 Hz. Neuronal activity in both BL and EPN was phase-locked with high-frequency (~200 Hz) field oscillations with a lower numbers of cycles and smaller amplitudes than hippocampal ripples. Both these EEG patterns and neuronal firing in the BL and EPN were clearly state dependent with a maximal occurrence during SWS, being lower during waking and PS. Cross-correlation between hippocampal ripples and EPN or BL patterns did not reveal an obvious synchrony. The results suggest multiple influences of transmitters, learning, and sleep on the modulation of ripple oscillations also in extrahippocampal medial temporal lobe structures related to the emotional aspects of memory.

INTRODUCTION

Synchronous neuronal activity reflects currently unknown principles of brain operation. Sharp waves and high-frequency oscillations (200 Hz, “ripples”) (Buzsaki, 1986; Buzsaki et al., 1992) in the hippocampus represent one of the most synchronous patterns of the normal brain. They can be critically involved in synaptic modifications associated with consolidation of memory traces (Buzsaki et al., 1987a). Issues of network mechanisms of the ripple oscillations have been extensively addressed (Csicsvari et al., 1999a;Ylinen et al., 1995a). A replay of neuronal firing patterns in slow wave sleep (SWS) takes place selectively during ripples (Kudrimoti et al., 1999; Wilson and McNaughton, 1994). However current knowledge about factors that regulate timing and intrinsic features of the ripple oscillations are very limited. They are represented mostly by the rather general findings of the dependence of ripples on an ongoing behaviour or sleep phase. Whatever the role of ripple oscillations in the brain, information about occurrence of these events across the sleep/waking cycle would place ripples in a context of long-term brain dynamics. This was the first aim of our study of ripple oscillation in freely behaving rats.

Another highly interesting aspect of ripple oscillations is their pharmacological modulation. Coherent oscillatory GABA-ergic inhibition of populations of hippocampal CA1 pyramidal cells is assumed to be one of the synchronizing mechanisms during ripples (Ylinen et al., 1995a). However there is only one observation regarding the suppression of sharp waves by GABA-ergic compounds (Buzsaki, 1986). A more detailed pharmacological analysis would help to elucidate the role of different interneuronal populations in 200 Hz oscillations. Monoamine transmitters exert multiple actions upon neural networks finally altering the efficacy of synaptic modification (Haas et al., 1995). It has been shown that the histaminergic system tonically inhibits ripple oscillations preferably via H_1-receptors in the medial septum(Knoche et al., 2003). It is not clear whether histamine acts in the same way in the hippocampus. Do the effects of hippocampal H_2- and H_3-receptor-activation observed in vitro play a role in the adaptive modulation of ripple oscillations in vivo? We studied actions of systemically administered ligands of the benzodiazepine site of the $GABA_A$ receptor and of antagonists of the histamine receptors upon ripple oscillations.

Finally, are ripple oscillations unique for the hippocampus and parahippocampal regions in the medial temporal lobe? What functional integration takes place between structures of the medial temporal lobe during ripples? We addressed these questions using parallel field and single-unit recordings from the basolateral nucleus of the amygdala (and the related endopiriform nucleus) and the temporal or septal poles of CA1.

LITERATURE REVIEW

Anatomical organization of the hippocampus and amygdala.

Hippocampal formation

The hippocampal formation comprises 6 cytoarchitectonically distinct regions including dentate gyrus, hippocampus, which is subdivided into three fields (CA1, CA2 and CA3), subiculum, presubiculum, parasubiculum and entorhinal cortex. The entorhinal cortex, in turn, is divided into two or more subfields (Amaral and Witter, 1989).

The laminar organization is similar for all fields of the hippocampus. The principal cellular layer is called pyramidal cell layer. The narrow, relatively cell-free layer next to the pyramidal layer is called stratum oriens, which is covered by the fiber containing alveus. In the CA3 field, but not in CA2 and CA1 a narrow acellular zone located just above the pyramidal layer is occupied by the mossy fiber axons. This narrow layer is called stratum lucidum. Superficial to the str. lucidum in CA3, and immediately above the pyramidal layer in CA2 and CA1, lies the stratum radiatum. The most superficial portion of the hippocampus is called the straum lacunosum-moleculare, where perforant pathway fibers travel and terminate, as well as some afferents from the nucleus reuniens of the midline thalamus.

The dentate gyrus consists of primary cells (the granule cells), which have no basal dendrites. The large pyramidal cells of the fields CA3 and CA1 are more reminiscent of those in the deep layers in the cerebral cortical areas. They have a basal dendritic tree that extends to the str. oriens and an apical dendritic tree that extends to the hippocampal fissure. Field CA3's cells are less likely to have a single apical dendrite than more classical pyramidal cells in CA1. CA3 possesses a local density gradient of its recurrent collateral system: within the local neighborhood, CA3 cells innervate each other more densely than remote cells.

The entorhinal cortex is characterized by the presence of a marked cell-sparse layer (lamina dissecans), which separates superficial layers I, II, and III from the deeper layers V and VI. There is no agreement about the organization of inputs to the entorhinal cortex. A widely accepted model assumes that afferents target neurons in the superficial layers I-III. According to this scheme, neurons in the deep layers receive the major output from the hippocampal fields CA1 and the subiculum and convey this to neighboring cortical areas of the parahippocampal region and subcortical structures such as the basal ganglia, claustrum, and thalamus. However, hippocampal output also reaches the superficial layers of the entorhinal cortex. Also cortical inputs have been described that either reach both superficial

and deep layers or selectively innervate only the deep layers of the entorhinal cortex. Another example is the recent observation that inputs from the presubiculum, which are known to distribute selectively to layers I and III of the MEC, also target dendrites of layer V pyramidal cells (van Haeften et al., 2000).

The rat hippocampal formation includes the following major fiber bundles: The surface of the subiculum is covered by a thin sheet of myelinated afferent and efferent fibers, the alveus. Many of these are pyramidal axons that extend further to the fimbria. The fornix splits around the anterior comissure to form a rostrally directed precomissural component, which innervates the septal nuclei and other basal forebrain structures, and a caudally directed postcomissural component, which is directed towards the diencephalon. A large number of fibres cross the midline before entering the columns of the fornix. Many of these fibres are true commisural fibres and are directed to fields in the contralateral hippocampal formation. Fornix and fimbria carry both efferent fibres of the hippocampus and subcortical afferent fibres to the hippocampal formation. The dorsal hippocampal comissure crosses the midline just rostral and ventral to the splenium of the corpus calossum. It carries fibres mainly originating from, or projecting to, the presubiculum, parasubiculum, and entorhinal cortex. Fibres of the dorsal hippocampal comissure are continuous laterally with a bundle of fibres that is interposed between the entorhinal cortex and the pre- and parasubiculum – angular bundle. This fiber system is the main route by which fibres from the ventrally situated entorhinal cortex travel to all septotemporal levels of the hippocampal fields.

The hippocampus receives polymodal sensory information from the entorhinal cortex via the perforant pathway, originally described by Ramón y Cajal (1911). This complex set of projections, together constituting the perforant pathway, originates from layers II and III of the entorhinal cortex, so that neurons in layer II project to the dentate gyrus and CA3, whereas layer III cells project to CA1 and the subiculum (Witter and Amaral, 1991). Layer II cells also send a few collaterals to the subiculum (Lingenhohl and Finch, 1991). The perforant pathway shows a topographical organization along the longitudinal axis of the hippocampal formation, so that a lateral-to-medial gradient in the entorhinal cortex corresponds to a septal-to-temporal gradient in the hippocampal formation. At all longitudinal levels of the hippocampus, each field receives inputs belonging to the functionally different components of the perforant pathway originating in the LEC and the MEC, respectively. The major point of this organization is that on the basis of its afferents, the entorhinal cortex can be divided into at least three longitudinal zones, which project to different parts along the hippocampal longitudinal axis.

Inside the hippocampus, granule cell axons (mossy fibers) project to CA3 pyramidal cells, which are also innervated by recurrent excitatory collaterals and thus contain a positive feedback loop (Miles and Wong, 1986). Pyramidal cells of CA3 can feed back information into the dentate gyrus, either by activating granule cells directly or through mossy cells (excitatory local circuit neurons of the hilus), or by silencing granule cells via inhibitory interneurons in the hilus (Penttonen et al., 1997). The main output from CA3 pyramidal cells is through the Schaffer collaterals, which project to CA1 pyramidal cells and interneurons. Once CA1 pyramidal cells are excited, they propagate their activity via the subiculum to the deep layers (V and VI) of the entorhinal cortex. CA1 pyramidal cells also project to the septum, from where the hippocampus receives GABAergic and cholinergic innervation. In contrast to the dentate–CA3 system, positive feedback loops are expressed only sparsely in the "output network" beginning at CA1 (Deuchars and Thomson, 1996).

The CA1-to-subiculum projection shows extensive longitudinal divergence, so that fibers from one particular point of origin distribute over approximately one third of the long extent of the subiculum. This longitudinal spread is thus comparable to that of the perforant pathway. Projections from the proximal part of CA1 terminate in the distal part of the subiculum. Conversely, projections from the distal part of CA1 predominantly reach the proximal part of the subiculum; projections from the center of CA1 reach the center of the subiculum. Intracellular fills of CA1 neurons have yielded comparable results and showed that the axon of any one particular neuron distributes along approximately one third of the transverse extent of the subiculum (Amaral et al., 1991). The CA1-subiculum projections extend throughout the stratum pyramidale and moleculare of the subiculum. The CA1-to-subiculum projections influence the proximal dendrites of the subicular pyramidal cells, but also influence the cell at the level of the soma and possibly the basal dendritic domain.

Projections from the hippocampal formation to the entorhinal cortex originate in CA1 and the subiculum. Most fibers terminate in layer V of the entorhinal cortex over its full transverse extent. (van Groen and Wyss, 1990). However, this projection also distributes to the superficial layer III of the entorhinal cortex. The projections from CA1 and the subiculum originate from the entire longitudinal extent of the hippocampal formation, and in rat, cat, and monkey, this projection shows a topographical distribution along the long axis, similar to that of the perforant pathway.

Amygdaloid complex: nuclei and its external connections.

The amygdala is a heterogeneous collection of nuclear groups located in the medial temporal lobe. The various nuclei can be distinguished on the basis of cytoarchitectonics, chemoarchitectonics and fiber connections. The deep nuclei include the lateral nucleus, basal nucleus, and accessory basal nucleus. The superficial nuclei include the anterior cortical nucleus, bed nucleus of the accessory olfactory tract, medial nucleus, nucleus of the lateral olfactory tract, periamygdaloid cortex, and posterior cortical nucleus. The remaining nuclei include the anterior amygdaloid area, central nucleus, amygdalohippocampal area, and the intercalated nuclei (Aggleton J.P., 2000;Chepurnov and Chepurnova, 1981;van Groen and Wyss, 1990).

The basolateral amygdala consist of the basolateral, lateral, and basal amygdaloid nuclei. The basolateral amygdala has reciprocal connections with many cortical regions and projections into the extended amygdala, basal forebrain, and ventral striatum. The extended amygdala includes parts of the central and medial amygdaloid nuclei that continue through the substantia innominata into similarly characterized regions of the bed nucleus of the stria terminalis. The extended amygdala has reciprocal connections with the hypothalamus, thalamus, midbrain, and brain stem (Gray, 1999).

The amygdaloid complex is reciprocally connected with the hippocampus and the surrounding cortex. The direct cortical input to the amygdala is segregated and selectively targeted to various amygdaloid subregions. Projections into the amygdala arise from the orbital and medial prefrontal cortex (limbic and anterior cingulate regions), lateral prefrontal cortex (containing the rostral tip of the insular cortex), insular cortex (gustatory, visceral, and somatosensory), perirhinal cortex, piriform cortex. The recipients of these projections are the lateral, basolateral, basal, and extended amygdaloid regions, although the majority of incoming cortical projections terminate within the basolateral amygdaloid nuclei. The basolateral and basal amygdaloid nuclei in turn project back upon the cerebral cortex in a highly recipriocally organized topographical manner. The extended amygdala has no direct cortical projections, but, rather, has extensive intrinsic connections and extrinsic pathways that innervate the hypothalamus and lower brain stem regions. In addition, the extended amygdala receives direct visceral and sensory input from the regions in the brain stem (nucleus of the solitary tract and parabrachial nucleus) and the thalamus.

Most of the amygdala-entorhinal interconnections occur between the lateral, basal, and accessory basal nuclei of the amygdaloid complex and the AE, DLE, DIE, and VIE subfields of the entorhinal cortex. Many of these connections appear reciprocal. The heaviest

projections from the amygdaloid complex to the entorhinal cortex originate in the lateral, basal, accessory basal, medial, and posterior cortical nuclei and terminate in layers 3 or 5 of the entorhinal cortex. Various subfields of the entorhinal cortex project to selective amygdaloid nuclei or nuclear subdivisions (Pitkanen et al., 2000).

The basal, accessory basal, and posterior cortical nuclei are the major sources of projections from the amygdala to the CA1 subfield. The parvicellular division of the basal nucleus projects moderately throughout the temporal half of the CA1 subfield (stratum oriens and stratum radiatum). The magnocellular division of the basal nucleus gives origin to a light projection that terminates in the stratum oriens and stratum pyramidale of the most septal end of the CA1/subiculum border (Pikkarainen et al., 1999). The magnocellular division of the accessory basal nucleus also sends a moderate projection to the CA1 subfield. The posterior cortical nucleus also provides a heavy projection to the temporal end of CA1 (stratum lacunosum moleculare and stratum radiatum) (Kemppainen and Pitkanen, 2000). According to anterograde and retrograde tracer studies, only the temporal end of the CA1 subfield projects to the amygdala (McDonald, 1998;Ottersen, 1982).

According to the available data, there are no monosynaptic interconnections between the amygdaloid complex and the dentate gyrus. The parvicellular division of the basal nucleus provides a substantial projection to the stratum oriens and stratum radiatum of the temporal end of the CA3 subfield. There are no data showing that the CA2 and CA3 subfields project to the amygdaloid complex. The magnocellular division of the basal nucleus projects lightly to the stratum oriens and stratum radiatum of the CA2 subfield.

The subiculum (temporal) also receives substantial projections from the basal and accessory basal nuclei of the amygdala. The projection is mostly directed to the deep portion of the molecular layer, although varicose terminals are also observed in the superficial portion of the pyramidal cell layer. The temporal end of the subiculum provides substantial projections to a large number of amygdaloid nuclei (lateral nucleus, basal nucleus, accessory basal nucleus, central nucleus etc). Thus, the temporal end of the subiculum gives origin to substantial projections to a large number of amygdaloid nuclei (e.g., compared to the CA1 subfield). Interconnections between the amygdala and the parasubiculum are unidirectional, that is, from the amygdala (the lateral, basal, and accessory basal nuclei) to the parasubiculum. Thus within the amygdaloid complex, the basal nucleus has the most extensive interconnections with the hippocampus. The amygdaloid complex provides more projections to the hippocampus than vice versa.

There are significant similarities between the anatomy, neurochemistry, and functions of subregions of the extended amygdala and the ventral striatum-accumbens areas. Both the extended amygdala and ventral striatum receive a dense input from the basolateral amygdaloid nucleus. These regions contain medium, spiny GABAergic neurons and receive a dense dopaminergic input from the brain stem. They also contain a dense innervation of enkephalin. The basolateral and extended amygdala and ventral striatum circuitry has an important function in associating previously neutral stimuli with positive and negative reward. These include the association of multiple stimuli with the rewarding properties of natural and pharmacological stimuli. The basolateral amgydala, in concert with prefrontal cortical circuitry and hippocampus, is involved in learning and memory, associated with assessing the magnitude and value reward or reinforcement (Aggleton, 2000).

Anatomical basis of amygdaloid processing.

Information flow within the amygdala takes place via dense and precisely organized intradivisional connections. Each nucleus is made up of separate subdivisions, which are connected via interdivisional pathways. Each subdivision, in turn, has its own intradivisional connections. Anatomical tracing studies suggest that input from the auditory thalamus terminate in the dorsolateral and ventrolateral areas, while input from cortical sensory areas terminate in all the divisions. The medial division receives most of its input from cortical regions, including the prefrontal and perirhinal cortical areas, and the hippocampal formation. The lateral nucleus sends heavy projections to most of the other amygdaloid nuclei. The major connectivity rule is that the various divisions of the lateral nucleus do not initiate substantial intradivisional projections, but rather, each rostrocaudal level projects only a short distance.

Although relatively little is known about local circuit organization in the amygdala, there is evidence that incoming signals are regulated locally by inhibitory interneurons in the dorsolateral division. Each rostrocaudal level of the dorsolateral division gives rise to dense projections to the other two divisions of the lateral nucleus. This allows information entering any part of the dorsolateral division to activate the other divisions. Information flow between these divisions is unidirectional, as the ventrolateral and medial divisions do not project back to the dorso-lateral division.

Unlike the lateral nucleus, the magnocellular, inter-mediate and parvicellular divisions of the basal nuclei have dense projections throughout their rostrocaudal extent. The only exception is the parvicellular division, in which the lateral and medial portions remain largely unconnected. The interconnections of the three divisions of the basal nucleus are selective.

The parvicellular division gives rise to most of the intranuclear projections within the basal nucleus and projects both to the magnocellular and intermediate divisions. Unlike the lateral nucleus, where there are no major reciprocal connections between the nuclear divisions, the magnocellular division of the basal nucleus sends a projection back to the lateral part of the parvicellular division. The intermediate division, however, does not give any substantial projections to the other divisions of the basal nucleus. These observations suggest that in contrast to the lateral nucleus, each division of the basal nucleus is able to distribute the input throughout the division, and the magnocellular and parvicellular divisions may selectively activate the other divisions as well.

The two divisions of the accessory basal nucleus, the magnocellular and parvicellular, also give rise to dense intradivisional projections, but are connection-ally separated from each other (Savander et al., 1997). Therefore, information arriving in one of the divisions is able to influence processes throughout most parts of that division but probably remains segregated from the content of the other division.

The central nucleus is the major output nucleus for amygdaloid projections to the brainstem and hypothalamus. It is also one of the amygdaloid nuclei to receive input from both the lateral, to the medial division; lateral division projects to the capsular and medial divisions; medial division projects back to the capsular division. The intermediate division is the only one that does not interact with the others. The capsular and medial divisions are the major recipients of the inputs from the lateral, basal and accessory basal nuclei. Inputs from these three nuclei mostly terminate in different divisions of the central nucleus. Each of the divisions of the central nucleus has heavy intradivisional projections along the rostrocaudal and mediolateral axes. In addition, there is extensive interdivisional connectivity: capsular division is reciprocally interconnected with the basal and accessory basal nuclei.

The different divisions of the medial nucleus are also interconnected. However, the projections between the medial and lateral divisions of the amygdalo-hippocampal area are directed from lateral to medial direction. The intra-amygdaloid projections of various amygdaloid nuclei are mainly segregated, but converge in select amygdaloid regions. Projections from various cortical and subcortical areas to the amygdala terminate in different amygdaloid nuclei. For example, projections from sensory processing areas terminate in the lateral nucleus; projections from the entorhinal cortex terminate most heavily in the basal nucleus; and projections from the hypothalamus terminate in the central, medial, basal and accessory basal nuclei. These data suggest that the information entering the amygdala from various cortical and subcortical systems will have multiple representations within the

amygdala. The lateral nucleus gives rise to the most extensive set of intra-amygdaloid connections (Aggleton, 1993). However, the basal nucleus, accessory basal nucleus, periamygdaloid cortex, medial nucleus, anterior cortical nucleus and posterior cortical nucleus (Canteras et al., 1995) also have projections to the other amygdaloid nuclei. This generates an extensive network of intra-amygdaloid connections, although there is little overlap between the terminal fields of projections originating in the different amygdaloid nuclei. The two regions where there is a significant amount of convergence of projections are the central nucleus and the amygdalo-hippocampal area.

Thus general principles of information flow between amygdaloid nuclei are as follows. After entering the amygdala, a stimulus will soon have several representations that are processed in parallel. After association of information from the other functional systems of the brain, each of the nuclei or nuclear divisions comes to have a unique representation of the stimulus qualities. The overlap of the projections in select amygdaloid nuclei might be important for the association and fine tuning of information processed in parallel within the amygdaloid networks.

The information flow within the amygdaloid complex is reciprocal rather than unidirectional. Virtually all main intra-amygdaloid targets of the lateral nucleus, with the possible exceptions of the central nucleus and the amygdalo-hippocampal area, send projections back to the lateral nucleus. The basal nucleus appears to send morphologically defined inhibitory and excitatory projections to the ventrolateral division of the lateral nucleus. The inhibitory component of this projection has also been demonstrated electrophysiologically *in vitro* by stimulating or applying glutamate to the basal nucleus and recording hyperpolarizing GABA receptor mediated responses from the lateral nucleus. The accessory basal nucleus sends an excitatory projection to the medial division of the lateral nucleus (Aggleton J.P., 2000). Moreover, the PAC division of the periamygdaloid cortex projects to the lateral nucleus. In addition, the anterodorsal part of the medial nucleus sends projections back to the ventrolateral and medial divisions of the lateral nucleus. The reciprocal connections are of substantial density even though they typically tend to be lighter than their input projections from the lateral nucleus. Also the basal nucleus and the accessory basal nucleus are reciprocally connected with their target regions, such as the anterior cortical nucleus or the medial and posterior cortical nuclei, respectively (Canteras et al., 1992).

The organization of the intra-amygdaloid connections of the central nucleus and the amygdalo-hippocampal area is different from the other amygdaloid nuclei. Even though they receive substantial projections from the lateral, basal and accessory basal nuclei, they send

few projections back to these amygdaloid areas. These data suggest that the major function of these nuclei is to execute output commands rather than modulate incoming information. It is accepted today that the amygdaloid output nuclei, especially the central nucleus, receive convergent information from several other amygdaloid regions and generate behavioral responses that reflect the sum of neuronal activity produced by different amygdaloid nuclei.

The dorsal endopiriform nucleus

The dorsal endopiriform nucleus (EPN) is a large elongated group of densely packed, multipolar neurons located deep to the piriform cortex over its full rostral to caudal extent and laterally to the basolateral complex of the amygdala (Behan and Haberly, 1999). EPN shares many features of connectivity and cellular organization both with the piriform cortex and the basolateral amygdala. The amygdala is connected with the EPN. The lateral, basal, and accessory basal nuclei, anterior and posterior cortical nuclei, medial nucleus, periamygdaloid cortex, and the amygdalo-hippocampal area project to EPN (Canteras et al., 1992;Luskin and Price, 1983;Ottersen, 1982). The heaviest projection to the endopiriform nucleus originates in the amygdalohippocampal area (Majak et al., 2002). EPN also receives projections from the olfactory bulb, as well as from the piriform, entorhinal, and perirhinal cortices. Notably EPN targets mostly cortical areas, including hippocampal formation rather than the nuclear structures. Although few studies have addressed the functional role of EPN on the basis of electrophysiologic, lesion, pharmacologic, and molecular studies, EPN and the claustrum are implicated as candidate gateways for the spread of seizure activity from the amygdala to other brain areas, particularly to the motor system, to which the monosynaptic amygdaloid projections are sparse. On the other hand, some observations suggest that it contributes to behaviors that depend on the convergence of olfactory cues such as mating behavior (Canteras et al., 1992). In vivo electrophysiological studies of the EPN have not been performed yet.

Oscillatory patterns of the hippocampus and amygdaloid complex

The hippocampal EEG displays the following synchronous patterns: Theta-rhythm - the rhythmic oscillatory field activity of 5 to 10 Hz is correlated to active states, especially exploration, and to paradoxical sleep (PS) (Vanderwolf, 1969). The underlying mechanisms are complex and may involve intrinsic properties as well as several intrahippocampal, corticohippocampal, and septohippocampal circuits (Chapman and Lacaille, 1999). Gamma-oscillations (Bragin et al., 1995a) are normally superimposed on the theta-rhythm and range from 40 to 100 Hz. They are generated by phasic, synchronous inhibition of principal cells

through interneuronal networks (Traub et al., 1996a). The term “large irregular activity” (Vanderwolf, 1969) was introduced for a non-theta state that is most pronounced during slow-wave sleep and consummatory behavior. Large irregular activity is generally slow and contains sharp waves. Sharp waves (Buzsaki et al., 1983) comprise a massive (50–100 msec) activation of CA3 pyramidal cells by their mutual excitation and are propagated to CA1 (Buzsaki, 1986) as well as to the dentate gyrus (Penttonen et al., 1997). Sharp waves are observed primarily during awake immobility, slow-wave sleep and consummatory behaviours. Superimposed on sharp waves are high-frequency events called ripples (O'Keefe, 1976). Dentate spikes are generated by the excitation of granule cells and certain hilar interneurons from the entorhinal cortex (Bragin et al., 1995a;Penttonen et al., 1997). In contrast to sharp waves, CA1 pyramidal cells are inhibited during dentate spikes, and thus the output from the hippocampus is silenced.

Hippocampal ripples.

High-frequency oscillations (~200 Hz) during large irregular activity were first noticed by O’Keefe (O'Keefe, 1976), but a detailed physiologic analysis began with the study by Buszáki et al. (Buzsaki et al., 1992). Chronically implanted single- and multi-electrodes recorded a peculiar pattern of spontaneous activity in the hippocampal CA1 region of freely moving rats: brief bursts of 5 to 15 sinusoidal waves in the stratum pyramidale with a cycle time of approximately 5 msec (200 Hz) that occur during slow-wave sleep, rest, or consummatory behavior. Ripples have small amplitudes of less than 500 μV but usually are superimposed on larger sharp waves (Buzsaki et al., 1983). They arise from CA3 pyramidal cells that, through their positive excitatory feedback loop, develop spontaneous, synchronous bursts of action potentials that then propagate to CA1. In extracellular field potential recordings this is reflected by a negative deflection at the level of the Schaffer collateral synapses in stratum radiatum. Intracellular somatic recordings reveal a depolarization of a few millivolts (Ylinen et al., 1995a).

Laminar profiles of ripples have been recorded with multielectrodes positioned perpendicular to the layered structure of the hippocampus (Ylinen et al., 1995a). By calculating the second spatial derivative of the smoothed voltage profile, such recordings can serve to identify current sinks (inward currents) and sources (outward currents). This current source density analysis (CSD) (Mitzdorf, 1985) revealed oscillating pairs of sinks and sources during ripples that were largely restricted to the pyramidal cell layer and its immediate vicinity. This pattern is in marked contrast to the distribution of sinks and sources caused by

sharp waves, theta-oscillations, or electrical stimulation of afferent fiber bundles, all of which show much more distributed CSD patterns, with current sinks in dendritic layers resulting from synaptic excitation. The concentration of ripples to the pyramidal layer restricts the possibly involved circuitry to perisomatic inhibition of CA1 pyramidal cells or synaptic excitation of the basal dendrites, which can occur through Schaffer collaterals and commissural fibers. A role for excitatory inputs has been excluded by Ylinen et al. (1995), who found different CSD for ripples versus Schaffer collateral or commissural pathway activation. Thus, ripples seem to involve mainly synaptic inhibition, although they can be triggered by sharp waves (Buzsaki et al., 1992;Traub and Bibbig, 2000) that are generated by excitatory input from the ipsi- or contralateral CA3 region.

Records revealed ripples with a zero average phase lag over at least 2 mm along the CA1 axis (Ylinen et al., 1995a). Later it was shown that some cycles of the oscillations can be coherent over distances as long as 5 mm in the rat (Chrobak and Buzsaki, 1996) and thus recruit the larger part of the whole CA1 region of one side.

Ripples are not restricted to CA1. Toward the hippocampal output pathway, sharp wave-associated ripples travel through CA1 and the subiculum into the deep layers (V, VI) of the entorhinal cortex, where they elicit a sharp wave with a concomitant ripple delayed by 5 to 30 msec relative to CA1 (Chrobak and Buzsaki, 1994;Chrobak and Buzsaki, 1996). Single and multiunit activity is correlated to the negative phase of the local field oscillation, although the degree of modulation for multiple cycles of the oscillation varies from site to site at sites within the hippocampal-entorhinal output network where high-frequency ripples can be observed. The peaks of ripple-ripple cross-correlograms do not indicate any significant (>5 msec or a single cycle) lag in the occurrence of presubicular ripples as compared with CA1 ripples. Entorhinal ripples are more variable and exhibit fewer oscillatory waves per ripple. Although an occasional entorhinal ripple precedes the occurrence of CA1 ripples, the majority (~95%) occurs either virtually simultaneously (±5 msec) or are delayed (>5-30 msec peak-amplitude wave to peak-amplitude wave) as compared with a dorsal CA1 site. Entorhinal and parasubicular single and multiunit activity is phase-related to local ripples, although the degree of oscillatory modulation is clearly less pronounced than at CA1, subicular or presubicular sites. Entorhinal neurons are phase-related to the negative peak of the local oscillation. Entorhinal ripples, observed as electrodes penetrate layers V-VI and enter layer III, were associated with a prominent negative-going wave that we refer to as entorhinal sharp waves. This slow potential reverses in polarity near layer II, suggesting that it represents a synchronized field EPSP in the apical dendritic zone of layer V-VI neurons. This entorhinal

sharp wave is similar to that described previously by Paré et al. (1995) in the cat. These authors also observed that deep layer EC neurons discharge regularly in association with these events, whereas superficial neurons discharged much less frequently. Bringing neurons within the hippocampal-retrohippocampal network together in time on such a short time-scale provides a potent means of enhancing their impact on common postsynaptic targets.

At the same time, sharp waves also excite dentate granule cells, probably through excitatory interneurons in the hilus—the mossy cells (Penttonen et al., 1997). Consistent with this "retrograde" propagation, ripples do occur in the dentate as well (Chrobak and Buzsaki, 1996;Ylinen et al., 1995a). Sharp waves with superimposed ripples often occur bilaterally at the same time, but have no strict cycle-to-cycle coherence between both hemispheres. Thus, ripples are initiated by sharp waves in CA3 (where superimposed lower frequency ripples are also present), and then travel bidirectionally into the dentate as well as through the CA1–subiculum–entorhinal cortex–output pathway of the hippocampus. In addition, the MSDB is inhibited by hippocampal ripples, in contrast to its activation during theta-oscillations (Dragoi et al., 1999). Because sharp waves are thought to be initiated by the recurrent collateral system of the hippocampal CA3 region, suppression of MSDB neurons is likely brought about by the increased activity of septally projecting GABAergic hippocampal interneurons. In return, the decreased activity of the target MSDB cells may have important consequences on the activity of hippocampal neurons as well. Decreased firing of MSDB GABAergic neurons may contribute to the termination of sharp wave bursts by disinhibiting hippocampal interneurons (Toth et al., 1995), suggesting a regulatory negative feedback role for the hippocampus-MSDB-hippocampus loop.

The synchrony of ventral CA1 sharp waves/ripples and occurrence of "up" membrane potential states of nucleus accumbens principal neurons (Goto and O'Donnell, 2001) provide a basis for the incorporation of hippocampal functions into motor planning and attentional mechanisms within the ventral basal ganglia circuits.

Ripples constitute a strong hippocampal–cortical output signal, involving an estimated 40,000 to 60,000 projection cells in the rat. CA3-generated sharp waves activate dentate granule cells that in turn project back to CA3 (Penttonen et al., 1997).

The propagation of sharp wave–ripple complexes is a unique pattern, different from the spread of dentate spikes (generated by input from the entorhinal cortex) with rare discharge of granule cells and a quiescent CA1 output pathway (Bragin et al., 1995b) or from theta- and gamma-oscillations, from which dentate granule cells receive mainly inhibitory potentials (Buzsaki and Eidelberg, 1981).

Investigation of sharp waves was also conducted in the early postnatal period in rats (Leinekugel et al., 2002). Depth distribution of spontaneous and evoked field potentials was recorded by 16-site silicon probes placed in the CA1-dentate gyrus axis of urethane-anesthetized rat pups (P3 to P6). The dominant hippocampal pattern was the field sharp wave followed by a long "tail" of population unit firing. These long, multiunit bursts were no longer observed in rats older than P10, in contrast to other hippocampal patterns (theta, dentate spikes) that progressively emerged during the second postnatal week. Amplitude-versus-depth profiles of sharp waves in P3 to P6 animals revealed a sharp phase-reversal just below the CA1 pyramidal layer. A major difference between the developing and adult forms of sharp waves was the absence of fast field "ripples" in the pyramidal layer in neonates. 140-200 Hz CA1 pyramidal layer oscillations were first observed in P10 animals.

Network and cellular mechanisms of ripple oscillations

Fox and Ranck (1975) observed that “theta cells” (probably interneurons of the stratum pyramidale and oriens) fire bursts of action potentials during sharp waves whereas “complex spike cells” (probably pyramidal cells) fire occasional single spikes during sharp waves. More detailed information is available on the firing behavior and phase relations of different hippocampal cell groups during sharp waves and ripples, through the work of Buszaki et al.

Unit recordings from putative projection neurons in CA1 revealed that approximately 10% to 15% of the pyramidal cells show action potentials that are phase coupled to field ripples (Buzsaki et al., 1992;Csicsvari et al., 1998;Csicsvari et al., 1999a;Ylinen et al., 1995a). These cells fire only one to a few action potentials during a field ripple; thus, they do not reach the network frequency of 200 Hz. However, their mean action potential frequency (1–2 Hz) is increased more than sixfold during sharp wave–ripple complexes.

Intracellular recordings (Ylinen et al., 1995a) revealed a slight depolarization of pyramidal cells during sharp waves, probably reflecting the excitatory drive from the Schaffer collaterals. Moreover, the membrane potential showed 1 to 5-mV oscillations in phase with the field ripples that reversed on hyperpolarization or after filling the cell with Cl^-. These findings indicate a role for $GABA_A$ receptor-mediated inhibitory postsynaptic potentials in the oscillations and largely exclude that the oscillation frequency is determined by intrinsic properties of the pyramidal cells. Pyramidal cells discharge preferentially at the negative peaks of the ripple oscillation. Pairs of pyramidal cells show a substantial cross-correlation during ripples with negligible phase lag and with repetitions at 5-msec intervals.

Inhibitory interneurons in the hippocampus not only balance excitation but coordinate principal cell discharge probability during complex network behaviors (Traub et al., 1996b). It is therefore crucial to look at the phase relation between field ripple oscillations and interneurons. Two recent studies (Csicsvari et al., 1998;Csicsvari et al., 1999a) show that during sharp waves, interneurons in the stratum pyramidale and the stratum oriens/alveus of the CA1 region increase their basal average discharge frequency of 12 to 14 Hz by approximately two- to threefold. When interneurons participate in a field ripple, they fire at high frequency, sometimes at every cycle of the field discharge, reaching 150 to 250 Hz. The discharge behavior of interneurons during ripples is highly heterogeneous, which is in line with the extreme functional and anatomic heterogeneity of interneurons (Freund and Buzsaki, 1996). In the alveus, some cells show no correlation at all with the field ripple, some are silenced instead of activated by ripples, whereas many other interneurons are consistently active during the ripples. Altogether, unit recordings from interneurons are not well predictive for ripples, in contrast to theta-oscillations that seem to be generated mostly by interneurons. The opposite is true for pyramidal cell units. Usually, interneurons fire 1 to 2 msec after pyramidal cells within a ripple, but still within the negative half-cycle. This delay points toward a monosynaptic activation of interneurons by action potentials of pyramidal cells (Traub and Bibbig, 2000). However, the efficacy of pyramidal cells to excite interneurons is lowest during sharp waves compared with other states of the network.

Two classes of high-frequency oscillations in the CA1 region were described (Csicsvari et al., 1999a). The amplitude of so called “fast ripple waves” was largest in the CA1 pyramidal layer. These large-amplitude, fast (>140 Hz) ripples were typically associated with a negative sharp wave in the stratum radiatum. The fast ripple waves reversed abruptly below the pyramidal layer, and their amplitude decreased steeply in stratum radiatum. In between large ripples, the fast (>100 Hz) oscillatory field activity was relatively small or entirely absent. These lower-amplitude events were of slower frequency (<140 Hz), and the oscillatory waves showed a phase reversal in either the stratum oriens or stratum radiatum.

Both fast (180 Hz peak) and slow oscillations (110 Hz peak) were associated with phase-locked discharge of both pyramidal cells and interneurons. The amplitude of both fast and slow oscillatory events correlated with the relative increase in firing frequency of neurons. The correlation with pyramidal cell discharges was linear, except for the lowest-amplitude events. Interneurons also increased their firing rate as a function of the field amplitude, but the rate of increase was considerably lower than it was for pyramidal cells. Wave-triggered averaging for the slow oscillatory event in CA1 revealed phase-locked field

activity in the CA3 region. In contrast, field activity in the CA3 pyramidal layer did not appear to be related to the individual waves of the fast ripples recorded in the CA1 field. In addition, cross-correlation between CA1 field activity and interneuronal discharge in the CA3 region revealed that unit discharges were phase-locked to the slow CA1 field activity but not with the large-amplitude, faster ripples.

Recently an alternative mechanism for the generation of 200-Hz oscillations has been proposed by A.Draguhn et al. Experiments in rat hippocampal brain slices in vitro revealed spontaneous, fast rhythmic activity in all principal cell layers reminiscent of ripples in vivo (Draguhn et al., 1998). It was found that the 200 Hz oscillations could not be blocked by antagonists of glutamatergic or GABAergic synapses. Even more, the oscillatory field activity of 150 to 200 Hz persisted in the absence of extracellular calcium ions and thus cannot depend on a network coupled by chemical synapses.

Several lines of evidence suggest that 200-Hz activity in rat brain slices depends on electrical coupling by gap junctions between pyramidal cells. The oscillations can be blocked by three different agents known to block gap junctions - halothane, octanol, and carbenoxolone - and they are enhanced in a calcium-free medium and increase on alkalization of cells. Lastly, recordings from a CA1 pyramidal cell in calcium-free extracellular medium revealed spikelet potentials (MacVicar and Dudek, 1982), also called fast prepotentials that were tightly coupled to the field rhythm. Such potentials have been suggested to be generated by electrical coupling through gap junctions (MacVicar and Dudek, 1982;Perez Velazquez and Carlen, 2000). Thus oscillations resembling 200-Hz ripples can be generated in electrically coupled networks of hippocampal pyramidal cells (Draguhn et al., 1998;Traub et al., 1999a).

Synchronization of neural networks by electrical coupling via gap junctions is increasingly regarded as a possible mechanism underlying physiologic and pathologic (epileptic) oscillations (Perez Velazquez and Carlen, 2000). There is functional and anatomic evidence for electrical coupling between hippocampal interneurons especially early in development (Cesare et al., 1996), and for electrically coupled interneuronal networks in the cortex (Galarreta and Hestrin, 1999). Evidence for electrical coupling between hippocampal principal cells comes from various physiologic and anatomic studies (MacVicar and Dudek, 1982;Perez Velazquez and Carlen, 2000;Schmalbruch and Jahnsen, 1981), but direct proofs and detailed data on the quantity and localization of such gap junctions are still missing.

Based on a realistic computer model of pyramidal cells, Traub et al. (Traub et al., 1999a) have modeled an electrically coupled network generating ripple oscillations. To mimic

the fast time course of experimentally observed spikelets, gap junctions were located between the axons of hippocampal principal cells. Axons have low capacitance, high input resistance, and a high density of Na+ channels that can amplify and accelerate the signal and result in extremely fast and efficient coupling. So far, axonal–axonal gap junctions have been described in the retina and within electrically coupled oscillating networks in electrical fish that work at high frequency (1,000 Hz) and with very high precision (Vaney, 1993). However, for the mammalian hippocampus, direct structural evidence for interaxonal gap junctions is still missing. A recent study by Maier et al (Maier et al., 2002) indicates that mice lacking the gap junction protein Cx36 display altered network behaviour in the hippocampus. A reduction in the frequency of occurrence of sharp waves and ripples as well as attenuated epileptiform discharges under 4-AP were found.

The model proposes that spikelets are ectopically generated action potentials that invade the soma antidromically. The oscillation can start from a few spontaneous ectopic action potentials. Subsequently, the activity will propagate through the axonal, electrically coupled network. Coupling is random and sparse. One surprising emergent property of this model is that the cycle duration (~ 5 msec) is determined by the average time needed for an axonal spike to travel through the gap junctions to a randomly selected secondary neuron in the net. Thus, the frequency is determined by the network topology and not by intrinsic or synaptic time constants. Another interesting feature is the fact that in such a model the activity of axons is largely independent from synaptic integration because the activity travels largely within the axonal circuit.

A way in that gap junctions and chemical synapses could work cooperatively to generate in vivo ripples has been proposed recently in the form of a network model(Traub and Bibbig, 2000). This model works as follows. During a sharp wave, populations of pyramidal cells and interneurons are presumed to receive a strong synaptic depolarization, lasting some tens of milliseconds. One consequence of this is a small depolarization of pyramidal cell axons. These latter axons are presumed to be interconnected by a sparse network of axonal gap junctions, as suggested by the experimental work and modeling results of Draguhn et al. (1998). Such an axonal network can, at least in principle, generate autonomously a 200 Hz network oscillation, consisting of temporally coherent axonal spikes. Orthodromic propagation of the oscillation will induce a 200 Hz series of excitatory postsynaptic potentials in interneurons receiving local collateral excitation. This explains why at least some interneurons can fire as fast as the collective oscillation itself. As the pyramidal axonal network is itself firing coherently, interneurons will be induced to fire coherently, and these

interneurons will induce phasic, but also coherent, inhibitory postsynaptic potentials in pyramidal cells, accounting for the intra- and extracellular rippling. The axonal spikes will also propagate antidromically into pyramidal cells. However, action potential firing of pyramidal cells will be infrequent, because of the inhibitory postsynaptic potentials, again in agreement with experiment. Antidromic conduction to the pyramidal cells occurs in a fraction of a millisecond after an axonal spike, but the time from occurrence of the axonal spike to an interneuron spike will be on the order of 1 to 2 msec because of the synaptic delay and generation of an excitatory postsynaptic potential in the interneuron (Csicsvari et al., 1998). Thus, on average, firing of pyramidal cells will lead firing of interneurons by a couple of milliseconds, as seen experimentally. Because the major component of intracellular rippling in this model is from inhibitory postsynaptic potentials, the rippling will phase reverse relative to the local average field potential, on hyperpolarization of a cell to a potential below the $GABA_A$ reversal potential. The proposed role of gap junctions is consistent with the blockade of in vivo ripples (not sharp waves) by the gap junction blocking agent halothane (Ylinen et al., 1995a).

Epileptogenesis: ultrafast ripples.

Conventional EEG recordings from human subjects cover the range of frequencies between approximately 0.5 and 30 Hz (and as high as 70 Hz), and therefore miss high-frequency phenomena. Recently, (Bragin et al., 1999a;Bragin et al., 1999b) recorded high-frequency extracellular and unit activity from the hippocampus and parahippocampal region of nine patients with implanted depth electrodes before epilepsy surgery. Two types of fast local field potentials could be identified: activity in the range of 80 to 160 Hz (ripples) and fast ripples at higher frequencies (250–500 Hz). Although slightly slower than in rats, the ripples showed several characteristics known from prior and concomitant work on rodents: they occurred spontaneously at variable frequency (0.1–20 ripples/min), often on top of sharp waves, and were coupled to the same functional state as in rats - namely, slow-wave sleep or awake rest. Their frequent bilateral occurrence is interesting in the light of the sparse interhemispheric connections between both hippocampi in humans. Ripples could precede interictal spikes, although there was no fixed relation between these events.

Fast ripples (250–500 Hz) occurred only in CA1 and in the entorhinal cortex of humans and kainic acid-treated rats (Bragin et al., 1999b). They were related to the same functional states as ripples but were largely confined to the lesioned area (rats) or to the epileptogenic focus in four of five patients, respectively. In contrast to kindled rats, the

chronic epileptic syndrome in kainic acid-treated animals goes along with severe structural damage, sprouting of axons, and remodeling of neuronal circuits. Thus, fast ripples may be pronounced in pathologically altered tissue or may even be restricted to such states. Fast ripples in the entorhinal cortex showed a different laminar distribution than conventional ripples and had no consistent relation to interictal spikes or sharp waves, although ripples, fast ripples, and interictal spikes occurred most frequently during the same behavioral state (slow-wave sleep and quiet immobility). The cellular mechanisms behind fast ripples are as yet unknown but may be different from ripples.

In kainic acid-treated rats, fast ripples can be observed at the beginning of a certain type of interictal event—the fast ripple–tail gamma-complex—that ends with oscillations in the gamma-range (30 to 80 Hz). Again, this activity pattern is confined strictly to the area of the epileptogenic lesion. The most frequent pattern of seizure onset in these rats started with or developed into fast ripple–tail gamma-complexes. Thus, fast ripples (250–500 Hz) seem to be a pattern closely related to epileptogenic tissue in the limbic system whereas typical ripples are, at most, loosely related to epilepsy. The behavioral correlate of fast ripple–tail gamma-complex-related seizures was slow-wave sleep or quiet immobility, in accordance with the general occurrence of fast ripples and ripples. Seizure onset reminiscent of fast ripple–tail gamma-complex has been reported previously from humans with implanted depth electrodes (Engel, Jr. et al., 1990).

Several groups have observed similar high-frequency discharges in experimentally induced epilepsy (Dichter and Spencer, 1969), including in vitro models in the absence of chemical synaptic transmission (Jefferys and Haas, 1982). It is feasible that electrotonic coupling of principal cells by gap junctions (Perez Velazquez and Carlen, 2000;Valiante et al., 1995)or interneurons (Traub, 1995) plays a causal role in the genesis of these synchronized fast oscillations.

Theta oscillations: sites and mechanisms.

Theta oscillations depend on ongoing behavior. Although no consensus has yet emerged regarding their specific behavioral correlates, theta waves are most consistently present during PS sleep (Jouvet, 1969) and during various types of locomotor activities (Vanderwolf, 1969). In general, theta waves are absent in the immobile animal but short epochs of theta trains can be elicited by noxious conditioned stimuli. Theta waves have been also assumed to be carriers of mnemonic processes (Lisman and Idiart, 1995). It should be noted here that field oscillations at theta/alpha frequencies have been observed in numerous cortical structures

(Lockery and Sejnowski, 1992). Intracranial recordings in humans indicate, however, that these patterns occur in different behavioral states and are not coherent with hippocampal theta waves (Kahana et al., 1999). Theta oscillation is most regular in frequency and largest amplitude in the str. lacunosum-moleculare of the hippocampal CA1 region. Both the amplitude and phase of theta waves change as a function of depth, whereas in the same layers they are robustly similar along the long axis of the hippocampus (Bullock et al., 1990). Theta oscillations are also present in the dentate gyrus and the CA3 region.

Several subcortical nuclei have been postulated to be critically involved in the rhythm generation of theta. Afferents from these nuclei release neurotransmitters that may allow for the emergence of network oscillations in the hippocampus and associated structures or may provide a coherent, theta frequency output. Because lesion or inactivation of MSDB neurons abolishes theta waves in all cortical targets, it has been regarded as the ultimate rhythm generator of theta. The MSDB is reciprocally connected to the supramamillary region (Borhegyi et al., 1998;Bullock et al., 1990), a second critical structure involved in pacing the theta rhythm. Whether the MSDB and supramamillary nucleus are true pacemakers or rhythmic firing of their neurons depends on the hippocampal and entorhinal feedback has yet to be determined (Brazhnik and Fox, 1999;Denham and Borisyuk, 2000;Lee et al., 1994). Neurons in several other subcortical structures are phase locked to hippocampal theta oscillation, including the dorsal raphe nucleus, ventral tegmental nucleus of Gudden, and anterior thalamic nuclei (Vertes and Kocsis, 1997). Finally, stimulation of several subcortical nuclei elicits hippocampal theta (Bland, 1986). However, these latter structures also project to the thalamus and/or neocortex as well, and they are part of a common ascending activation system rather than structures specifically involved in theta rhythm generation.

In the first and simplest theta model, the MSDB has been postulated to be the rhythm generator (pacemaker), which supplies phasic modulation to the hippocampus. On the assumption that the extracellular field is generated by the summed activity of IPSPs and EPSPs on the somata and dendrites of principal cells, respectively, these models utilized a single canonical CA1 pyramidal cell with passive membrane properties. It has been assumed that all pyramidal cells receive coherent excitatory (from perforant path) and inhibitory (from septum to feed-forward inhibitory neuron) inputs. The interplay between these two current generators is assumed to be responsible for the unique amplitude/phase versus depth profiles of hippocampal theta oscillation. According to this scheme, the most strongly excited minority of the population would discharge at the same time when nonspiking neurons are maximally depolarized.

Theta waves in the waking rat show a gradual phase reversal between CA1 str. oriens and the hippocampal fissure (Winson, 1974), consistent with the coordinated activity of at least two current generators. Because the largest amplitude theta waves are observed at the hippocampal fissure, rhythmic excitation of the distal dendrites by the entorhinal afferents is assumed to play the most important role in the current generation of extracellular field theta. A second theta dipole in the CA1 region is assumed to be generated by somatic IPSPs. These IPSPs are brought about by the theta frequency discharge of basket and chandelier cells, repeated at theta frequency (Kamondi et al., 1998;Leung and Yim, 1986;Ylinen et al., 1995b). The rhythmic drive and/or inhibition of basket cells may arrive from the MSDB (Buzsaki et al., 1983;Stewart and Fox, 1990), although several other inputs, including the entorhinal afferents, CA3 afferents, CA1 recurrent collaterals, and other interneurons with intrinsic oscillatory properties, may also be involved. CSD analysis, showing a strong sink in the CA1 str. lacunusom-moleculare and a source in the pyramidal layer also support the above scheme (Buzsaki, 1986). The gradual phase shift of the theta waves with depth (Winson, 1974) and the lack of a clear "null" zone are explained by the phaseshifted nature of the somatic and dendritic dipoles.

Research over the past several years points out a number of inadequacies of the above model (Buzsaki, 2002). (1) Although both CSD analysis and unit recording studies suggest that dendritic excitation is coupled to somatic inhibition, in the classic theta model a controversy exists between the timing of the excitatory and inhibitory inputs as postulated from field/ CSD studies and the actual discharge of the pyramidal cells and interneurons. If the major excitatory drive during theta is the entorhinal input, CA1 pyramidal cells are expected to discharge maximally at the peak of the sink in str. lacunosum-moleculare. However, the highest probability of discharge in the behaving rat occurs around the positive peak of theta recorded at the level of the distal dendrites, corresponding to the negative phase of the theta waves in the pyramidal layer. (2) Another finding, which is at odds with the classic model, is that the theta phase relationship of pyramidal cells is not fixed but changes dynamically as a function of behavior, this is the theta phase precession phenomenon. (3) Recent work indicates that pyramidal neurons in various limbic structures are endowed to oscillate at theta frequency. These intrinsic mechanisms may be as important in the generation of transmembrane currents as postsynaptic potentials. (4) The complex interconnections among the numerous hippocampal interneuron classes pose further questions about their involvement in rhythm generation. (5) More recent knowledge indicates that the recurrent circuit of the CA3 region may function as an intrahippocampal theta oscillator. (6) Finally, the

mutual connections between MSDB and the hippocampus/entorhinal cortex indicate that the model is overly simple.

Neurons in all hippocampal regions are phase modulated by theta oscillation (Buzsaki et al., 1983;Fox et al., 1986). Therefore, both the numerous granule cells and CA3 pyramidal cells are expected to generate their own theta fields. Although theta phase does not fully reverse across the granule cell layer, the waves recorded in the outer molecular layer and the hilus are phase shifted by approximately 90º. Furthermore, large phase jumps (180º) have been described in the molecular layer (Buzsaki, 1986). Elimination of CA1 pyramidal neurons by forebrain ischemia results in a dramatic decrease of theta amplitude (Buzsaki et al., 1989;Monmaur et al., 1986).

The CA3 pyramidal cells contribute to theta fields recorded in both the CA3 and CA1 regions. The CA3 output contributes directly to the theta field recorded in the CA1 region, as demonstrated by a sink in CA1 str. radiatum (Buzsaki, 1986). Despite the similar cytoarchitecture of the CA1 and CA3 regions, the extracellular theta currents in the CA3 region are considerably smaller than in CA1. Several factors may be responsible for this conspicuous difference. First, the distal dendritic arbor of CA3 pyramidal cells is considerably smaller than that of the CA1 pyramidal neurons (Pyapali et al., 1998). Second, in addition to the inputs common to CA3 and CA1, CA3 pyramidal neurons receive perisomatic excitation near their somata from the large mossy terminals of granule cells (Henze et al., 2000). Finally, the excitatory drive from the entorhinal layer II and layer III neurons to CA3 and CA1 pyramidal cells may be different.

After surgical removal of the entorhinal cortex, all remaining theta appears to depend on the integrity of the CA3 region, and theta signals in all layers are highly coherent with each other (Bragin et al., 1995a). In contrast, the coherence of theta signals in CA1 str.radiatum and str. lacunosum-moleculare in the intact brain is low and the powers of theta signals in these layers are inversely correlated with each other (Kocsis et al., 1999). On the other hand, theta waves in CA1 str. radiatum and in the inner third of the dentate molecular layer are strongly related. Since these layers are the targets of the intrahippocampal associational projections (Amaral and Witter, 1989), the findings suggest that the recurrent network of CA3 pyramidal cells and possibly hilar mossy cells forms an intrahippocampal oscillator. The intrahippocampal theta oscillator requires cholinergic activation because in the absence of the entorhinal input, the remaining theta is abolished by atropine. The notion that the cholinergic component of theta emerges in the CA3 recurrent collateral system implies that this form of oscillation can also be studied in the isolated hippocampus.

Konopacki et al. (Konopacki et al., 1987) observed that when a hippocampal slice is bathed in a solution containing the muscarinic drug carbachol, short bursts of field oscillations (4 to 15 Hz) occur intermittently. Depending on the concentration of the drug, the magnitude of the field oscillation and the synchrony of the neuronal population vary from in vivo theta-like pattern to overt epileptic patterns. The carbachol-induced rhythm is generated in the CA3 region and attenuated by AMPA receptor blockers. In the CA1 region, theta waves are reversed in phase in the str. oriens/pyramidale and str. radiatum.

The mechanisms by which theta-like oscillations emerge in the hippocampal slice preparation have yet to be disclosed. Pyramidal neurons are endowed with intrinsic properties to oscillate at theta frequency. Appropriate activation of such intrinsic oscillatory mechanism may elicit theta rhythm in single cells. Acetylcholine or carbachol induces dendritic depolarization and can affect several K^+ and other channels (I_h, I_A, I_{AHP}, I_M, and $I_{K[Ca]}$) (Madison et al., 1987). When the oscillating cells communicate with each other, a network oscillation is expected to occur. In contrast to the continuous theta in the intact brain, theta-like oscillations in vitro consist of only a limited number of cycles (Konopacki et al., 1987;Traub et al., 1992;van Der et al., 1999). When these conditions were created in vivo by grafting the fetal septal region into the subcortically denervated hippocampus, theta oscillation failed to emerge (Buzsaki et al., 1987b;Segal et al., 1985) even though release of acetycholine from the graft reached physiological levels. A broader implication of these observations is that in the behaving animal, the intrahippocampal (CA3) theta oscillator can change its frequency and phase relatively independently from the extrahippocampal (entorhinal) theta inputs (Kocsis et al., 1999). The phase differences, in turn, can have a profound effect on the timing of action potentials in the activated principal neurons.

Pharmacology of theta oscillations.

Generally, drugs affecting the field theta waves may interfere with the rhythm and/or the current generators. Blockade or potentiation of GABAA receptors during picrotoxin-induced epilepsy or pentobarbital anesthesia, respectively, eliminates theta by affecting both rhythm generation and current generation. Theta activity can be influenced by a variety of drugs (Vanderwolf, 1988). Vanderwolf (Kramis et al., 1975)suggested that, on the basis of pharmacological sensitivity, two types of theta could be distinguished: atropine-sensitive and atropine-resistant. The idea of an atropine-sensitive form of theta comes from early observations that muscarinic blockers, such as atropine, completely eliminate theta oscillations in anesthetized animals. In contrast, in the awake, walking rat, the amplitude and

frequency of theta oscillation do not substantially change even after large doses of systemically administered muscarinic blockers, although the wave shape and depth profile of theta under atropine are quantitatively different from those in the drug-free animal. This persisting form of theta is referred to as “atropine resistant”. Complete surgical removal of the entorhinal cortex or surgical isolation of the entorhinal cortex from its nonhippocampal afferents eliminates the theta dipole localized on the banks of the hippocampal fissure. Such lesions render the remaining theta oscillation atropine sensitive and its depth versus voltage profile somewhat similar to that observed under urethane anesthesia (Kamondi et al., 1998;Ylinen et al., 1995b).

Activation of NMDA receptors might be critical for the atropine-resistant form of theta oscillation (Buzsaki, 2002). The depth versus voltage profile of theta under the NMDA receptor blocker, ketamine, is similar to that described under urethane (Soltesz and Deschenes, 1993). Combination of ketamine or other NMDA receptor blockers and atropine or scopolamine abolished all theta activity in the hippocampus. A candidate target of the NMDA blockers is the entorhinal afferent synapses on the distal apical dendrites of CA1 pyramidal neurons.

The precise targets of systemic atropine in hippocampal theta generation are unknown. The remaining theta sinks and sources after bilateral lesion of the entorhinal cortex are more compatible with associational/commissural inputs and perisomatic inhibition than with the distribution of septo-hippocampal cholinergic terminals, which are present in all layers (Kamondi et al., 1998). This observation suggests that cholinergic-muscarinic receptors in the hippocampus are not responsible directly for the extracellular theta currents. Release of acetylcholine may simply depolarize pyramidal cells and interneurons and/or affect voltage-dependent conductancies, such as I_M, I_h, and I_A (Hoffman et al., 1997).

An alternative mechanism to the direct excitation of pyramidal cells by acetylcholine in theta generation is the cholinergic modulation of interneurons. Tonic cholinergic excitation of interneurons, coupled with their phasic septal GABAergic inhibition, has been suggested to be responsible for the rhythmic discharge of hippocampal interneurons (Freund and Antal, 1988;Stewart and Fox, 1990). In turn, the theta frequency discharge of the interneurons imposes rhythmic IPSPs on their target principal cells (Kamondi et al., 1998;Soltesz and Deschenes, 1993;Ylinen et al., 1995b).

There is an unresolved discrepancy between the pharmacologial blockage of the muscarinic M1 receptors and the absence of MSDB cholinergic neurons. Whereas the amplitude of hippocampal theta is only modestly affected after atropine treatment, it is

reduced several-fold after selective elimination of MSDB cholinergic cells (Lee et al., 1994). This discrepancy suggests that muscarinic M2 and/or nicotinic receptors (Ji and Dani, 2000) may also be involved in the regulation of theta. Because the atropine-resistant type of theta in the hippocampus is conveyed by the entorhinal input, the theta generated in the entorhinal cortex is likely not affected by muscarinic blockade.

Interneurons and theta-rhythm

Ample evidence supports the critical involvement of hippocampal interneurons in theta oscillations (Buzsaki et al., 1983). Hippocampal interneurons are the exclusive targets of the GABAergic septo-hippocampal projection as well as the sole hippocampal output to the neurons of MSDB(Freund and Antal, 1988). Thus, they are in a strategic position to amplify the hypothesized septo-hippocampal pacemaker connection.

In the behaving rat, the majority of CA1 interneurons discharge on the descending phase of theta in the pyramidal cells layer (ascending phase in the apical dendritic layers) (Bragin et al., 1995b). However, it is not known whether interneurons with different preferred theta phases represent different classes of cells or whether interneurons of the same class can discharge at different phases. At least three classes of interneurons deserve special attention: (1) basket and chandelier cells with perisomatic targets, (2) oriens lacunosum-moleculare and hilar interneuron with perforant path axon projection interneurons (Halasy and Somogyi, 1993; Freund and Buzsaki, 1996), which specifically innervate the termination zones of entorhinal afferents, and (3) interneurons with feedback septal projection.

Perisomatic inhibition plays an important role in timing the action potentials of principal cells within the theta cycle. Basket and chandelier cells discharge rhythmically at theta frequency on the descending phase of the pyramidal layer theta and provide rhythmic hyperpolarization to the perisomatic region of pyramidal cells via GABAA receptor-mediated IPSPs (Leung and Yim, 1986;Soltesz and Deschenes, 1993;Ylinen et al., 1995b). A functional consequence of such perisomatic shunting is periodic “isolation” of the somatic and dendritic compartments of pyramidal neurons at the time of maximum somatic inhibition. In the majority of pyramidal cells, the $GABA_A$ receptor-mediated transmembrane currents are very small because most pyramidal cells are silent during theta activity (Harris et al., 2000). The role of $GABA_B$ receptors in theta oscillation is not clear. Activity of a single presynaptic interneuron rarely activates postsynaptic $GABA_B$ receptors (Csicsvari et al., 1999b). However, because at least 60% of putative basket cells discharge synchronously during the

theta cycle, the amount of GABA released in the intact brain during theta may be sufficient to activate postsynaptic $GABA_B$ receptors.

Oriens lacunosum-moleculare and hilar interneurons specifically innervate the termination zones of entorhinal afferents on pyramidal cells and granule cells, respectively (Freund and Buzsaki, 1996). Since an important excitatory input to these interneurons is the local collaterals of CA1-CA3 pyramidal cells and granule cells (Blasco-Ibanez and Freund, 1995;Sik et al., 1995;Sik et al., 1997), the feedback dendritic inhibition can provide a "winner-take-all" mechanism and thereby prevent the discharge of weakly activated pyramidal neurons and granule cells. A third group of cells that may be critically involved in the rhythm generation of theta oscillation is septally projecting interneurons. Septally projecting interneurons discharge rhythmically during theta. Interneurons with septal collaterals are in a unique position to coordinate rhythmic discharge of large neuronal populations in both hippocampus and septum. Finally, a small group of interneurons, termed "antitheta" cells, may also hold a key in understanding the emergence of theta oscillations because of their reciprocal firing relationship with all the other interneuron classes. Antitheta cells are virtually silent during theta oscillations, but fire rhythmically at 15–25 Hz in the absence of theta (Buzsaki et al., 1983;Mizumori et al., 1990). Their anatomical identity is unknown (Buzsaki, 2002).

Interneuron network gamma (ING).

The concept of an inhibition-based network oscillation centres upon the mutual inhibition of a population of interconnected inhibitory interneurons. The activation of the interneurons can be either tonic or phasic or both. In the carbachol model the phasic activation of interneurons is generated by the synchronous firing of excitatory neuronal axons in the neocortex and area CA3 of the hippocampus. The degree and extent of this inhibitory neuron to inhibitory neuron connectivity can therefore govern whether or not an area is capable of generating such an oscillation when excitatory neurons do not participate. In the hippocampus inhibitory connections between GABAergic neurons have been directly demonstrated using recordings of synaptically connected basket cell pairs in the CA1 area. Following the stimulation of afferent fibres, such as the Schaffer collateral pathway, presumably locally generated di-synaptic IPSPs could be elicited in several classes of anatomically identified interneurons (Buhl et al., 1996). Moveover, these findings are also corroborated by anatomical data, showing, for example, the interconnectivy of hippocampal CCK- and parvalbumin-containing basket cells (Sik et al., 1995). Interestingly, the degree of interneuronal connectivity is

strongly dependent on their anatomical or neurochemical phenotype. While axo-axonic cells exclusively target principal neurons, several classes of interneuron are specialised to innervate other interneurons.

The interneuron population must consist, at least in part, of neurons with intrinsic firing frequencies faster than the population rhythm. Firing frequencies higher than the gamma range (more than 80 - 90 Hz) are common in directly depolarised inhibitory interneurons in the CNS (Whittington et al., 1997). If a population of such neurons is excited, then the firing frequency of the population response is governed by the timecourse of the mutual inhibition present from one neuron within the population to its synaptically connected neighbours (Traub et al., 1996a;Wang and Buzsaki, 1996;Whittington et al., 1995).

If a population of interconnected interneurons is depolarised then each action potential will generate an IPSP in each connected target interneuron. If enough interneurons fire action potentials at approximately the same time then convergent inhibitory inputs generate a temporally summated IPSP of sufficient magnitude to prevent further action potential generation until the IPSP fades. The basic frequency of network oscillation depends on two major parameters; 1) the magnitude and kinetics of the $GABA_A$ receptor-mediated inhibitory synaptic potentials between interneurons, and 2) the magnitude of tonic driving force (Whittington et al., 1996). The magnitude of the synaptic inhibition between interneurons governs the frequency of ING. This is the case for both absolute magnitude changes in the postsynaptic response and the kinetics of the response itself. A broad range of endogenous and exogenous agents can modify the $GABA_A$ receptor mediated IPSP and many of these have been shown to alter the frequency of gamma oscillations in experimental models. These agents include anaesthetics (Halothane (MacIver et al., 1991), sedatives, sex steroids and other neuromodulators (Segal and Barker, 1984).

The tonic driving force causing the excitation of the interneuron network has to be of sufficient magnitude: it must be large enough to cause individual interneurons to fire faster that the frequency produced by the network as a whole (gamma band). As driving force decreases from optimal a decrease in the frequency of the population oscillation can be seen until the population oscillation is no longer manifest. This occurs at frequencies around 15 Hz (Traub et al., 1996b). As driving force increases, oscillation frequency can also increase (up to 80 Hz) but, in the case of metabotropic glutamate receptors activation, the dependence of frequency on drive is non-linear, and experimentally ‘over-excited’ networks can demonstrate a decrease in oscillation frequency.

ING alone produces rhythmic trains of IPSPs in pyramidal cells, which would be expected to influence the timing of action potential responses to afferent excitatory input. However ING does not generate an excitatory projection neuron output. If excitatory neurons are concurrently depolarised along with the inhibitory network then the IPSP trains can generate precisely temporally controlled action potentials in these neurons. However, many excitatory neurons in the CNS have calcium-activated potassium conductances which markedly attenuate long periods of spike generation. Thus, without metabotropic activation, excitatory neurons cannot participate in inhibition-based gamma and beta oscillations for longer than a few periods. Metabotropic glutamate (and acetylcholine) activation alters this situation by reducing the magnitude of a number of potassium conductances that take part in the post-spike AHP (Charpak et al., 1995). If these longer-duration hyperpolarising voltage transients are attenuated to such an extent that the IPSP is the longest duration significant post-spike event in excitatory as well as inhibitory neurons, and if the excitatory neurons are depolarised, then these excitatory neurons will fire repeated action potentials at gamma frequencies along with, and synchronously with, the local interneuron network.

In an ING rhythm, the interneurons recover from inhibition and fire without excitation from other cells; as mentioned in the section on ING, these cells must then have sufficient drive to be able to fire even in the presence of inhibition, so their natural firing rate would be larger than the gamma frequency. The excitatory pyramidal cells are then basically gated by the rhythm created by the interneurons, and fire in the periodic intervals when the inhibition is low. If the drive to the excitatory neurons is relatively high (but not so high that they fire before the interneurons on a given cycle), then these excitatory neurons can fire in most cycles and still have an inhibition-driven rhythm (ING).

The rhythm produced by pyramidal - interneuron network gamma oscillations (PING) requires that the excitatory neurons recover from inhibition before the inhibitory cells do; the resultant firing of the excitatory neurons then causes the interneurons to fire. During a PING rhythm, agents that change the size and time course of inhibition have an effect that depends on the excitability of the excitatory neurons, while for ING rhythms their effect depends on excitability of the interneurons alone. This explains the difference between the effects of GABAergic drugs in the intact slice network, and when the ionotropic synaptic excitation is blocked.

In addition to the effects of EPSPs in interneurons on the stability of locally generated gamma rhythms, these EPSPs also allow spatially separated sites to oscillate at gamma frequencies with approximately 1 ms mean phase differences. This occurs experimentally

using the tetanus when there are 2 stimulating electrodes in the CA1 region of hippocampal slices, with spacing between the stimulated sites of about 1 mm up to at least 4.5 mm (Traub et al., 1995;Traub et al., 1996a;Whittington et al., 1997). An interneuron at one site will be synaptically excited, almost immediately, by the synchronous firing of nearby excitatory neurons; and, it will be excited, after an axon conduction delay, by the synchronous firing of distant excitatory neurons at the second oscillating site. If the two sites are approximately in phase, and if the excitatory neuron/interneuron connections are strong enough, then the later EPSP should be able to generate a second interneuron spike a few milliseconds after the first interneuron spike that occurs nearly in phase with nearby excitatory neurons. Such a spike pair is a doublet. The existence of doublets was predicted on theoretical grounds, and shown to occur experimentally during 2-site oscillations, but very rarely during 1-site oscillations (Traub et al., 1999b). Experimental manipulations, such as AMPA receptor blockade, that interfere with doublets also interfere with 2-site synchrony.

At a system level recent findings suggest that two gamma current generators reside in the hippocampus. The gamma oscillator in the dentate gyrus requires an extrahippocampal drive, because, following surgical removal of the entorhinal cortex, the power of dentate gamma activity virtually disappears, whereas it increases several-fold in the CA1 region (Bragin et al., 1995). A similar large increase in CA1 gamma power has been described after transient impairment of the entorhinal cortex following afterdischarges (Leung and Buzsaki, 1983). Furthermore, the discharge frequency of layer II, III entorhinal cortical neurons is increased during theta-associated behaviors (Chrobak and Buzsaki, 1998), which may contribute to the selectively increased gamma current power in the dentate gyrus during theta relative to nontheta epochs. In contrast to the dentate oscillator, gamma rhythm generation in the CA3-CA1 regions does not require external inputs. The precise behavioral conditions that specifically enhance the coherence between the gamma oscillators at the input and output stages of the hippocampus remain to be uncovered.

Oscillations in the amygdaloid complex.

Unlike the situation with well-characterized hippocampal oscillations, relatively few studies were performed on rhythmogenesis in the amygdala. Most extensively oscillatory patterns were studied in the basolateral complex of the amygdala. The lateral nucleus of the amygdala (L) and perirhinal cortex generate a highly synchronized slow oscillatory activity despite the fact that the distance between the L and different longitudinal levels of the perirhinal cortex varies widely (Collins et al., 2001). These results suggest that the rhinal cortices can generate

slow oscillations independently of the neocortex and impose this slow rhythm on the amygdala. Importantly, both perirhinal and L oscillations are associated with prominent fluctuations in firing probability, which indicates that these focal oscillations are generated locally and are not volume conducted from the cortex. Moreover, as in the neocortex, the slow amygdala oscillation is associated with cyclical fluctuations in the amplitude of beta and gamma waves. However, whereas the slow oscillation remains synchronized even at distant (up to 10 mm) amygdala and perirhinal sites, the coherence of gamma oscillations decreases abruptly with distance.

BL amygdala neurons exhibit a clear tendency to oscillate at the delta frequency during SWS (Pare and Gaudreau, 1996). Moreover, the phase relationship is tightly coupled to the delta oscillation of the rhinal cortices. Because a previous study revealed that correlation between rhinal and neocortical oscillations tended to be low (Collins et al., 1999), it is likely that amygdala delta oscillations also bear little relationship to those in the neocortex.

Whereas sleep spindles are prevalent in the neocortex, they are absent from the BL amygdala and rhinal cortices. During neocortical spindles, the amygdala exhibits trains of slow delta waves (Forslid et al., 1986;Pare and Gaudreau, 1996). The lack of spindles in the rhinal cortices is consistent with the comparatively meager thalamic projections to these cortical fields (Room and Groenewegen, 1986). Moreover, the dorsal thalamic nuclei that project to the entorhinal cortex, namely the reuniens and anterior thalamic nuclei, do not receive inputs from the reticular thalamic nucleus (Pare et al., 1987), which, as mentioned above, plays a crucial role in the genesis of spindles. Similarly, most of the thalamic nuclei that project to the BL complex (Turner and Herkenham, 1991) do not receive inputs from the reticular thalamic nucleus. Thus, compared with the neocortex, the rhinal cortices and BL amygdala depend largely on cortico–cortical connections for the transfer of thalamically generated spindle oscillations. In this context, the lack of spindle oscillations in these areas suggests that the rhythmic thalamic volleys accompanying spindles are gradually disorganized as they are transmitted through successive cortico–cortical links. Alternatively, it is possible that the neocortical inputs converging in the amygdala and rhinal cortices are insufficiently synchronized for EEG spindles to emerge.

It has been found that during SWS, and under barbiturate anesthesia, the BL amygdala generates synchronized population bursts (Pare et al., 1995a). These synchronized population discharges give rise to brief, large-amplitude potentials (termed ‘sharp potentials’) in the rhinal cortices (Collins et al., 1999) and, after a brief delay, in the dentate gyrus. These sharp

dentate potentials are associated with a marked increase in the amplitude of fast oscillations around 80 Hz in the dentate gyrus and rhinal cortices. These events might correspond to the dentate spikes previously described in rats (Bragin et al., 1995b).

During PS, theta activity is readily observed in the BL amygdala and perirhinal cortex, although in both structures it remains less prominent than the theta oscillation of the entorhinal cortex and hippocampus (Pare and Gaudreau, 1996). For instance, Collins et al., found that as many as 46% of entorhinal neurons displayed a statistically significant modulation in firing rate in this frequency range compared with only 16% in the perirhinal cortex. In the perirhinal cortex at least, the theta oscillation is related to a cyclical modulation in the amplitude of gamma waves, as in the hippocampus. Moreover, perirhinal and amygdala theta is phase locked to entorhinal (Pare and Gaudreau, 1996), and thus to hippocampal, theta. During the waking state, the theta oscillation is prominent in the amygdala only during periods of intense arousal, as produced by the anticipation of a noxious stimulus (Pare and Collins, 2000) or alimentary instrumental conditioning (Aleksanov, 1983). Moreover, it was reported that arousal was associated with an increased coherence of theta activity in the amygdala and frontal cortex. Three non-exclusive factors probably contribute to the appearance of theta oscillations in the BL complex during anticipation of noxious stimuli. First, BL neurons are endowed with intrinsic membrane properties that predispose them to oscillate in this range of frequencies (Pare et al., 1995b) Pape, 98, 98). Second, the BL complex receives synaptic inputs from the rhinal cortices and hippocampal formation where rhythmic neuronal activity in the theta range has been observed (Buzsaki et al., 1983), (Collins et al., 1999). Third, the BL amygdala receives inputs from thalamic nuclei, such as the anterior thalamic nuclei and nucleus reuniens that could transmit the hippocampal theta rhythm to the amygdala.

Several studies have reported that arousal is accompanied by increases in the amplitude of fast focal activities in general, and of ‘amygdala spindles’ in particular. Although they have the typical spindle shape, these events should not be confused with sleep spindles because they occur during a different behavioral state and comprise much faster waves (in the beta/gamma range), as previously described in the adjacent pre-pyriform cortex (Pare et al., 2002). Whether amygdala spindles are volume conducted from the pre-pyriform cortex or reflect a true amygdala rhythm remains unknown.

These findings reviewed above indicate that the amygdala reflects a unique pattern of state dependent oscillations. Like the rest of the brain, focal waves recorded in the amygdala during slow-wave sleep are dominated by waves of high amplitude and low frequencies. By

contrast, faster activities of lower amplitude are predominant during wakefulness and PS. The lack of sleep spindles in the amygdala, the variable temporal relations seen between the slow amygdala and faster neocortical oscillations, and the presence of theta during EEG-activated states, all suggest that the amygdala is functionally closer to the hippocampal formation and rhinal cortices than to the neocortex.

These findings take on a particular significance when considered in the light of data indicating that the amygdala facilitates consolidation of emotionally arousing memories (Cahill and McGaugh, 1998). Although previous work has emphasized the individual contributions of the amygdala and hippocampal system to distinct forms of memory, the functional similarities and reciprocal connections between these structures suggest that they engage in cooperative interactions. Because theta oscillations are present in the amygdala only during emotional arousal, they represent a likely physiological substrate for the facilitated consolidation of emotional memories by the amygdala. Importantly, amygdala theta occurs in conditions that can have a negative or a positive valence (Aleksanov, 1983;Pare and Collins, 2000). It has been proposed that the theta activity of amygdala neurons during emotional arousal promotes memory by facilitating interactions between neocortical storage sites and the declarative memory system of the temporal lobe (Pare et al., 2002). First, it should be noted that glutamatergic projection neurons of the BL complex have extremely low firing rates, even during emotional arousal (Pare and Collins, 2000). Thus, the temporal clustering of neuronal discharges at the theta frequency greatly enhances the depolarization produced by BL activity on target structures. Second, much of the temporal lobe shows theta frequency oscillation during emotional arousal, and amygdala and hippocampal theta are highly correlated. Third, coherent oscillations cause short recurring time windows that facilitate synaptic interactions between phase-locked oscillators. And fourth, coincident pre- and post-synaptic activity is crucial to synaptic plasticity (Bliss and Collingridge, 1993). Amygdala oscillations at the theta frequency exert a depolarizing action that promotes synaptic plasticity in co-active structures of the temporal lobe and neocortex. Consistent with this idea, the conduction times of BL axons to the rhinal cortices adjust to compensate for variations in distance between the BL complex and distinct rostrocaudal rhinal sites (Pelletier and Pare, 2002). As a result, BL neurons can generate simultaneous rhythmic depolarizations at spatially distributed rhinal sites and facilitate Hebbian associations between coincident activity patterns. In rats, intra-amygdala lidocaine injections up to six hours post-learning interfere with the facilitating effects of emotion on recall days later (Parent et al., 1988).

Memory processing during sleep

David Hartley (1791) first suggested that dreaming might alter the strength of associative memories. On the basis of patterns of brain electrical activity measured in the EEG, eye movements, and muscle tone, sleep can be broadly divided into PS and slow-wave sleep (SWS), with the human PS-SWS cycle typically having a 90-min period. Recent evidence strengthens the hypothesis that sleep plays a role in learning and memory processing at several levels, including the PS-dependent developmental wiring of binocular cells in visual cortex (Frank et al., 2001), procedural learning of a visual discrimination task (Karni et al., 1994; Stickgold et al., 2000), and the development of problem-solving skills.

Evidence from behavioral studies

Smith proposed the existence of "PS windows" (Smith, 1985), periods of time after procedural training when rats show increased amounts of PS and during which PS deprivation leads to diminished retention. For many of the early PS deprivation studies, the apparent decrease in recall after deprivation may have been the consequence of deprivation-induced stress (Horne, 2000). But other studies have demonstrated performance decrements 20 hours after PS deprivation, but not 8 to 16 hours after deprivation (Smith and Butler, 1982).

However, substantial memory consolidation occurs during normal waking, and many memory tasks are unaffected by subsequent PS deprivation (Horne, 2000). Furthermore, memory consolidation is most likely not the only function of PS sleep, not explaining, for example, the decrease in PS during the first year of life.

In humans, post-training PS deprivation impairs retention of procedural learning. Declarative memory tasks in general have not shown any sleep dependence, although some studies have suggested that deep SWS early in the night may aid in their consolidation (Plihal and Born, 1999). PS may also enhance the processing of emotional memories. There is enhanced recall for emotionally salient memories after periods of sleep rich in PS (Wagner et al., 2001), and several older studies similarly support a role for PS in processing emotional memories. In addition, shortenings of PS latencies and increases in PS densities have been reported in major depression and posttraumatic stress disorder (Kupfer and Foster, 1972).

Some of the strongest evidence for human learning being sleep dependent comes from a visual texture discrimination task (Stickgold et al., 2000). On this task, improvement is not seen until after post-training sleep, and sleep deprivation in the night after training eliminates all benefits of training, even when measured after two full nights of recovery sleep. Karni et

al. found no improvement after a night with selective PS deprivation, but did see improvement after selective SWS deprivation (Karni et al., 1994). Other studies suggest that both SWS and PS are required, a result in keeping with the two-step model proposed by Giuditta et al. (1995) for the consolidation of learning in rats (Giuditta et al., 1995).

More generally, studies suggest that PS might modify neocortical networks in general, rather than simply those involved in procedural learning, with PS effects reported for learning of complex logic games, for foreign language acquisition, and after intensive studying (De Koninck et al., 1989).

Physiological correlates of trace consolidation during sleep: synchrony and reactivation.
Steriade (Steriade, 2000) has hypothesized that high rates of ~10-Hz firing of neocortical neurons during the long-lasting depolarization phase of SWS oscillations might induce long-term potentiation (LTP) at cortical synapses (Huerta et al., 1995; Otto, 1991), which could serve to reorganize or respecify connections within neural networks and functionally connect distant cortical regions. Similarly, sharp wave potentials seen in SWS might facilitate information flow from the hippocampus to the neocortex (Buzsaki, 1986).

In contrast, theta rhythms in PS may support information transfer from neocortex to hippocampus, where theta waves enhance LTP, considered critical for hippocampal memory formation (Otto et al., 1991). Neural network simulations (Hinton et al., 1995) have suggested that such an alternating "hippocampo-neocortical dialog" could enhance the encoding of hippocampus - dependent memories in the neocortex.

Phasic ponto-geniculo-occipital (PGO) waves, which activate visual and motor cortices as well as the amygdala and hippocampus, are seen during the transition from SWS to PS and throughout PS. These waves may play an important role in memory consolidation in the rat (Datta, 2000) and have been proposed to reactivate memory traces during PS dreaming (Hobson and McCarley, 1977).

Stronger evidence of the possible role of these processes in learning and memory comes from analyses of neuronal activity in the rat hippocampus. During sleep, replay of recent waking patterns of neuronal activity is seen within the CA1 layer of the hippocampus. This reactivation is seen during SWS for about half an hour after learning (Pavlides and Winson, 1989; Wilson and McNaughton, 1994) and in PS after 24 hours (Louie and Wilson, 2001). Although this replay in SWS may simply reflect continued activity unrelated to sleep, the presence of replay in PS only after 24 hours demonstrates that these patterns of neuronal activation are specifically reactivated during PS.

At the level of individual hippocampal cells, the firing pattern during sleep depends on previous waking experience. The firing rates in CA1 place cells exposed to their place field during a previous waking period was increased during subsequent sleep, as compared with the firing rates in unexposed cells. The hippocampal place cells that show highly correlated firing during a food-seeking spatial task maintained high firing correlation during the post-training sleep, especially during SWS. The temporal aspect of waking discharges seems to be maintained during postexposure sleep. The order in which pairs of place cells fire during post-training sleep (mainly SWS) reflects, within a time window of 200 ms, the order of firing during the previous waking session (Skaggs and McNaughton, 1996). Sequences involving more than a pair of cells, within a similar time window, were replayed during SWS recorded after a wheel-running task (Nadasdy et al., 1999). In the most recent design (Lee and Wilson, 2002) rats repeatedly ran through a sequence of spatial receptive fields of hippocampal CA1 place cells in a fixed temporal order. A novel combinatorial decoding method reveals that these neurons repeatedly fired in precisely this order in long sequences involving four or more cells during SWS immediately following, but not preceding, the experience. The SWS sequences occurred intermittently in brief (100 ms) bursts, each compressing the behavioral sequence in time by approximately 20-fold. This rapid encoding of sequential experience is consistent with evidence that the hippocampus is crucial for spatial learning and the formation of long-term memories of events in time in humans.

The time course of these reactivations, over several nights, has not yet been thoroughly investigated. However, during PS sleep, there is evidence that the novel representations are strengthened whereas the older ones are weakened (Poe et al., 2000). Hippocampal firing for novel experience during postexposure sleep occurs in phase with the theta rhythm, a condition known to induce long-term potentiation. In contrast, cells coding for familiar environments tend to fire out of phase with the theta rhythm, a situation that may lead to depotentiation.

At the network level in the rat, the activity of hippocampal cells is reflected in two types of macroscopic patterns (Buzsaki, 1996). On the one hand, gamma oscillations (40 to 100 Hz) and theta rhythm (4 to 7 Hz) are recorded in the superficial layers of the entorhinal cortex, the gyrus dentatus, and the CA3 and CA1 fields of the hippocampus during exploratory activity and PS sleep. Awake immobility and SWS are characterized by sharp waves, crowned by high-frequency ripples (140 to 200 Hz). Ripples and sharp waves are initiated in CA3 and recorded in CA1 and the deep layers of the entorhinal cortex. It is believed that, during gamma and theta oscillations, neocortical inputs transmit information

about the external world to the hippocampal structures through the entorhinal cortex. In contrast, during ripples and sharp waves, hippocampal information is thought to be played back to the entorhinal cortex (Chrobak et al., 2000) and through it, to neocortical areas (Siapas and Wilson, 1998). This two-stage operation could consolidate the memory trace, as has been suggested by computational simulations (Lorincz and Buzsaki, 2000).

Neuronal reactivations do not only occur in the hippocampal formation. Cortical neuronal activities during sleep can also be modified following training on a hippocampus-independent task. In the cat, fast (30 to 40 Hz) neocortical oscillations can be enhanced by instrumental conditioning during wakefulness, and a selective increase in these oscillations is observed during subsequent SWS and PS. More generally, SWS oscillations are associated with rhythmic spike bursts in thalamic and cortical neurones, which lead to persistent excitability changes (Steriade, 2000). These short-term plasticity processes could be used to consolidate memory traces acquired during wakefulness. It has been proposed that in the early stages of SWS, spindle activity would be related to massive Ca^{2+} entry into spindling cells (Sejnowski and Destexhe, 2000). This would open the gate to subsequent long-term modifications in cortical networks. During SWS, large populations of thalamic and cortical neurons fire synchronously in a slow oscillation (<1 Hz), alternating phases of hyperpolarization and of depolarization (Steriade et al., 1993). During the depolarized phase, the bursting neurons generate brief periods of fast oscillations that would iteratively recall and store information embodied in the assemblies primed during spindling. Alternatively, the neurons recruited by the slow oscillations would preferentially be those with the largest number of synapses recently potentiated during wakefulness (Timofeev et al., 2000).

Postexposure brain reactivations during sleep seem to generalize across species. In order to learn their own song, young zebra finches have to establish the correspondence between their vocal production and the resulting auditory feedback. This cannot be done during wakefulness because the bird song arises from a tightly time-coded sequence of activity in the song area, whereas the auditory feedback, necessary to correct the vocal production, is inevitably delayed. During sleep, however, stored sensory feedback could easily be compared to the brain activities underlying the motor output. This seems to be the case, because spontaneous activity during sleep in a premotor area of the song system matches the activity recorded while the bird is singing during wakefulness (Dave and Margoliash, 2000).

Preliminary results suggest that experience-dependent reactivations of neuronal populations also occur in humans during sleep. Using positron emission tomography, it was shown that during PS, some brain areas were more active in human subjects previously trained

on a serial reaction-time task than in naïve subjects (Datta, 2000). These results suggest that memory traces were reprocessed during PS, for two reasons. First, the activated areas were among those previously engaged in the execution of the task. These cerebral regions were actually reactivated during posttraining PS. Second, the subjects' performance on the task was improved in a postsleep retest session, suggesting that the influence of these reactivations, if any, was beneficial to memory traces.

Sleep and neuromodulators

The PS-SWS cycle also displays marked shifts in levels of neuromodulators in the brain. Systems that control the PS-SWS cycle include the noradrenergic locus coeruleus, the histaminergic TM in the posterior hypothalamus, the serotonergic (5-HT) dorsal Raphe nucleus, and the cholinergic nuclei of the dorsolateral pons (Hobson et al., 1975). Whereas SWS is characterized by decreases in all three neuromodulators compared with waking, acetylcholine levels in PS are equal to or higher than during waking, and levels of noradrenaline and 5-HT drop to near zero (Kametani and Kawamura, 1990).

Other evidence from electrophysiological studies, mainly in the cat, has shown that histamine neuron firing varies across the sleep/waking cycle (Monti, 1993;Sakai et al., 1990). A circadian rhythm of histamine release has been demonstrated (Friedman and Walker, 1968). Icv injection of histamine causes phase-shifts in locomotor activity, the direction and magnitude of which are dependent on the phase of the circadian cycle when histamine is applied (Itowi et al., 1991). A similar action of histamine can be observed on the firing rate of suprachiasmatic nucleus neurons maintained in vitro (Cote and Harrington, 1993). Injection of α-FMH reduces light-induced circadian phase-shifts and disrupts free-running circadian rhythms of locomotor and drinking activities (Eaton et al., 1995). The phaseshifting effects of histamine do not appear to be mediated by classical histamine receptors but rather by an action on the NMDA receptor (Meyer et al., 1998). Bilateral transection of the posterior hypothalamus (Nauta, 1946)or injections of muscimol into this region (Lin et al., 1989) leads to a state of somnolence or hypersomnia.

Injection of histamine or H_1 agonists icv or into various brain sites causes a desynchronisation of the EEG, a dose-dependent augmentation of wakefulness and a diminution of deep SWS (Lin et al., 1988;Lin et al., 1994;Lin et al., 1996;Monnier and Hatt, 1969;Monti, 1993). The H_1 antagonist mepyramine blocked these effects. Injection of α-FMH intraperitoneally in cats or in rats, led to a depletion of neuronal histamine and concurrently a reduction of the time spent awake (Lin et al., 1988;Monti et al., 1988). Upregulation of

neuronal histamine levels by oral administration of the H_3 receptor antagonist, thioperamide, strongly enhanced wakefulness in the cat whilst the H_3 receptor agonist, *R*- α -methylhistamine enhanced deep SWS (Lin et al., 1990;Monti et al., 1991).

Regional brain activation during sleep and biochemical correlates.

Positron emission tomography (PET) studies have demonstrated unique patterns of regional brain activation across wake-sleep states (Hobson et al., 1998). Almost all brain regions become less active in SWS compared with waking. But although many regions remain relatively inactive in PS, thedorsolateral prefrontal cortex, which is involved in decision making and memory, becomes further inactivated in this state (Braun et al., 1997), while at the same time, several midline limbic structures, including both the anterior cingulate and medial orbitofrontal cortices and the amygdala, become reactivated to levels at or above waking levels. Both the consolidation of learning and the formation of new associations can be mediated by pontine reticular formation activation during sleep. In addition, a correlation between an increased density PGO waves during posttraining PS and subsequent improved task performance has been reported, suggesting that PGO waves facilitate learning in the rat (Datta, 2000).

Both protein synthesis and phosphokinase A (PKA) are required for hippocampally mediated learning, and their inhibition during PS windows produces effects similar to those produced by PS deprivation (Graves et al., 2001;Gutwein et al., 1980). In addition, exposure to an enriched learning environment induces the immediate early gene zif-268 during subsequent REM. Zif-268 expression normally coincides with synaptic modification and, during REM, presumably reflects the consolidation of learning. These and related findings led to the suggestion that the PKA signaling pathway mediates sleep-dependent learning and memory processes.

Dreams and memory.

Dreams presumably reflect the activation and recombination of memories, and both these memories and associations to them may be altered in some ways in the process. Dream elements often appear to arise from memories of waking events. But the fact that an element can be traced to a specific waking event does not necessarily mean that an episodic memory was used for dream construction. Episodic memory is defined as a memory of an event, recalled as an integrated whole, with the actual waking event (or "episode") replayed in one's mind. Episodic memories are thought to consist of multiple hippocampus-linked memory

traces located within neocortical regions and dependent on the hippocampus for their integrated recall. When subjects identify waking events as the sources of dream elements, the dreams themselves rarely replay episodic memories. This suggests that the brain sources for dream elements are not hippocampally mediated episodic memories, but cortical traces of discrete components of the episodic memories, which then presumably are combined with associated semantic memories. With dorsolateral prefrontal cortex deactivated in both PS and SWS (Braun et al., 1997; Maquet et al., 1996; Maquet et al., 1997) and the hippocampal formation producing only minimal cortical output in PS, actual episodic memories may be inaccessible and hence irrelevant to the dream construction process.

In PS, the central nucleus of the amygdala plays a crucial role in the activation of medial prefrontal cortical structures associated with the highest order regulation of emotions. This adds to the deactivation of dorsolateral prefrontal cortex, normally associated with higher cognitive functions, in PS (Nofzinger et al., 1998). Thus, the brain appears to be biased toward emotional processing in this state. There is evidence for both emotion-enhanced PS and PS-facilitated retention of emotionally salient memories (Goldman-Rakic, 1996). Moreover, both depression (Lauer et al., 1987) and the presleep viewing of unpleasant films correlate with reports of negative emotion in early night PS dreaming. How specific aspects of emotional events affect dream construction remains obscure, as it has been difficult to reliably induce the incorporation of waking events or emotions into subsequent dreams.

During PS, limbic forebrain structures are activated while both dorsolateral prefrontal cortex and the locus coeruleus become less active. This presumably inhibits the ability of dorsolateral prefrontal cortex to allocate attentional resources. At the same time, the inhibition of hippocampal outflow would prevent the reactivation of episodic memories (Buzsaki, 1996). Dreams would thus be constructed largely from those primarily weak neocortical associations available during PS (Stickgold et al., 1999).

Sleep-deprivation: waking-promoting substances.

There are a number of uncertainties about the molecular bases of other efficacious wake-promoting compounds - amphetamines and modafinil. Amphetamines block plasma membrane transporters for DA, NE, and 5-HT and inhibit the vesicular monoamine transporter (VMAT2), releasing monoamines from the synaptic vesicles into which VMAT2 pumps them (Seiden et al., 1993). Noradrenergic mechanisms have been proposed to explain the wake-promoting effects of amphetamine-like stimulants. However, dopamine-specific reuptake blockers can promote wakefulness in normal and sleep-disordered narcoleptic

animals better than NE transporter-selective blockers (Nishino and Mignot, 1997). Furthermore, the wake-promoting effect of amphetamine is maintained after severe reduction of brain norepinephrine produced by lesions of the noradrenergic cells of the locus coeruleus in cats (Jones et al., 1977).

The mode of action of modafinil, a new wake-promoting compound (chemically a benzydrylsulfinyacetamid) used in the treatment of sleepiness associated with narcolepsy, is even more uncertain. Studies have suggested that modafinil increases wakefulness by activating α-1 noradrenergic transmission (Duteil et al., 1990) or hypothalamic cells that contain orexins (Chemelli et al., 1999), or that it may work by modulating GABAergic tone (Ferraro et al., 1996). Central pharmacological blockade or genetic ablation of alpha-1B-adrenoreceptors markedly attenuates the behavioral modafinil-induced activation (Stone et al., 2002). Modafinil exhibits a weak affinity for the dopamine transporter (DAT) (Mignot et al., 1994). To identify the molecular basis for the wake-promoting effects of amphetamines and modafinil, the responses to these compounds were studied in DAT knock-out mice. It was found that the wake-promoting effects of classical stimulants and modafinil are abolished in DAT knock-out mice (Wisor et al., 2001). On the other hand, modafinil, in contrast to amphetamine, was unable to modify in vivo the firing patterns of dopaminergic neurons in substantia nigra and ventral tegmental area and noradrenergic neurons in locus coeruleus (Akaoka et al., 1991). Injections of haloperidol blocked significantly the amphetamine- but not dopamine-induced arousal (Lin et al., 1992).

Histaminergic system

Anatomy.

Histamine neurons are confined to a small region of the posterior hypothalamus — the tuberomamillary nucleus (TM). These neurons have widespread, diffuse projection patterns (Panula et al., 1984; Watanabe et al., 1984). The name, TM, derives from the anatomical term tuber cinerum, denoting an ashen swelling located rostral to the mamillary bodies and caudal to the optic chiasm, forming the floor of the third ventricle in the hypothalamus (Kruger et al., 1995).

The TM in rats has been subdivided by Ericson et al. (Ericson et al., 1987) into three subgroups: (1) the medial tuberomamillary subgroup (TMM), which consists of around 600 neurons located on either side of the mamillary recess; (2) the ventral tuberomamillary subgroup (TMV), which contains approximately 1500 neurons around the mamillary bodies;

and (3) the diffuse part of the TM (TMdiff or E5), which is made up of about 100 HD-immunoreactive perikarya scattered within or between various hypothalamic nuclei. Inagaki et al. (Inagaki et al., 1988) further subdivided the TMM into a dorsal (TMMd or E4) and ventral (TMMv or E3) part and the TMV into a rostral (TMVr or E2) and caudal (TMVc or E1) part to give five nuclei (E1–E5). At the present time there is little evidence to suggest that these five nuclei play different roles and thus, they can be considered as a single functional group (Wada et al., 1991). Histaminergic neurons are mainly large cells, approximately 25–30 μm in diameter, which contain, in addition to histamine, a number of other neuroactive substances (or at least their synthesising enzymes), including GABA, adenosine, met-enkephalin, galanin, and substance P (Ericson et al., 1991;Kohler et al., 1986). They lie on the ventral surface of the brain and send out several primary dendrites, which subdivide into long, secondary dendrites (Wouterlood et al., 1986). The dendrites from a single neuron often overlap with dendrites from other histamine neurons. Interestingly, some of these dendrites may project into the mamillary recess and come into contact with the CSF.

Substances present in the CSF, such as cytokines, may, thus, influence the firing of histaminergic neurons. Unusually, the axons of the histaminergic neurons arise from primary dendrites and not from the soma (Ericson et al., 1987). It is well known that other aminergic neurons, in particular dopaminergic neurons located in the substantia nigra can release transmitter from their dendrites or somata and activate local autoreceptors(Leviel et al., 1979). Although it is known that histamine neurons possess somatic H_3 autoreceptors, the source of the histamine to activate these receptors is not clear. The presence of vesicles in the dendrites of histamine neurons is controversial (Schwartz et al., 1991) - alternatively, histamine may be released from local axon collaterals (Eriksson et al., 1998).

The histamine neurons in the TM send out axons which innervate practically the entire brain, and parts of the spinal cord. Two ascending pathways and one descending pathway have been identified (Panula et al., 1989). The ventral ascending pathway remains on the ventral surface of the brain, providing innervation to the hypothalamus, diagonal band, septum and olfactory bulb whilst the dorsal pathway leaves the TM dorsally, following the lateral side of the third ventricle to innervate the thalamus, hippocampus, amygdala and rostral forebrain structures. The descending pathway in rats is associated with the medial longitudinal fasciculus and provides input to the brain stem and spinal cord.

As mentioned above, the five histaminergic cell groups can be considered as one functional group (Wada et al., 1991). One main reason for this classification is the similarity of their projection patterns. Single neurons from each of these groups send widely divergent

projections to many different areas of the brain with considerable overlap. Single neurons may even send out both descending and ascending axon collaterals. Anatomical studies have not identified any precise topographical organisation of the histaminergic projection field, e.g. a strong projection to motor areas rather than sensory areas, however, there are marked differences in the densities of fibres in different brain regions (Inagaki et al., 1988;Panula et al., 1989). The highest density of histaminergic fibres is found in the hypothalamus, with all nuclei receiving a strong or moderate innervation. Other structures innervated by the ventral ascending pathway also receive a powerful input including the diagonal band, septum and olfactory tubercle. Structures innervated by the dorsal ascending pathway tend to have a somewhat lower density of fibres, with the amygdala being the most prominent. The cerebral cortex has a moderate density of fibres in all areas and layers with a slightly increased level in the outer layers whilst the innervation of the thalamus is concentrated upon the periventricular nuclei. The hippocampal formation is most strongly innervated in the subiculum and dentate gyrus, with a low density of fibres present in CA3 and CA1; a similar low to moderate level innervation is present in the striatum and nucleus accumbens. Projections to the midbrain, brain stem, cerebellum and spinal cord tend to be of lower density than the ascending projections, with some notable exceptions. All of the other aminergic cell groups receive at least a moderate density of fibres, with the substantia nigra and ventral tegmental area being strongly innervated. In addition, the inferior and superior colliculi, periaqueductal gray, nucleus of the trigeminal nerve and nucleus tractus solitarius receive prominent projections.

Histaminergic axons do not in general form synaptic specialisations, instead histamine is released from varicosities - swellings containing synaptic vesicles - located periodically along the axon (Takagi et al., 1986). Thus, histamine release sites and histamine receptors are not directly apposed to one another. Rather, histamine has been proposed to act like a local hormone, acting on neurons, glial cells and blood vessels in a concerted manner (Wada et al., 1991).

Histamine receptors: H_1 receptors.

Central histamine H_1 receptors are the main site responsible for the sedative effects of antihistamines. The gene for the human histamine H1 receptor is located on chromosome 3 (Le Coniat et al., 1994) and encodes a member of the large, 7-transmembrane-spanning, G-protein-associated receptor family. Intracellularly, the receptor is associated with the $G_{q/11}$ GTP-hydrolysing protein which, when activated by histamine binding to the receptor, stimulates the activity of phospholipase C (Leurs et al., 1994). Phospholipase C in turn

hydrolyses phosphatidyl-4, 5-bisphosphate to form two second messengers, DAG and IP3. DAG potentiates the activity of PKC, whilst IP3 binds to the IP3 receptor located on the endoplasmic reticulum, allowing the release of stored calcium into the cytoplasm. In addition, histamine H_1 receptor activation leads to the formation of arachidonic acid, most likely through the action of phospholipase A2 and to the formation of cGMP (Richelson, 1978). Finally, histamine H_1 receptor stimulation can potentiate the formation of cAMP by substances acting at receptors coupled to the Gs (Baudry et al., 1975), e.g. histamine acting at the H_2 receptor or adenosine acting at the A_2 receptor.

H_1 receptors, labelled by [^{3}H]mepyramine or [^{125}I]Iodobolpyramine, have been shown to have a widespread distribution in the central nervous system (Chang et al., 1979;Martinez Mir et al., 1990). Particularly high levels of H_1 receptors are present in areas involved in arousal, i.e. thalamus, cortex, cholinergic cell groups in the mesopontine tegmentum and in the basal forebrain as well as the locus coeruleus and raphe nuclei. In addition, high densities of H_1 receptors are present in the limbic system, including many nuclei of the hypothalamus, most septal nuclei, medial amygdala and several hippocampal areas.

H_2 receptors.

A second class of histamine receptors was identified by Black and colleagues based on the different pharmacological profile of the histamine receptor responsible for stimulating gastric acid secretion (Hill et al., 1997). The gene for the histamine H_2 receptor is located on human chromosome 5 and encodes a 7-transmembrane domain, G-protein coupled receptor (Traiffort et al., 1995). The Gs G-protein is associated with the receptor, activation of which leads to stimulation of adenylyl cylase and enhanced production of the second messenger molecule cAMP. One prominent target of cAMP is the cAMPdependent PKA which can phosphorylate target proteins in the cytosol, in the cell membrane or translocate to the nucleus and activate the transcription factor CREB (Sheng et al., 1991).

Like the histamine H_1 receptor, the H_2 receptor has a widespread expression in the brain and spinal cord, as demonstrated using labelling with [^{125}I]iodoaminopotentidine (Traiffort et al., 1995). Particularly high densities are found in the basal ganglia and in parts of the limbic system such as the hippocampal formation and amygdala. In contrast to H_1 receptors, H_2 receptors are present in low densities in septal areas, hypothalamic and thalamic nuclei. H_1 and H_2 receptors are colocalised in several areas of the.brain including pyramidal and granule cells in the hippocampal formation and in the other aminergic cell groups (locus coeruleus, raphe nuclei, substantia nigra, ventral tegmental area) where the receptors can act

synergistically, e.g. in the stimulation of cAMP production. In the cerebral cortex, H_2 receptors are denser in the superficial layers (I–III) and are most likely located on the dendrites of pyramidal cells. A similar expression of H_2 receptors by principal cells in the hippocampus proper and dentate gyrus exists. In the cerebellar cortex H_2 receptors are expressed by both Purkinje and granule cells.

*H*3 *receptors.*

The histamine H_3 receptor was described in 1983 by Arrang and colleagues as an autoreceptor regulating the release and synthesis of histamine (Arrang et al., 1983). It has very recently been cloned (Lovenberg et al., 1999), and as expected (Hill et al., 1997) it is a G-protein coupled receptor which is pertussis-toxin sensitive, similar to many other presynaptic inhibitory receptors. Interestingly, the H_3 receptor gene shows a low overall homology to all other biogenic amine receptors. In various cell lines, H_3 receptor activation led to an inhibition of forskolin-stimulated cAMP formation. H_3 receptors in rat brain have been labelled using [^{3}H](R)α-methylhistamine (Pollard et al., 1993). In the cerebral cortex, H_3 receptors are present in all areas and layers, with a higher density rostrally and in the deep layers (IV–VI). High densities of H_3 receptors are also found in nucleus accumbens, striatum, olfactory tubercles and the substantia nigra whereas only moderate levels are found in the hypothalamus. H_3 receptors are present, however, on the cell bodies of the histamine neurons in the TM.

Hisminergic modulation of NMDA-receptors.

It has been known for some time that histamine can modulate currents gated by the glutamate NMDA receptor (Haas, 1984). However, only recently has it been demonstrated that this can result from a direct action on the NMDA channel complex as well as indirectly through classical histamine receptors. Histamine could dramatically enhance NMDA receptor-mediated currents in acutely-isolated or cultured hippocampal pyramidal cells (Bekkers and Stevens, 1993; Vorobjev et al., 1993). This action of histamine could not be blocked by application of antagonists of the histamine H_1, H_2 or H_3 receptors, was unaffected by the external calcium concentration and was not blocked by saturating glycine concentrations. Further experiments showed that the enhancement by histamine was occluded by the polyamine spermine, which has certain similarities in structure to histamine. It was concluded that histamine acts on the polyamine site of the NMDA receptor. At much higher concentrations, histamine actually inhibits NMDA currents.

Electrophysiological effects of histamine in the hippocampus.

Although the hippocampal formation receives only a weak to moderate histamine innervation (Panula et al., 1989), many prominent effects of histamine have been demonstrated in vitro and in vivo. In the rat, the only one of the main excitatory synaptic pathways which is affected by histamine is the perforant path input to the dentate gyrus (Brown, 1996;Brown and Reymann, 1996;Greene and Haas, 1990). Here, histamine depresses synaptic transmission by around 30% via presynaptic H_3 receptors located on the perforant path terminals. This effect can also be observed in vivo following icv administration of a H_3 receptor agonist (Manahan-Vaughan et al., 1998) or following stimulation of the TM during exploratory behaviour (Weiler et al., 1998). In mouse hippocampal slices, however, this effect is lacking. A facilitation of the mossy fibre input to the CA3 region has been described (Segal, 1981;Yanovsky and Haas, 1998) which is likely to be due to postsynaptic excitability increases rather than a direct action on the synapses themselves.

Histamine has strong effects on excitability in the hippocampus. All the principal cells are strongly excited by histamine acting on histamine H_2 receptors (Greene and Haas, 1990;Haas and Greene, 1986;Haas and Konnerth, 1983). Extracellularly, in vitro, one can observe an increase in the size of the population spike which reflects the firing of many cells or increases in the frequency of spontaneously occurring bursts (Brown et al., 1995;Haas and Greene, 1986;Yanovsky and Haas, 1998). These effects can be very long-lasting. In freely moving animals, the population spike amplitude is modulated in a complex manner by H_2 receptors. Intracellularly, histamine causes depolarisation by enhancing I_h current (Pedarzani and Storm, 1995) and blocks the calcium-sensitive potassium channel responsible for the slow afterhyperpolarisation and accommodation of firing (Haas and Konnerth, 1983). These effects on excitability are reproduced in co-cultures of hippocampus and TM (Diewald et al., 1997). Histamine has dramatic effects on interneuron excitability, enhancing the spontaneous firing of cells in the alveus/oriens region (Yanovsky and Haas, 1998) and leading to a large increase in spontaneous IPSPs in pyramidal cells in CA1 and granule cells in the dentate gyrus (Greene and Haas, 1990;Haas and Greene, 1986). Again these effects seem to be mediated via histamine H_2 receptors. Histamine affects the hippocampal formation indirectly through its effects on the medial septum, which provides the cholinergic input to the hippocampus.

Histamine strongly depolarizes cholinergic septal neurons (Gorelova and Reiner, 1997), mainly through histamine H_1 receptors, which should lead to an increased acetylcholine release in the hippocampus.

Neurophysiological actions of histamine: reinforcement and learning.

Many antagonists of histamine H_1 receptors can act as reinforcers — either when applied alone or in combination with other reinforcers such as opiates, cocaine or amphetamine (Katz and Goldberg, 1986;McKearney, 1982a;Privou et al., 1998;White and Rumbold, 1988). These reinforcing effects are likely to reflect a combination of the antihistamine, antimuscarinic and dopamine-uptake blocking effects of these compounds.

Several lines of evidence support a role for the central histamine system. In squirrel monkeys, the potency of three different H_1 receptor antagonists on reinforcement was found to correlate better with their antihistamine action than with their antimuscarinic or dopamine-uptake blocking efficacy (McKearney, 1982b).

Injection of histamine or histidine but not histamine metabolites into the lateral hypothalamus specifically suppressed self-stimulation on the side ipsilateral to the injection (Cohn et al., 1973). The histamine effect was blocked by H_1 receptor antagonists. Unilateral electrolytic or ibotenic-acid lesions of the TM specifically suppressed lateral hypothalamic self-stimulation on the side ipsilateral to the injection (Wagner et al., 1993). Tasaka et al. (Tasaka et al., 1985) found that icv administration of histamine or H_1 receptor agonists inhibited a conditioned active avoidance response in rats. H_1 receptor antagonists but not H_2 receptor antagonists blocked the effect of histamine.

The effects of manipulation of the histamine system have been tested in other learning paradigms. In a so-called social memory test icv histamine, histidine or thioperamide decreased investigation time of a juvenile rat by an adult rat, possibly reflecting improved memory, whereas α-FMH and the H_3 receptor agonist immepip had the converse effect (Prast et al., 1996). Histidine was also found to ameliorate learning deficits induced by scopolamine in the elevated plus-maze test, an action blocked by α-FMH, the H_1 receptor antagonist pyrilamine but not the H_2 receptor antagonist zolantidine (Miyazaki et al., 1995).

The neuronal histamine system exerts a negative influence on learning and memory formation. Bilateral electrolytic or ibotenic acid lesions of the TM region improved performance in several different paradigms in adult and aged rats: habituation learning, inhibitory avoidance, discrimination learning and the Morris water maze (Frisch et al., 1998;Huston et al., 1997;Klapdor et al., 1994). Immunohistochemical studies revealed that these lesions led to a marked decline of neurons staining for histamine in the rostral part of the TM nucleus. One other study found that bilateral ibotenic acid lesions in the posterior hypothalamus did not affect performance in a passive avoidance task but in this study the effect of the lesion on the histamine neurons was not reported (Alvarez et al., 1994).

Furthermore, the Huston group has reported that the H_1 receptor antagonist, chlorpheniramine facilitates learning in aged rats when injected immediately after but not 5 h following an inhibitory avoidance task (Frisch et al., 1997). Recently, several different brain-penetrating H_3 receptor agonists and antagonists have been tested in learning paradigms. In general, the antagonists had a facilitatory action and the agonists were inhibitory (Blandina et al., 1996;Flood et al., 1998;Meguro et al., 1995). The facilitatory effects of the antagonists could reflect an enhanced release of histamine or of other ransmitters, such as acetylcholine.

Several brain regions are likely to be involved in the memory modulating actions of histamine. Many of the paradigms mentioned above are partly or predominantly dependent on the hippocampal formation and injection of histamine directly into the ventral hippocampus inhibits performance in an active avoidance task by acting on H_1 receptors (Alvarez and Banzan, 1995). Although in vitro studies of principal neurons in the hippocampus tend to suggest a memory-facilitating role for histamine (increased excitability, facilitation of NMDA receptors and LTP (Haas et al., 1995)), these actions of histamine could be overridden by actions on interneurons or extrahippocampal inputs, such as the septum.

Agonists of H_2 or H_3 receptors injected into the septum of mice improved retention in a T-maze avoidance task, whereas antagonists of these receptors had the opposite effect (Flood et al., 1998), implicating this region in histamine modulation of memory formation. Clearly much remains to be done to elucidate the role of the neuronal histamine system in reinforcement, learning and memory. More sophisticated behavioural paradigms, which enable the exclusion of effects on arousal, anxiety, locomotor activity or perception as being responsible for performance in the learning tasks are essential. The precise timing of histamine release in particular brain structures and the nature of the task may determine whether histamine has a facilitatory or inhibitory effect.

HYPOTHESES

I hypothesize that:

1. The probability of occurrence and structure of a ripple is determined by the event timing in the sleep/waking cycle.

I used pharmacological (amphetamine and the atypical waking promoting drug modafinil) as well as natural sleep deprivation to study the impact of the different types of waking on the occurrence and structure of ripples during SWS. Furthermore, temporal dynamics of ripple oscillations were investigated during SWS and in relation to PS episodes.

2. Modulation of $GABA_A$-receptor mediated IPSPs alters the structure and occurrence of ripple oscillations.

To address this issue I studied actions of systemically administered ligands of the benzodiazepine site at the $GABA_A$ receptor on the occurrence and structure of ripple oscillations with reference to the drug effect on the dominant hippocampal rhythmic state.

3. Histamine exerts divergent actions upon ripple oscillations via different histamine receptor subtypes.

I investigated effects of systemically applied histamine H_1, H_2 and H_3 receptor antagonists on ripple oscillations in the hippocampus.

4. High-frequency (>100 Hz) field oscillations are present in the amygdaloid complex independently from hippocampal ripple oscillations.

Parallel field and single-unit recordings from the basolateral nucleus of the amygdala (and the related endopiriform nucleus) and the temporal or septal poles of CA1 were performed in freely behaving rats. Local field potentials and neuronal activity were cross-correlated between these regions and analyzed in relation to the vigilance state.

METHODS

Animals.

Sixty one male Wistar rats (280-450 g) were used in the study. They were housed at 22 ± 2°C with a 12 h light/dark period and supplied with food and water ad libitum. All experiments were conducted in compliance with German law and with the approval of the Bezirksregierung Duesseldorf. All efforts were made to minimize the pain and discomfort of the experimental animals.

Surgery.

The rats were anesthetized with a mixture of ketamine (75 mg/kg, Ketavet, Upjohn GmbH, Heppenheim, Germany), xylazinhydrochlorid (4.4 mg/kg, Rompun, Bayer AG, Leverkusen, Germany) and acepromazinemaleat (1 mg/kg, Vetranquil, Sanofi-Ceva GmbH, Duesseldorf, Germany) intraperitoneal injection and were operated in a stereotaxic apparatus (Kopf Instruments, USA). Pain reflexes were regularly checked and, if necessary, additional anesthetic was given.

For recording of hippocampal high-frequency oscillations four adjustable or stationary electrodes were implanted in the left CA1 area (AP: -3.8, L: 1.6, V: 2.7 or 2.7 – 3.3 respectively), consisting of 50 µm tungsten-steel wires (California Fine Wire Company, Grover Beach, USA) with a distance of 0.5 mm. Electrodes differed in length by ~ 0.2 mm. An electrode array was mounted on a microdrive allowing gradual advancement of the electrode tips into the brain tissue. Alternatively the electrode array with adjusted electrodes length (3 mm for the middle-length microwire) was implanted directly into CA1 stratum pyramidale.

The following modification of the microwire technique was applied in experiments with single unit and field recordings. Two single-barrel microdrive assemblies were implanted unilateraly 1 mm above EPN (AP 2.1 L 5.6 V 6.6) or BL (AP 2.1 L 5 V 7) and the temporal (AP 6 L 5 V 6) CA1 area. Microwire arrays served for recording ripple oscillations from the septal CA1. Bundles of 5 microwires, formvar-insulated 25 µm stainless-steel wire for the amygdala or the EPN and 50 µm tungsten wire for the hippocampus (California Fine Wire Company, Grover Beach, USA) were inserted into the barrel of the microdrive cannula after its stabilization in a proper stereotaxic position with dental acrylic cement. Two stainless steel wires, striped from the insulation in at least 3 mm, were placed bilaterally in the neck muscle for electromyogram (EMG) recording. Two stainless steel screws driven into the bone above

the cerebellum served as indifferent and ground electrodes. The prefrontal cortical EEG electrode was a screw in the skull. The entire assembly was anchored to the skull with dental acrylic and anchor screws.

Histology.

Following completion of the experiments the rats were deeply anesthetized, perfused intracardially with 10% formalin-sucrose solution and decapitated. Brains were fixed for three days in 30% formalin-sucrose. The brains where then frozen, cut in 40 μm slices and stained with cresyl violet. Recording and cannula sites were confirmed (fig.1).

Recording and data processing.

Within a week following surgery the rats were placed four times for several hours for adaptation in a plastic transparent box (30 cm in diameter, 30 cm height) situated in a sound-attenuated shielded recording chamber. Then the rats were connected with a flexible cable to the amplifier and the CA1 electrode positions were adjusted for maximal ripple amplitudes when movable electrode arrays were applied.

In pharmacological experiments a day before recording, the rats were placed in the recording chamber and connected to the cable. The next day the experiment started (at 10:30 a.m.) with one hour recording followed by a drug or vehicle injection (i.p.). In sleep deprivation experiments recording went on for 7-10 hours; for the other treatments physiological parameters were registered for 1-3 hour following a drug administration. During sleep deprivation experiments behavioural waking, theta activity in the hippocampal EEG and desynchronised neocortical EEG were maintained for 3 hours by touching vibrissae with a brush following the administration of vehicle.

Seven rats were injected with amphetamine 0.5 mg/kg, modafinil, 64 and 128 mg/kg, and vehicle. Two other rats were sleep deprived for 3 hours or injected with vehicle following 1 hour of baseline recording. Seven rats were injected i.p. with diazepam, 1 and 0.1 mg/kg, and saline. Eight other rats were given flumazenil, 10 mg/kg, zolpidem, 10 mg/kg, and saline. Antagonists of histamine receptors were administered in 6 additional rats. All drug injections were performed i.p. in a randomized order with 3 days time interval between treatments. Out of these experiments recording session of good quality (well detectable ripples, few movement artefacts) were selected for analysis.

The hippocampal signal was analogue filtered (0.1 - 1 kHz) and amplified by a differential AC amplifier (Model 1700, A-M system, WA, USA), digitized at 2 kHz and

stored on a PC, using a Digidata-1200 A/D-converter (Axon Instruments, Union City, CA, USA). Neocortical EEG and EMG signals were online band-pass analogue filtered (0.1 – 120 Hz and 1 – 120 Hz respectively).

For parallel recording of amygdaloid and hippocampal activities in 6 rats, the CA1 electrode positions were first adjusted for optimal ripple detection. Twenty five rats were used for trial single unit recordings and improvement of the technique. Then BL or EPN electrodes were advanced in 5-20 μm steps until stable and well-isolated amygdaloid single- or multi-units were seen on an oscilloscope (signal to noise ratio at least 3). After amplification signals were wideband (1 Hz - 10 kHz) digitized at 25 kHz using Powerlab 1401 (CED, Cambridge, UK).

All analysis was carried out off-line using a feature detection program (H. Yokoyama, for the data recorded with Axoscope 1.1 software only), Spike2 software (CED, Cambridge, UK) and MATLAB software (The Mathworks Inc., USA). Data aquired with the pClamp package were also translated into the Spike2 data file format using the import editor. For semiautomatic detection (H. Yokoyama) ripples were defined by several characteristics including peak-to-peak potentials, frequency and shape. Automatic ripple detection was based upon the following conditions (fig. 2). The first two peaks above a threshold of 0.15 mV occur in an interval less than 30 msec. Within this interval no peak amplitude is larger than 130% of the threshold. Within 50 msec after the first peak the maximal positive or negative peak must be greater than 130% of the threshold. Peak 5 of the ripple must follow within 5 msec after peak 4 and cross the threshold. The frequency accessed between the second threshold crossing peak and the lowest amplitude peak must be above 170 Hz. If any of the parameters did not fit these requirements the program marked the event in colour to allow a later decision by the experimenter. Motor artifacts or single units were not detected by the program.

Detection of ripple oscillations was performed also with a spectral density threshold based algorithm. A fast Fourier transformation (FFT) was performed on successive 150 msec blocks of 130-250 Hz digitally filtered hippocampal EEG. All power spectra were calculated by a Spike2 based system for user defined spectral analysis. Periods of waking were excluded from analysis in accordance with the hypnogram (see below). Average power (root mean square) and SD were calculated for detection threshold setting. Events with a power of more than one SD above mean were detected, counted per minute with following normalization (see statistical analysis).

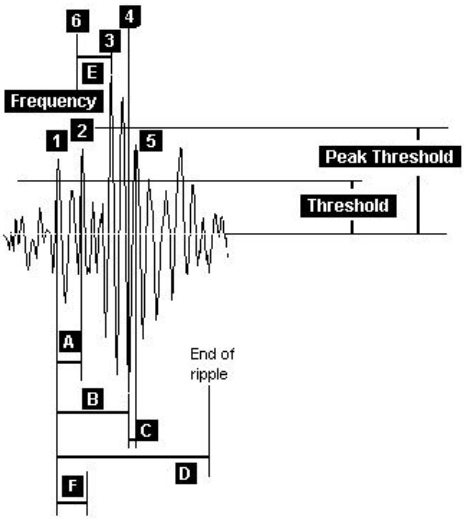

Fig. 2. Criteria for automatic detection of high-frequency ripples. Definition of the amplitudes 1-5: 1: first peak above threshold; 2: second peak above threshold; 3 + 4: amplitude maximum for both polarities; 5: first peak after peak 4. Definitions of the time intervals A-C in between the amplitudes: A < 30 msec; B < 50 msec; C < 50 msec. F: the frequency was evaluated between the second and the fourth peak.

The duration of ripples was calculated in a 130-250 Hz digitally filtered, rectified and smoothed (5 ms time constant) signal. The beginning and the end of oscillatory epochs were marked at points where the amplitude of a detected ripple fell below 0.5 SD. The amplitude and the frequency of a ripple were then calculated from the corresponding block of EEG. The maximum of the continuous wavelet (Morlet) transformation-based power spectrum served to compute ripple frequency. To control the contribution of slow (<140 Hz) and fast ripples the analysis of ripple features was performed for all the events detected and for those with a frequency below or above 140 Hz.

For digital filtering of aquired signal Finite Impulse Response (FIR) filters were applied. Each output point was generated by multiplying the waveform by the filtering coefficients and summing the result. The coefficients were then moved one step to the right and the process repeated. The filter coefficients were the impulse response of the filter. The impulse response was the output of a filter when the input signal was all zero except for one sample of unit amplitude. The frequency properties of a FIR filter were invariant when expressed as fractions of the sampling rate, not when expressed in Hz. With an even number of coefficients, there is a time shift in the output of half a sample period. Bandpass filter transition gaps were set to minimize rippling and maximize supression (up to 80 dB/octave) in stop bands.

A template matching algorithm was applied for spike sorting in 500 Hz – 10 kHz bandpass digitally (FIR) filtered recording. The template building algorithm worked as follows. (1). The first spike formed the first template with the template width estimated. This was a provisional template. (2) Each new spike was compared against each template in turn to see if sufficient points fall within the template. If there were any confirmed templates, these

were considered first, and if a match was found, the provisional templates were not considered. (3) If a spike could belong to more than 1 template, the spike was added to the template that represents the minimum distance from the spike. Distance was defined as the sum of the differences between the spike and the template. (4) If a spike could only belong to one template, it was added to it. (5) If a spike belonged to no templates, a new provisional template was created. (6) Adding a spike to a template changed the template shape and width. Once a pre-set number of spikes had been added to a template, it was checked against existing confirmed templates to prevent generation of two templates for the same data. If no match was found, the template was promoted to confirmed status. If a match was found, the provisional template was merged with the confirmed one unless the confirmed template was locked, in which case a new confirmed template was created with the same code as the one it matched. Each time a spike was added to a provisional template, the provisional template decay count was reset. (7) Each time a spike was added to a template, all provisional templates had their decay count reduced by 1. If any decay count reached 0, that template had 1 spike removed from its spike count and the decay count was reset. If the number of spikes in a provisional template reached 0, the provisional template was deleted. A template was stored as a series of data points. Each point of the template had a width and a minimum and maximum allowed width associated with it. The width represented the expected error in a signal that matches the template at that point. Spikes matched a template if more than a certain percentage of the points in a spike fell within the template. The template width was twice the mean distance between the template and the spikes that created it, but was not allowed to become greater than the maximum width or less than the minimum.

Spikes were detected by the input signal crossing a trigger level. There were two trigger levels, one for positive-going and one for negative-going spikes. Captured spikes were aligned on the first positive or negative peak. To avoid problems due to baseline drift, the data capture routines passed the data through a high pass filter. The time periods captured before and after the peak were 0.5 and 2.5 ms respectively. The spike detection algorithm was as follows: (1) waiting for the signal to lie within half the trigger levels. (2) waiting for the signal to cross either trigger level. If it crosses the upper trigger level go to step 3. If it crosses the lower level, go to step 4. (3) tracking the positive peak signal value. If the signal falls below the peak, seeing if there are sufficient post-peak points to define the spike. If so, go to 5. If the signal falls below half the upper trigger level, ignore further peaks (as for the second spike in the diagram). (4) tracking the negative peak signal value. If the signal rises above the peak, see if there are sufficient post-peak points to define the spike. If so, go to 5. If the signal rises

above half the lower trigger level, ignore further peaks. (5) save the waveform and first data point time and go to step 1 for the next spike. Limit levels outside the trigger levels were set to reject events with a peak amplitude outside this range. In this case the trigger and associated limit acted as an amplitude window on the data.

No more than one unit was extracted from one trace. The isolation of single units was verified by the absence of a peak in the autocorrelogram with a lag <1 ms, reflecting the refractory period.

BL/EPN high-frequency field oscillations were detected by a peak-detection algorithm (script for Spike2) in a low pass filtered (500 Hz), downsampled (to 1 kHz) and bandpass refiltered (140-300 Hz) signal from the same microwires that recorded the units. Derived events were used for cross-correlational analysis. Every trigger generated one sweep of analysis. The zero times of each sweep were aligned, and then the sweeps were accumulated to form a histogram. An estimation of the mean number of cycles in HFO was achived by averaging HFO-containing waveforms and taking cycles with an amplitude exceeding 7 SD above mean of the HFO-free recording.

Interval histograms (frequency histogram of the intervals between events) were constructed using Spike2 software. Event times were rounded down to the nearest base time unit, so an event time of t base units means that the actual time was greater than or equal to t and less than t+1 units. An interval of n units means that the real time interval between two events was greater than n-1 units and less than n+1 units. To form interval histograms of very short periods, the duration of the base time unit was set short enough to resolve the information required.

The sleep scoring was done with 30 sec resolution according to standard criteria for waking (desynchronised neocortical EEG and phasic or tonic activity at the EMG), SWS (slow-wave activity and decreased muscle tone) and PS (desynchronised neocortical EEG, theta activity at the hippocampal EEG and muscle atonia) on the basis of neocortical EEG and EMG activity with a reference to neocortical EEG spectral density in the 0.8-4 Hz band and hippocampal EEG. Spike2 based scripts (R. Parmentier) were used for semiautomatic sleep scoring and calculation of sleep episode statistics. Intermittent transition sleep episodes were included either in PS or waking on the hypnogram. In the analysis transition sleep was recognized by the presence of delta waves and spindles mixed with theta activity that was apparent in the power spectra as peaks at 1-5 Hz and 7 Hz of similar amplitudes and increased density at 11-12 Hz (Mandile et al., 1996). The cumulative duration of sleep stages for sleep-

waking profiles was calculated and averaged within treatment groups for 1 hour blocks of polygraphic data.

Drugs.

Modafinil (Lafon Laboratoire, France)

[(Diphénylméthyl)sulfinyl]-2 acétamide, M.W. 273.3

Atypical (non-dopaminergic) stimulant, although its waking promoting action depends on the dopamine reuptake transporter.

Dosage - 64 and 128 mg/kg, vehicle – 10% DMSO.

Amphetamine (Sigma, Deisenhofen, Germany).

Methylphenethylamine sulfate, M.W. 368.5.

Blocks catecholamine (mostly dopamine) reuptake and induces its release, adrenergic receptor agonist, waking promoting agent.

Dose – 2.5 mg/kg, vehicle – saline.

Zolpidem (Tocris, UK)

N,N,6-Trimethyl-2-(4-methylphenyl)imidazo[1,2-a]pyridine-3-acetamide, M.W. 307.39

Benzodiazepine agonist with high selectivity for α1 subunit-containing $GABA_A$ receptors (BZ/ω1 site) and very high intrinsic activity.

Dosage - 10 mg/kg, vehicle – 10% DMSO.

Flumazenil (Tocris, UK)

8-Fluoro-5,6-dihydro-5-methyl-6-oxo-4H-imidazo[1,5-a][1,4]benzodiazepine-3-carboxylic acid, ethyl ester, M.W. 303.29.

Benzodiazepine antagonist, non-selective for α1, α2, α3 or α5-containing GABAA receptors.

Dosage – 5 mg/kg, vehicle – 10% DMSO.

Diazepam (Valium, Roche, Switzerland)

7-Chloro-1-methyl-5-phenyl-3H-1,4-benzodiazepin-2(1H)-one, M.W. 284.7

Benzodiazepine agonist, non-selective for a1, a2, a3 or a5-containing GABAA receptors.

Dosage – 0.1 and 1 mg/kg, vehicle – 10% DMSO.

Pyrilamine (Research Biochemicals International, USA)

N-(4-Methoxyphenyl)methyl-N-dimethyl-N-(2-pyridinyl)-1,2-ethanediamine maleate, M.W. 401.5.
Selective antagonist for the H1 receptor.
Dosage - 5 mg/kg, vehicle – saline.

Zolantidine
N-[3-[3-(1-Piperidinylmethyl)phenoxy]propyl]-2-benzothiazolamine dimaleate, M.W. 613.68
Selective antagonist for the H2 receptor.
Dosage - 5 mg/kg, vehicle – saline.

Thioperamide (Tocris, UK)
N-Cyclohexyl-4-(imidazol-4-yl)-1-piperidinecarbothioamide maleate, M.W. 408.51.
Selective antagonist (or inverse agonist) for the H3 receptor.
Dosage - 5 mg/kg, vehicle – saline.
All listed substances cross the blood-brain barrier after systemic (i.p.) administration. Drugs were dissolved in a volume of 0.4 ml just before injection. In control experiments and before sleep deprivation rats were treated with the same volume of vehicle.

Statistical analysis.
The first hour of recording provided the baseline of ripple occurrence. In pharmacological experiments the second hour in each of the experimental groups (diazepam, flumazenil, zolpidem, pyrilamine, zolantidine, thioperamide) was compared with control group (vehicle). Non-parametric cretiria were used in statistical analysis because of non-gaussian distributions of samples. Comparisons between groups were made using the Mann-Whitney U-Test. Parameters of ripple structure were compared between baseline period of recording and post-treatment period utilizing Wilcoxon signed rank test. The drug effects during the second hour are presented as mean ± SEM. All P values given were considered to be significant when $P < 0.05$. In the sleep deprivation study ripple numbers were normalized for individual experiments taking the mean ripple occurrence during SWS in the baseline recordings as 100%. Then Mann-Whitney U-Test was applied. Ripple structure was compared between baseline SWS and post-treatment SWS using Wilcoxon signed rank test. Correlational analysis was performed utilizing the Spearman rank coefficient. P values given were considered to be significant when $P < 0.05$ in cases of single comparison. When multiple comparisons were performed resulting P values are presented solely as a mesures of effect.

RESULTS

Sleep-related dynamics of ripples after stimulant-induced waking.

Ripple rebound following different treatments

During pre-treatment baseline SWS ripple occurrence was 23 ± 7, 21 ± 2, 20 ± 3, 26 ± 6, 25 ± 3 / min in the amphetamine, modafinil 64 mg/kg and 128 mg/kg, sleep deprivation and control groups respectively. Thus, there was no difference in pre-treatment SWS ripple occurrence between groups. Treatment with amphetamine (2.5 mg/kg) caused continuous waking for nearly 3 hours (167 ± 13 min, n=5). It was accompanied by prominent theta activity and very rare if any occurrence of ripples in the hippocampal EEG (fig. 3A-C). With the following SWS onset ripple occurrence rose much higher than during normal (baseline) SWS (to 211 ± 34%, $p<0.01$, see fig.3D). The first SWS episodes were interrupted by two or three relatively short waking periods, then PS occurred between SWS episodes (see tab.1, 2 and fig. 3D-F). During this time ripple occurrence gradually decayed to the baseline level (decay time 155 ± 36 min, fig. 2 and 3). Only at the beginning of SWS the temporal pattern of ripple occurrence was similar to the delta spectral band rebound after amphetamine induced waking (fig. 3E).

To ensure correct representation of the rebound of ripple occurrence by normalized values, direct comparison of ripple numbers during pre- and post-treatment periods and its normalized difference was performed (fig.4). For this purpose ripple occurrence was detected with increasing thresholds (from 1 to 7 SD from the mean power in 140-250 Hz spectral band) in the amphetamine treated group. As expected the number of ripples detected dropped as threshold increased. The rebound of ripple occurrence expressed as absolute number of ripples decreased from the low to high detection thresholds. However, the normalized rebounds had the same values for all the detection thresholds (p=0.74).

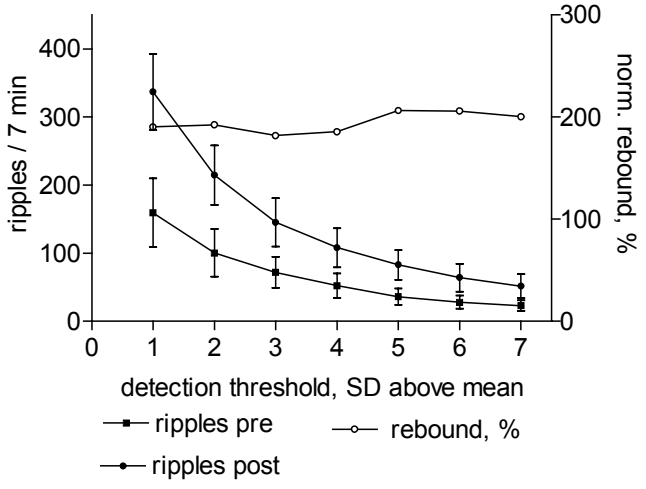

Fig. 4. Verification of the normalized representation of ripple rebound. Amphetamine-treated group.

Waking evoked by modafinil was more frequently interrupted by SWS episodes, which appeared after a shorter latency than after amphetamine treatment (79 ± 22 min, n=4, 64 mg/kg, and 56 ± 10 min, n=6, 128 mg/kg; see also tab.1 and 2 for sleep episode statistics). The cumulative waking time tended to be longer ($p=0.071$) within 3 hours after administration of 128 mg/kg, than 64 mg/kg (fig.5). The duration of consolidated waking caused by modafinil was shorter than one induced by amphetamine ($p=0.021$ for modafinil 128 mg/kg and $p=0.0077$ for modafinil 64 mg/kg). The rebound of ripple occurrence was 137 ± 15 % (128 mg/kg, $p<0.01$), and 145 ± 14 % (64 mg/kg, $p>0.05$) (fig. 6A, 7A, tab. 3). Recovery time was not significantly different (19 ± 8 min and 44 ± 19 min respectively).

In the control experiments rats were awake for 13 ± 2 min after vehicle injection. This waking was also followed by elevated ripple occurrence in subsequent SWS (to 135 ± 9% with recovery time 12 ± 6, n=6). Ripple occurrence after 3 hours of non-pharmacological sleep deprivation was increased to 203 ± 16 % (n=2) being similar to that in the amphetamine treated group.

The increase of ripple occurrence was directly linked with the duration of waking evoked by any treatment but not with the type of treatment (Spearman's correlation coefficient $r = 0.5$, $p=0.0198$, n=22; fig.6B). Conversely, the necessary time to get back to the baseline ripple occurrence correlated with the ripple occurrence rebound during the first SWS episode after the waking ($r=0.7$, $p<0.0001$, n=23, fig. 6C).

The mean intrinsic frequency of ripples was increased by up to 20 Hz during a post-treatment SWS episode ($p<0.0001$, tab. 4). This effect was observed for events >140 Hz only. Unlike ripple occurrence, an increase of ripple frequency was not correlated with the duration of waking ($p=0.6408$). The maximal elevation of ripple frequency was found in experiments with sleep deprivation. The amplitude of ripples was markedly elevated during post-treatment SWS only after amphetamine administration ($p=0.0004$, rank sum test, see tab.5). The duration of ripples was not different between pre- and post-treatment SWS in any group (tab.5).

Dynamics of ripple rebound during SWS

The decay of ripple occurrence to the pre-treatment level during SWS was measured as the difference of ripple occurrence between the first and the last 3 min of a continuous SWS episode. The decay of ripple occurrence was strongly dependent on SWS duration ($r=0.4$, $p=0.0367$, n=31 for amphetamine, $r=0.5$, $p=0.0265$, n=17 for modafinil 64mg/kg and $r=0.5$, $p=0.0160$, n=24 for modafinil 128mg/kg; see also fig. 7A).

Since a sequential order of sleep stages has been shown to be important for hippocampal processing (Vescia et al, 1998) we have compared the decay of ripple occurrence in two types of SWS episodes, which differed with respect to the nature of the preceding theta state: PS or waking. The decay of ripple occurrence during SWS preceded by waking made a higher contribution to the recovery of ripple occurrence in cases of relatively weak ripple rebound (15 ± 3 %, p=0.0057 for modafinil 128 mg/kg, 18 ± 4 %, p=0.03 for modafinil 64mg/kg and 18 ± 3%, p=0.0084 in the control group, U-test; fig. 7B, tab.6). In the treatments with a profound rebound (amphetamine and sleep-deprivation), ripple occurrence equally decreased during SWS preceded by PS or by waking (27 ± 10 and 20 ± 13% for amphetamine, 28 ± 20 and 20 ± 21% for sleep deprivation). On the other hand, ripple occurrence was not changed or was even elevated during SWS in about 10% of the cases in both types of SWS episodes.

The dynamics of intra-ripple frequency during SWS were estimated by the correlation with ripple timing within a sleep episode. The correlation was inverse (r=-0.1 to -0.2, p<0.05) during post-treatment SWS suggesting a gradual decay of intraripple frequency. Conversely, in the sequence of post-treatment SWS episodes the mean frequency of ripples was decreasing (p=0.0035, rank sum test, tab. 4). The mean ripple amplitude also displayed a clear decay over the 4 first SWS episodes (p=0.0008, rank sum test), although without obvious decay within the individual SWS episodes (p=0.0914).

PS regulates ripple occurrence during SWS

A role of PS in the dynamics of the ripple occurrence decay during SWS was revealed by an analysis of the last 3 min of SWS preceding PS (late SWS1) and the first 3 min of SWS following PS (early SWS2) in amphetamine-treated and control rats (see fig. 9A). Only in these groups we observed sufficient numbers of PS episodes and consolidated SWS episodes longer than 6 min.

PS was associated with a further decrease of ripple occurrence during early SWS2 only if ripple occurrence in the preceding late SWS1 had still been high (from 138 ± 17 % to 110 ± 16 % to baseline, p=0.0805, fig. 8A, tab.7). In contrast, when ripple occurrence had largely recovered during SWS, to 97 ± 13 %, the ensuing PS evoked a profound elevation to 133 ± 18 % (p=0.0331, U-test) during the next SWS period. Conversely, there was also a clear correlation between ripple occurrence in late SWS1 and the change of ripple numbers following PS both in amphetamine-treated and control rats (r=0.4, p<0.05, n=22 and r=0.5, p<0.05, n=24 respectively, fig. 8B, C). After PS-evoked elevation, ripple occurrence

markedly dropped during the following SWS to a level near baseline (to 92 ± 13 %, $p<0.0249$, U-test). In amphetamine treated rats PS was on average associated with increased ripple occurrence (fig. 9).

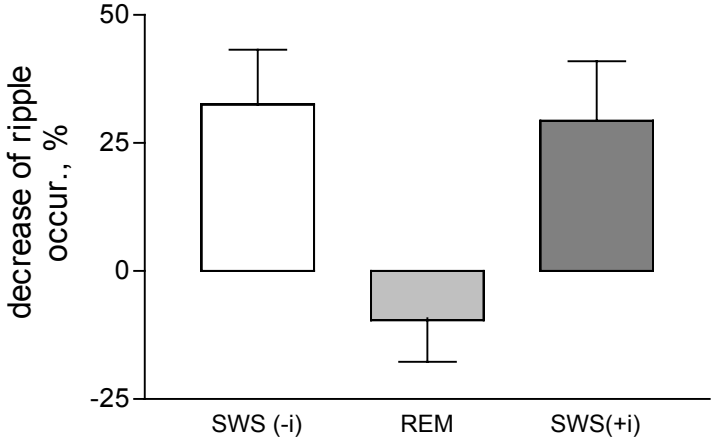

Fig. 9. An overall change of ripple occurrence associated with PS (difference of ripple numbers between the last 3 min and the first 3 min of two subsequent SWS) in amphetamine treated rats.

Durations of the SWS1, PS and SWS2 did not differ significantly between the two data sets representing the up or down of ripple occurrence during early SWS2 (tab. 8). The mean order of PS episodes analysed was similar in both sets (4.3 and 3.7). However, we found that short transition sleep episodes had occurred between late SWS1 and PS more frequently (71% versus 38% of PS episodes) when ripple occurrence was elevated after PS. The duration of transition sleep was shorter in the first set (21 ± 3 sec for PS associated ripple occurrence elevation and 29 ± 2 sec for PS followed by a decrease of ripple numbers, $p<0.05$, U-test). In the two subsequent PS episodes, PS that preceded early SWS2 was usually followed by transition sleep, when the next PS episode led to an increase of ripple occurrence (43%, 22 ± 3 sec duration versus 25%, 14 ± 2 sec duration).

A striking feature was that changes of ripple occurrence associated with PS predicted the change of ripple numbers during the following SWS2 ($r=-0.6$, $p<0.0006$, $n=40$, fig 8D). If ripple occurrence was increased between late and early SWS it was usually reduced during SWS2. We found no differences of ripple structure (frequency, amplitude, duration) in the periods bordering PS episodes.

In summary, at the end of the recovery period PS acted like waking, elevating ripple occurrence during subsequent slow wave sleep episodes. On the other hand, PS decreased ripple occurrence if recovery was not yet complete.

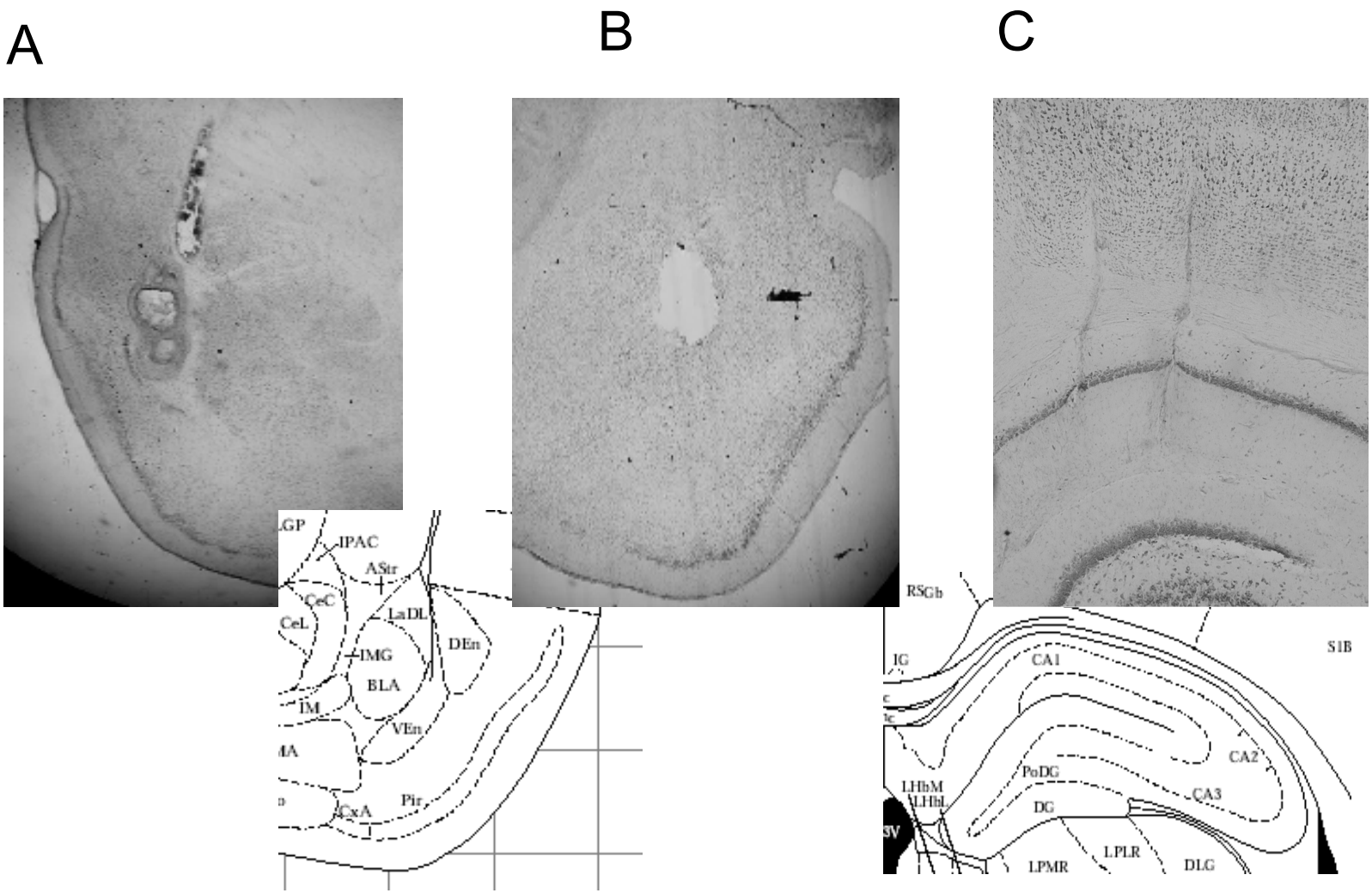

Fig. 1. Histological control of the electrode tips position in the target regions: dorsal endopiriform nucleus DEn (A), basolateral nucleus of the amygdala, BLA (B) and dorsal hippocampal CA1(C).

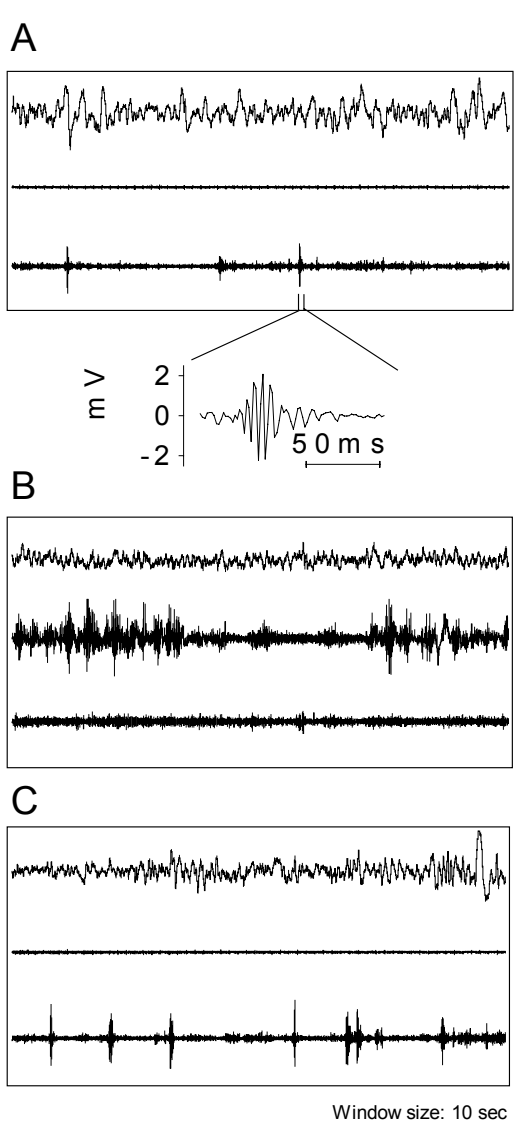

Fig.3 .Recordings of neocortical EEG (upper), EMG (middle) and hippocampal EEG (lower) traces. A: baseline period before treatment, representing SWS, B: during amphetamine evoked waking, C: at the onset of post waking SWS; periods of 10 sec duration. Neocortical EEG and EMG signals are on-line bandpass filtered between 0.1 and 120 Hz and 1 and 120 Hz respectively. The hippocampal waveform was digitally filtered at 130-250 Hz. Inset shows example of an oscillatory epoch. Ripples occur more frequently during SWS after amphetamine evoked waking than before treatment and are absent during theta state with high phasic EMG activity.

Temporal dynamics of ripple occurrence (D) in comparison with delta band power density (E) and sleep phases (F). Amphetamine was administered i.p., 2,5 mg/kg. Recovery of ripple occurrence to baseline pre-treatment level took about 1.5 h. Second PS episode in post treatment period elicited an increase of ripple occurrence in the beginning of subsequent SWS.

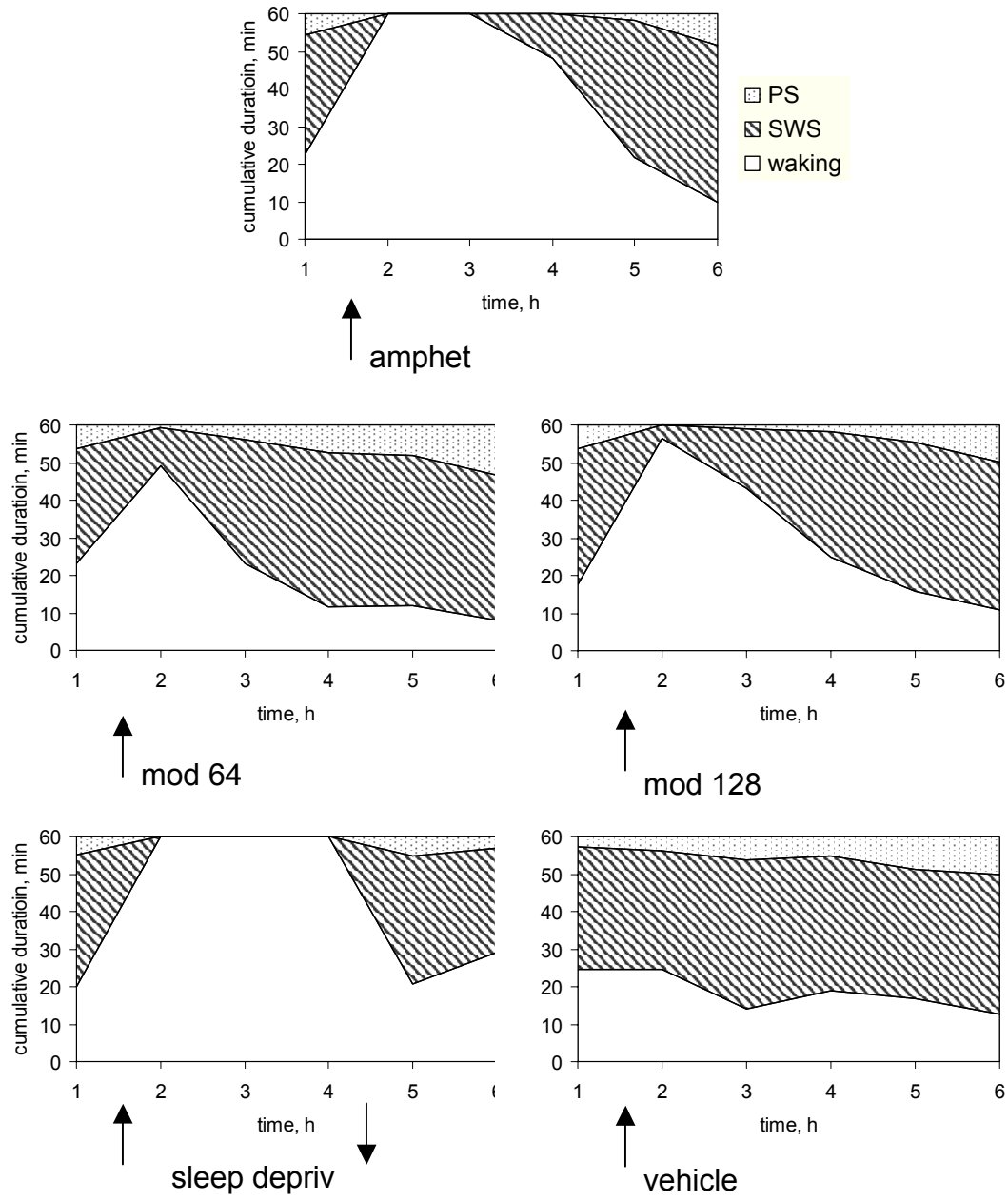

Fig. 5. Waking/sleep pharmacodynamic profiles for different treatment groups. Cumulative time spent in a vigilance state is summarized for 1 h periods. N=23

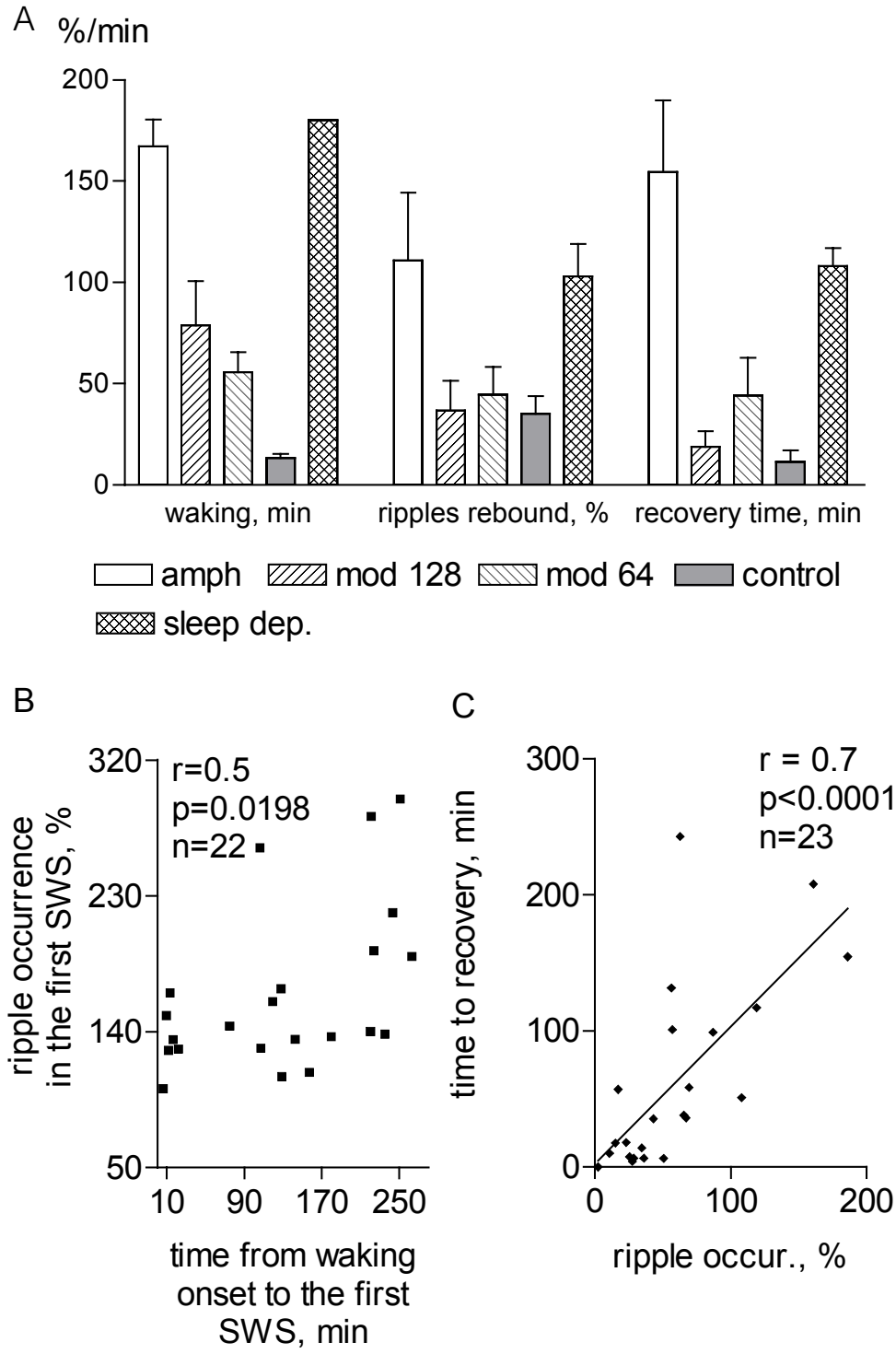

Fig 6. (A) Relationship between waking time (min), rebound of ripple occurrence (% of baseline) and its recovery time (min) in different experimental groups. N=23 Data are shown as mean ± SEM. (B) Ripple rebound depends on waking duration and (C) predicts the time needed for ripple occurrence to recover to the prewaking level. r – Spearman's correlation coefficient.

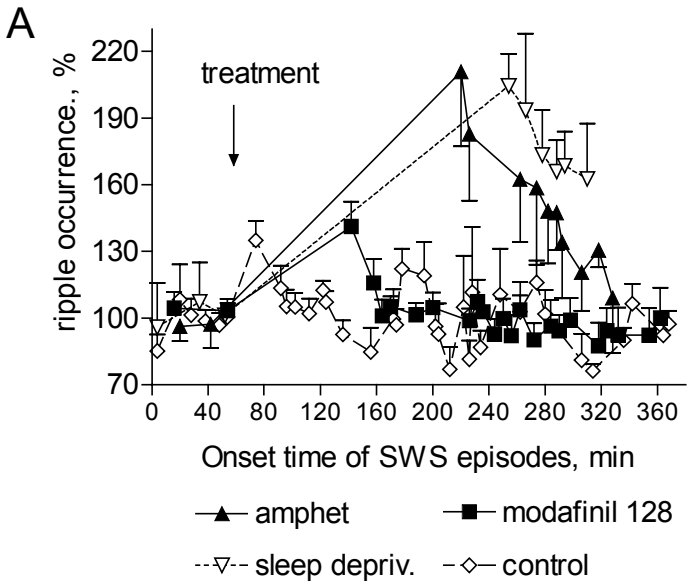

Fig. 7. (A) Ripple rebound dynamics after different treatments. The ordinate represents the mean (± SEM) ripple occurrence during consolidated SWS episode, the abscissa represents the average onset time of SWS episodes. After 1 hour of baseline recording rats were injected modafinil (128 mg/kg), amphetamine (2.5 mg/kg) or 10% DMSO (control). Sleep deprivation in the corresponding group lasted for 3 hours. The ripple occurrence during SWS episodes increased ($p<0.01$ for modafinil, 128 mg/kg, and amphetamine), than gradually decreased to the pre-treatment level. N=19

(B) SWS duration determines the change in ripple occurrence during given SWS episode. r –Spearman's correlation coefficient. (C) Decrease of ripple occurrence (mean ± SEM) in SWS episodes during recovery from waking-evoked ripple rebound. Ripple occurrence significantly decreased during SWS preceded by waking in modafinil – treated and in the control rats. SWS preceded by waking contributed significantly more than SWS preceded by PS in modafinil 128 mg/kg treated and in the control rats. Recovery from ripple rebound during SWS preceded by PS was more marked in amphetamine than in modafinil 128 mg/kg treated and control groups (* - $p<0.05$, ** - $p<0.01$). N=137.

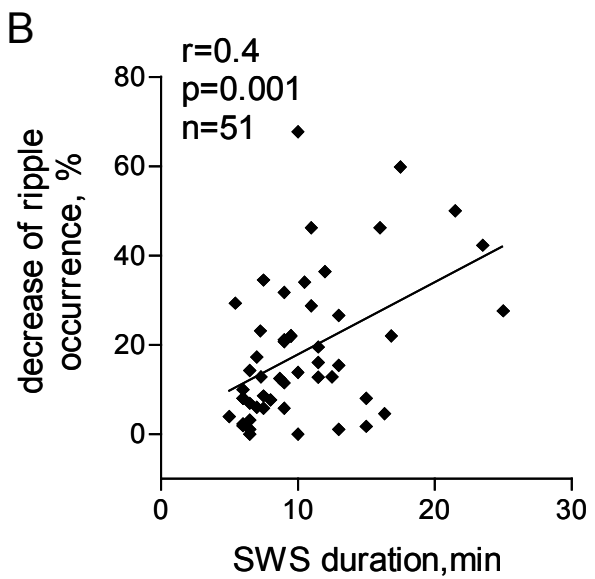

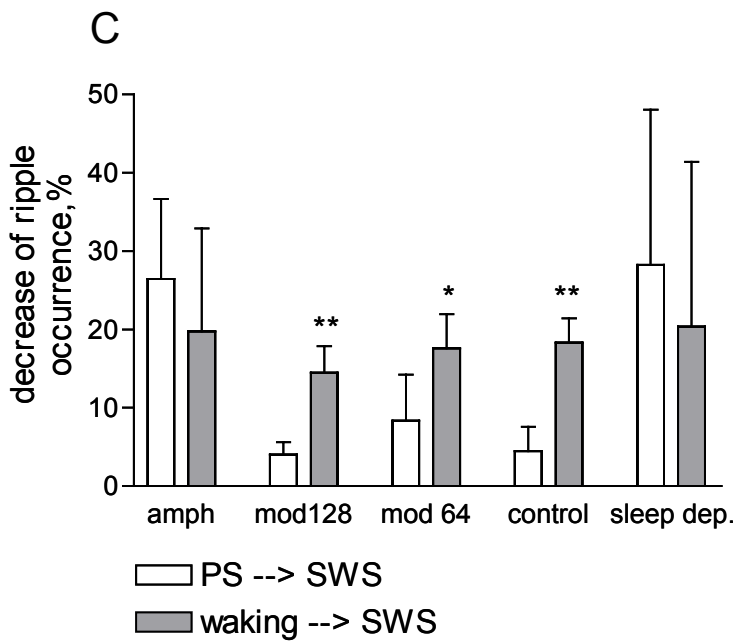

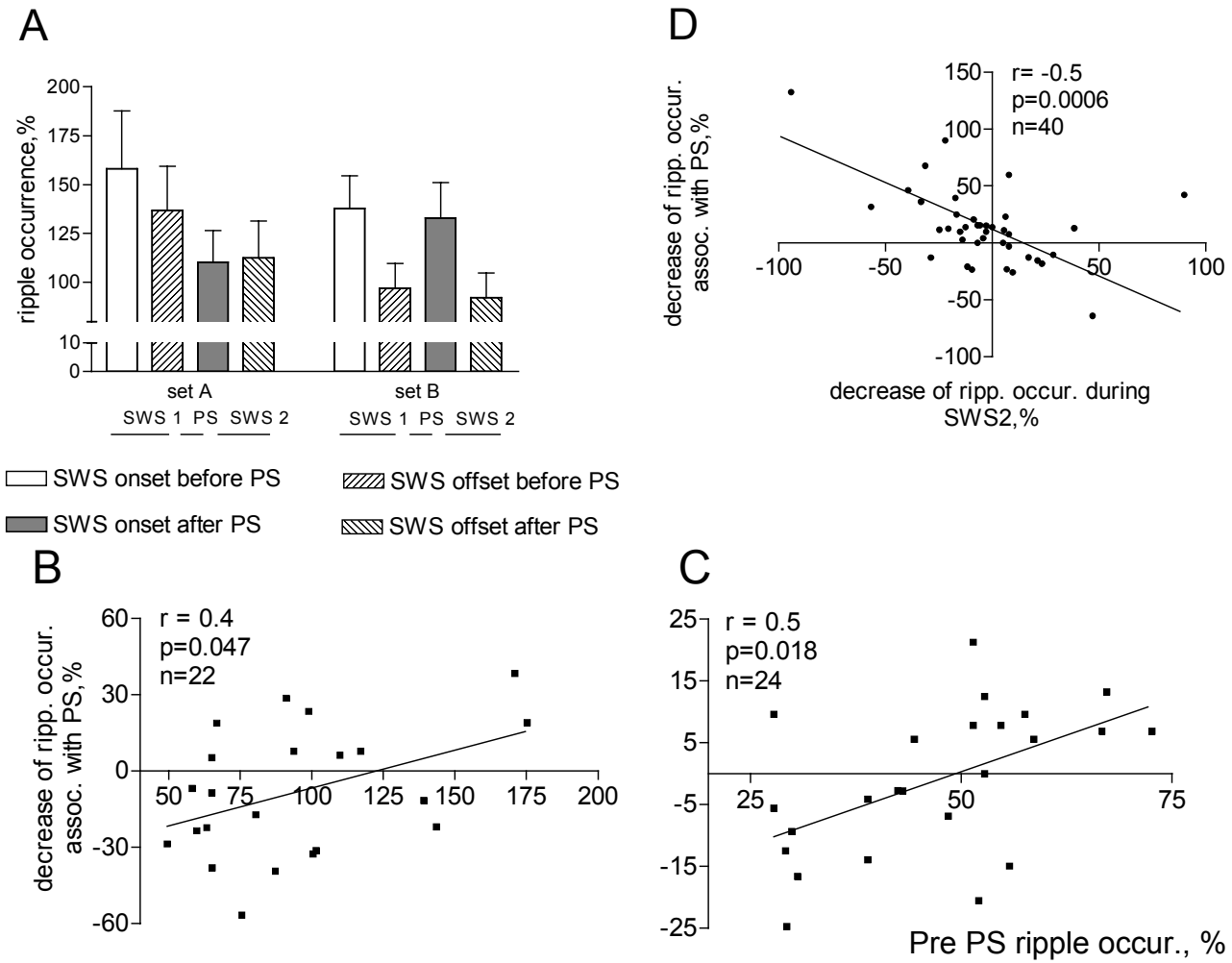

Fig. 8. (A) PS evoked changes in ripple dynamics depend on ripple occurrence in the previous SWS episode (amphetamine treated rats). Columns represent 3 min periods of the onsets and offsets of two sequential SWS episodes separated by PS. Sets A and B differ in the way how PS altered ripple occurrence in the subsequent SWS in comparison with the preceding one. In the set A ripple occurrence just before PS was significantly higher than in the set B. During the next SWS after PS the ripple number decreased to the level at the end of SWS before PS that coincided with initial pretreatment baseline.N=34 SWS. (B, C) Direction of PS evoked modulation of ripple occurrence depends on ripple occurrence in the last 3 min before PS (late SWS1, amphetamine-treated group). (C) Change of ripple occurrence associated with PS and subsequent SWS (SWS2) are negatively correlated. Y-values represent the difference of ripple occurrence between 3 min intervals at the offset of SWS before PS and at the onset of SWS after PS. r –Spearman's correlation coefficient.

On the role of GABA-receptors in the mechanisms of ripples: effects of benzodiazepine-site ligands.

A nonselective agonist of the benzodiazepine site of $GABA_A$ receptor, diazepam, a selective agonist of the benzodiazepine site of the $GABA_A$ receptor, zolpidem, and a benzodiazepine antagonist, flumazenil, were used to elaborate GABA-ergic mechanisms of ripple oscillations.

Diazepam, 1 mg/kg, effectively abolished high-frequency oscillatory activity in the hippocampal CA1 (Fig. 10A, n=5, p=0.0204, tab.9). An abrupt decline of ripple occurrence started 5 min after the drug administration, reached a maximum in 10 min. After a short period of behavioural activation (locomotion and grooming) lasting not longer than 10 min following i.p. injection, rats were immobile with a gradual transition to SWS.

In contrast, a lower dose of diazepam, 0.1 mg/kg, had no significant effect on the occurrence of ripples (p=0.710, n=4, tab. 9). The parameter was only transiently reduced within 10 min following the drug administration.

Zolpidem, 10 mg/kg, resulted in a profound drop of the number of ripples, peaking 20 min following the drug administration (p=0.0397, n=5, see fig. 11A, tab.10). Recovery started 30 min following administration. Ripple occurrence did not differ from that in the vehicle treated group and in the baseline recording 50 min following treatment. Conversely, spectral density in the high-frequency band, 140-300 Hz, corresponding to CA1-originating ripples (Csicsvari, 99), was markedly suppressed for 40 to 50 min after zolpidem injection. These changes were not accompanied by behavioural alertness – following a short (~10 min) period of activation deep SWS was evident from polygrafic recordings. Suppression of PS was also typical for treatment with both, zolpidem 10 mg/kg, and diazepam, 1 mg/kg, being in contrast with baseline and control recordings. Treatment with both benzodiazepine agonists resulted in a prevalence of slow irregular activity on the hippocampal EEG for the most period of ripple occurrence assessment.

Surprisingly, the antagonist at the benzodiazepine-site flumazenil, 10 mg/kg, also decreased the occurrence of ripples. This action of the drug began 10 min after drug administration and lasted 160 min (significant difference from the recordings with vehicle treatment, $p<0.05$, n=5, fig. 12A, tab.10) although a tendency of reduced ripple numbers was observed for up to 180 min. In contrast to benzodiazepine agonists, flumazenil evoked rather long (up to 50 min) periods of behavioural activation, including locomotion and rearing behaviours that were however frequently interrupted by immobility. This was accompanied by theta oscillations in the hippocampal EEG. As expected, ripple occurrence was the lowest

during this period (down to 64% of the baseline period of recording). During the next 2 hours of recording SWS was the prevalent state of vigilance. The structure of SWS was somewhat atypical, with relatively high amplitude tonic EMG, moderate synchronization of the neocortical EEG and fragmentation due to incorporation of short episodes of immobile waking. These waking episodes came along with some theta activity in the hippocampus that was reflected as slighly increased power density in the theta band (5-10 Hz). Thus although an initial reduction of ripple occurrence by flumazenil could be explained by a shift of the hippocampal rhythms towards theta, the overall decrease of ripple numbers is due to an intrinsic action of the drug upon sharp waves/high-frequency oscillations.

Analysis of ripple structure revealed reduction of all the parameters (ripple amplitude, duration and frequency) within 1 h following treatment with diazepam, 1 mg/kg (fig. 10B, $n=1769$, $p<0.0001$, tab.11). A similar tendency was observed for intraripple frequency and ripple duration but not for ripple amplitude following treatment with diazepam, 0.1 mg/kg ($n=1450$, $p>0.05$). Zolantidine, 10 mg/kg, decreased ripple amplitude and frequency but increased ripple duration (fig. 11B, $n=2555$, $p<0.0001$) within 1 h following the drug administration. Elevation of ripple duration by zolpidem was associated with increased occurrence of double-peak ripples accompanied by sharp waves of corresponding duration. Flumazenil reduced ripple duration ($n=2206$, $p<0.0001$) without effects on ripple amplitude and frequency (fig. 12B).

In summary, both agonists and the antagonist at the benzodiazepine site of the $GABA_A$ receptor reduce both sharp wave and ripple occurrence independently of its effects upon vigilance state. Ripple amplitude and frequency get affected by lower dose of diazepam than ripple occurrence. Zolpidem is different from diazepam in ability to prolong ripples, but has similar with diazepam effects upon ripple amplitude and frequency. On the other hand, antagonist of the benzodiazepine site flumazenil reduced ripple duration.

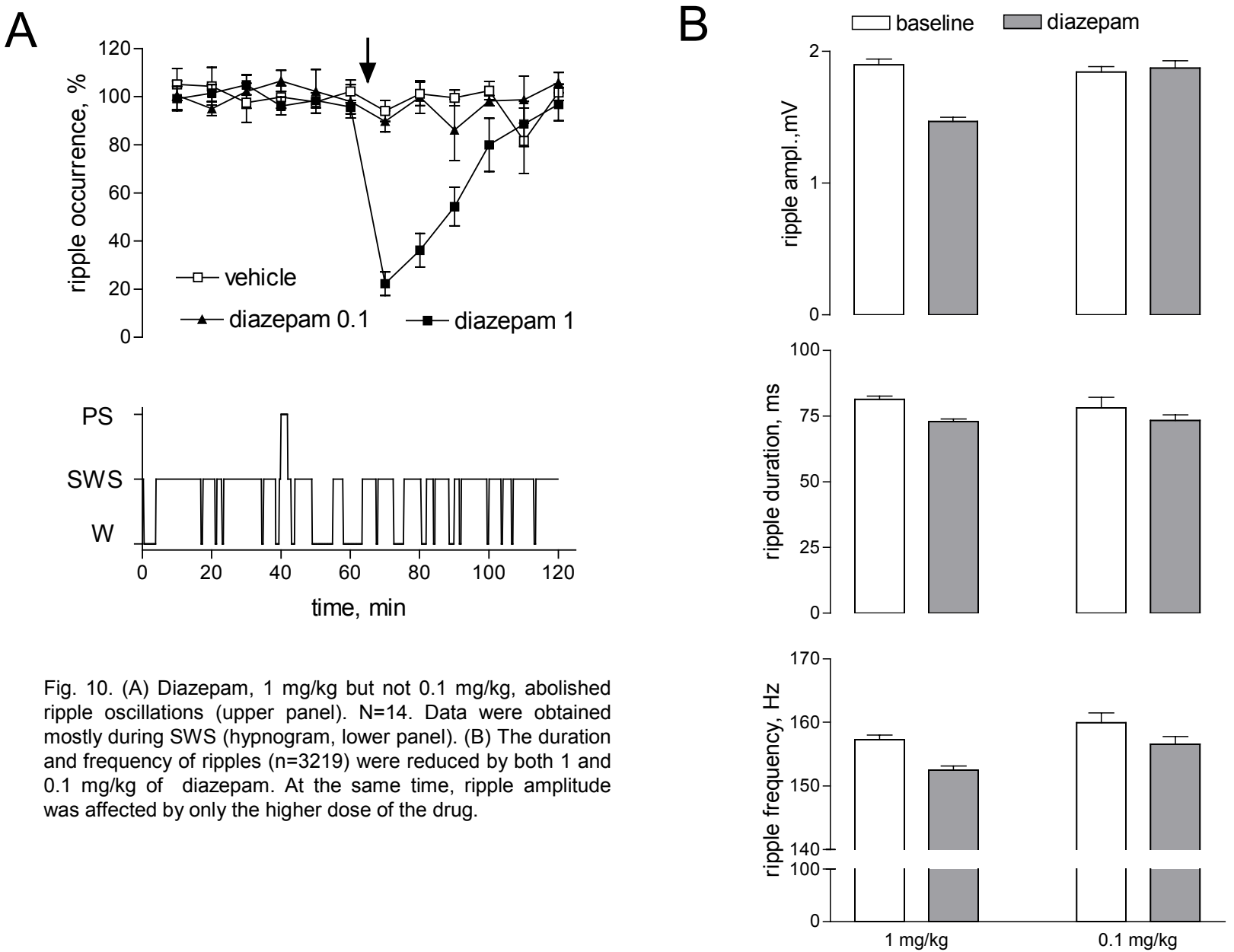

Fig. 10. (A) Diazepam, 1 mg/kg but not 0.1 mg/kg, abolished ripple oscillations (upper panel). N=14. Data were obtained mostly during SWS (hypnogram, lower panel). (B) The duration and frequency of ripples (n=3219) were reduced by both 1 and 0.1 mg/kg of diazepam. At the same time, ripple amplitude was affected by only the higher dose of the drug.

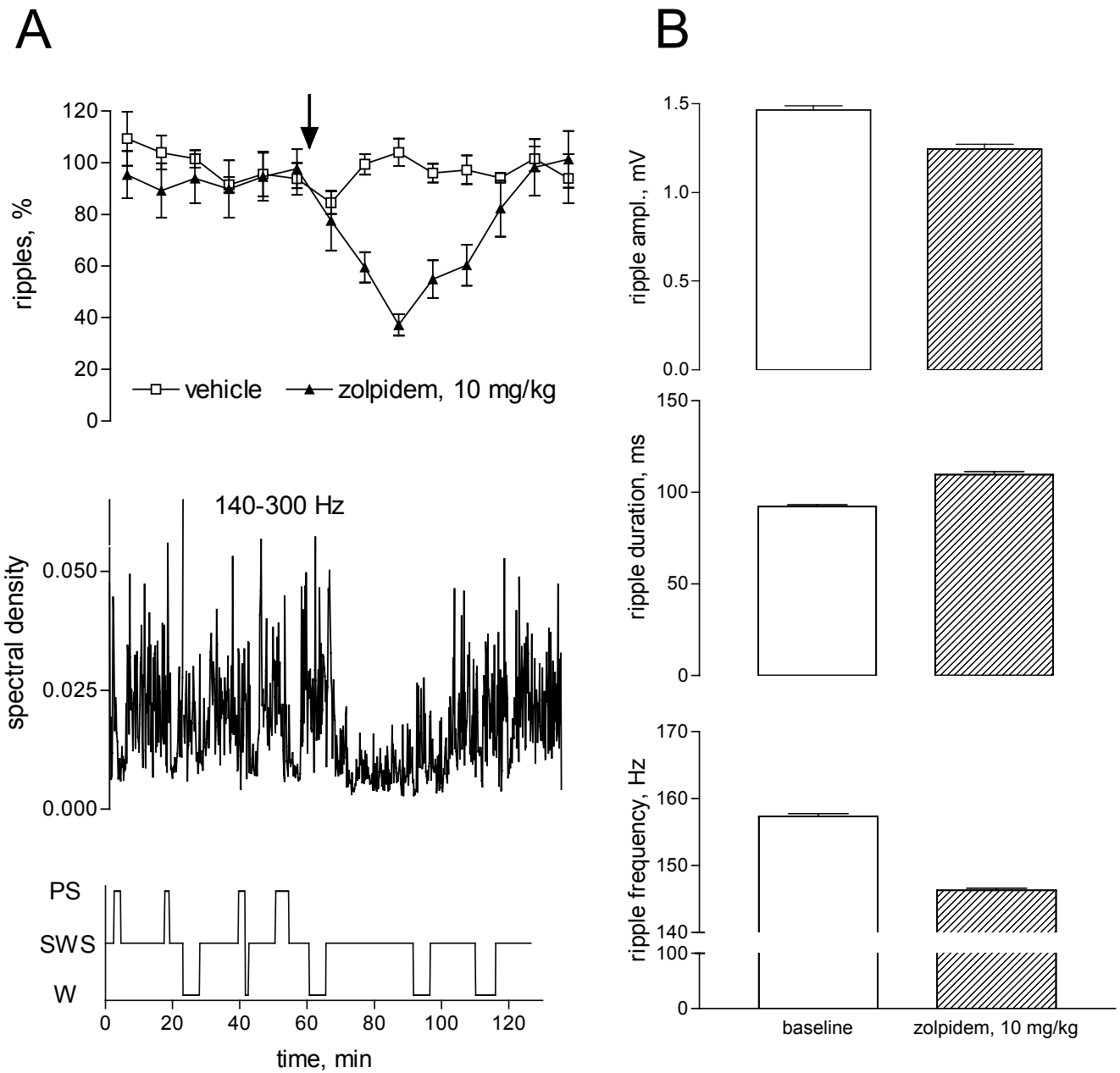

Fig. 11. Zolpidem reduced number of ripples (upper plot) without unidirectional alteration of the sleep/waking cycle (hypnogram, lower plot). N=10. Spectral density in the ripple related band is shown in the middle plot (A). Ripple (n=2555) amplitude, duration and frequency following treatment with zolpidem (B).

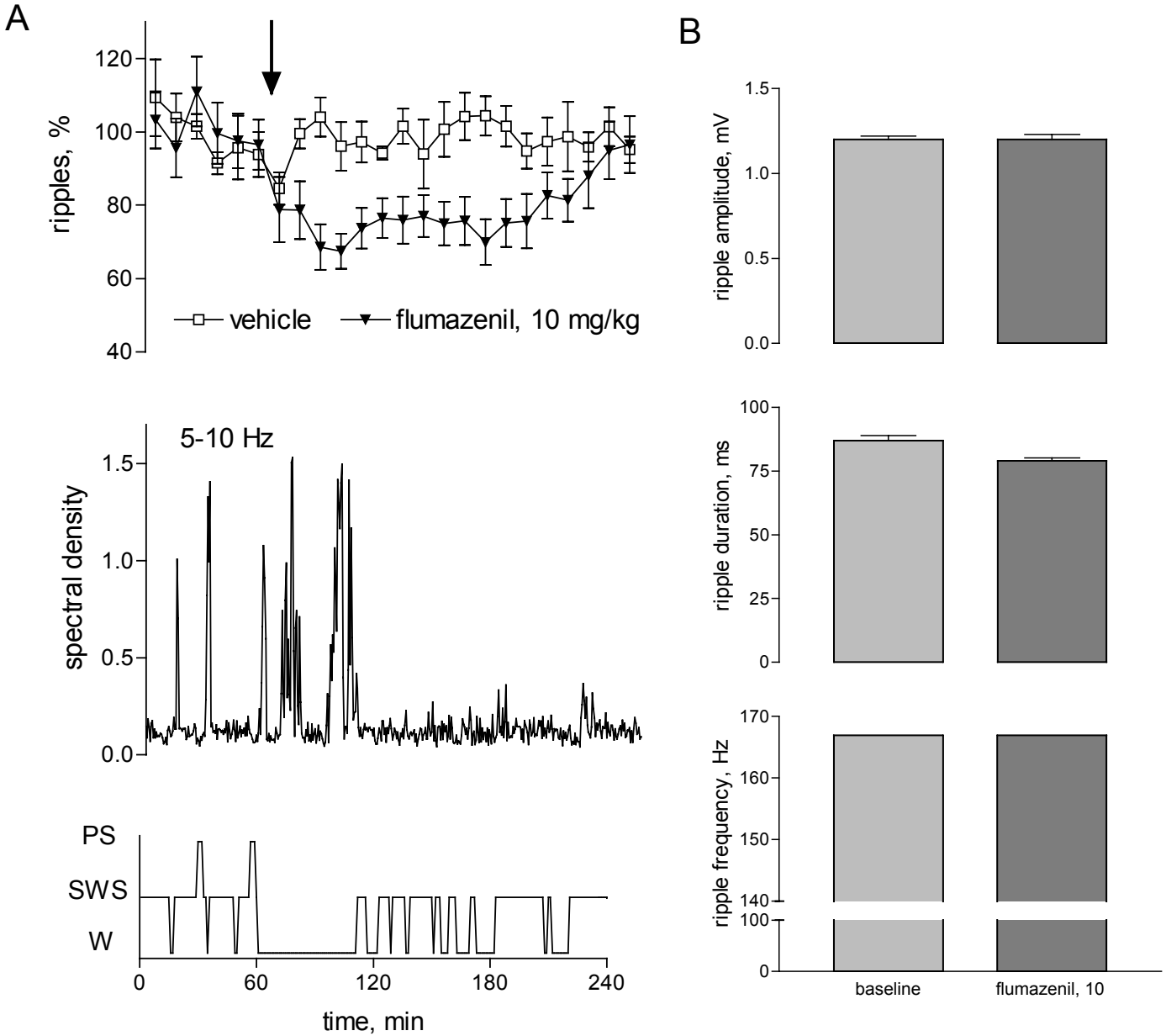

Fig. 12.(A) Supression of ripple oscillations by flumazenil (upper plot) was accompanied by only transient increase in theta spectral band (middle plot). N=10. Hypnogram (lower plot) shows prevalence of slow-wave sleep (SWS) over waking (W) and paradoxical sleep (PS) durinf post-treatment period. (B). Frequency and amplitude of ripples (n=2206) were unaffected by flumazenil, but ripple duration was reduced.

The histaminergic system shapes synchronization in the hippocampus

Histamine receptor antagonists were applied systemically to elucidate contribution of different receptor types in the tonic histaminergic modulation of ripple oscillations. Systemic (i.p.) administration allowed almost simultaneous impact of the drug upon brain structures involved in regulation or/and generation of ripples.

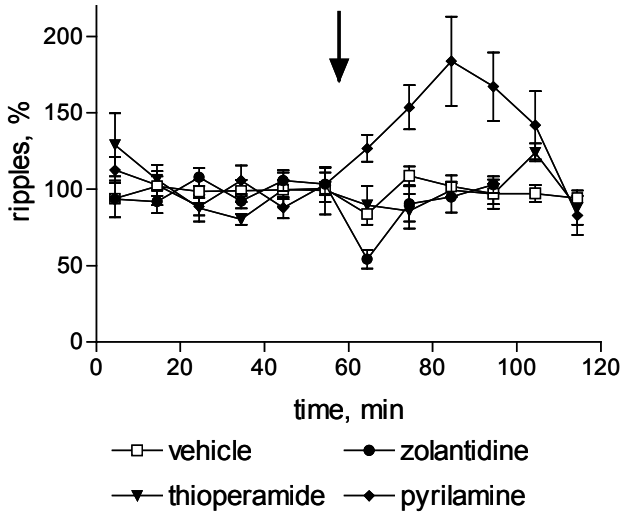

Fig.13. Effects of histamine receptor antagonists (5 mg/kg for pyralamine and thioperamide and 10 mg/kg i.p. for zolantidine) on the occurrence of ripple oscillations (inset) on the hippocampal EEG. Arrow indicates time of a drug administration.

The histamine H_2-receptor antagonist zolantidine (10 mg/kg, i.p., n=5, tab. 12) decreased the frequency of ripple occurrence to 54 ± 6 % of baseline (p=0.031). The average duration of this inhibitory effect was 20 min (fig. 13). However the lower dose of zolantidine (5 mg/kg) did not change the number of ripples. In contrast, the H_1-antagonist pyrilamine (5 mg/kg, i.p., n=5) facilitated the occurrence of ripples. The number of oscillatory epochs was gradually increased (p=0.014) following drug administration, peaking after 20 min (184 ± 29 % from baseline). Complete recovery to pretreatment ripple occurrence was achived by 60 min of the posttreatment period.

Surprisingly, the administration of the H_3-receptor antagonist thioperamide (5 mg/kg, i.p., p=0.7599, n=5) had no effect on the frequency of ripple occurrence. Both amplitude and intraripple frequency were unaffected by systemic histamine receptor antagonists. These actions of histamine receptor antagonists were not accompanied by significant alterations in vigilance state.

High-frequency synchronization in the basolateral amygdala (BL) and dorsal endopiriform nucleus (EPN).

In this chapter the neuronal firing patterns in the BL and EPN are compared. Furthermore, high-frequency oscillations in these nuclei are described and related to ripple oscillations in the dorsal and ventral hippocampus.

Common firing patterns of the basolateral amygdala (BL) and dorsal endopiriform nucleus (EPN).

Sixty-nine neurons were recorded in four rats, 40 from the basolateral complex and 29 from EPN. Spikes had a bi-phasic shape and durations of 1.9 ± 0.2 and 2.1 ± 0.2 ms in the BL and EPN respectively. Units from these structures exhibited a similar irregular firing pattern (fig. 14). In a majority of neurons (31 in the amygdala and 23 in the EPN) background firing was occasionally interrupted by bursts of 2-8 spikes with a firing frequency 100 – 400 Hz. Higher peak rates were associated with lower background firing. Seven neurons in the basolateral complex (6 of which were located in L), fired <0.01 Hz, are not considered here due to non-sufficient numbers of spikes for analysis in the individual recordings. Notably, mean firing rates in EPN were typically lower than 1 Hz, whereas units in the BL fired from less than 1 Hz (bursting units, n=29) to 17 Hz (phasic units) (tab.13). Autocorrelograms of single units showed a sharp peak at 4-6 ms (usually with shorter lags for EPN units) and different distributions of longer interspike intervals (Fig. 15A, 16D, 18D).

Neuronal activity in both BL and EPN appeared not to correlate with specific types of behaviour. Burst firing occurred irregularly and not following slower rhythms. With respect to the sleep/waking cycle neuronal firing in the BL and EPN was clearly state dependent (Fig. 19). The maximal neuronal discharge (bursting) occurred during SWS. Activity of EPN and BL neurons was low during waking and PS. However, averaged firing rates did not differ significantly for EPN and were even higher in the BL during PS than during waking (Tab. 13).

Firing of both BL and EPN units exhibited a clear tendency to be state dependent with mean rates maximal during SWS, intermediate during PS and almost two times lower during W (for BL in the case of SWS / W, $p=0.0208$, and PS / W, $p=0.0315$). Units of BL and EPN fired more bursts (instantaneous frequency >100 Hz) in relation to low frequency firing (<20 Hz) during SWS than during PS or waking (not significant due to large variability). In the

EPN and BL waking corresponded to tonic firing (<20 Hz) without bursts, whilst in the EPN there was low or sometimes no firing during PS. (see Fig. 19).

High-frequency oscillations in the BL and EPN.

The EEG signal displayed high-frequency oscillations (HFO) mostly at the time of neuronal discharge in BL and EPN. Power spectra- and autocorrelograms revealed a frequency of the field HFO of approximately 200 Hz (Fig. 15B, 16A, 17). Firing of both bursting and phasic single units appeared synchronous with a positive HFO peak when relatively long intervals at cross-correlograms (3 s) were considered. Cross-correlograms for EPN units were slightly sharper around the HFO peak than those for BL units, reflecting the higher mean firing rates rates (see also tab.13). At a higher resolution neuronal discharge was phase-locked with positive peaks of HFO at least for three oscillatory cycles. A striking feature was the tendency (not significant) for the number of cycles in an individual HFO epoch to correlate with the number of spikes in a burst both in EPN (Fig. 15C) and BL. Single spikes were associated with a short (10 ms) field potential whilst trains of 8 spikes corresponded to a similar number of oscillatory cycles (HFO duration up to 80 ms). Amygdaloid and EPN HFO had on average a lower number of field cycles than observed in hippocampal rippless (3 to 6 vs 11 cycles in averaged waveforms, see methods) and smaller amplitudes (see fig.18C) but belonged to the same frequency band (~140-200 Hz). Auto-correlograms (up to 3 s) of HFO did not reveal any intrinsic slow rhythms in the occurrence of these events.

HFO coincided with sharp potentials in a band 1-20 Hz lasting 15 – 100 ms depending on HFO duration (fig. 15B, 16B). These sharp-potentials were clearly seen in the averaged waveforms (1-20 Hz band) triggered by HFO markers; the peak of such a sharp potential corresponded in the averaged waveforms with the maximal amplitude field-cycle of the HFO. However, many HFO epochs lacked a link with slow-band potentials.

Like in the hippocampus HFO in the BL and EPN were state dependent following temporal dynamics of the burst firing (Fig. 19, Tab.13). Maximal HFO numbers (up to 20/min in the EPN and 23 in the BL) were observed during SWS. In comparison, hippocampal ripples occurred up to 20/min during SWS, around 2/min during waking with tonic EMG activity and were virtually absent during PS and waking with phasic EMG. Frequency of BL/EPN HFO occurrence varied markedly in individual recordings and accross behavioural states. Further recordings to obtain longer epochs of PS waking periods free of movement artifacts are needed to clarify the state dependence of HFO in the EPN and BL.

Short and long scale correlation of amygdaloid and EPN activity with hippocampal ripples was also assessed both for HFO and single units. Averaged cross-correlograms were triggered by the positive peak of either temporal or dorsal hippocampal ripples for units (n=17 for EPN, and n=20 for BL) and field HFO from the same electrodes did not reveal a significant time-relation with any signal. Individual cross correlograms for single units were more heterogenous: some BL and EPN units tended to discharge well before (up to 2 s) the peak of hippocampal ripples but others fired at almost zero lag (Fig. 18A, B). Two neurons from BL displayed a right-shifted lag (several hundred ms) from a hippocampal ripple's positive peak. Hippocampal ripple triggered cross-correlograms for EPN and BL HFO peaks showed no lags.

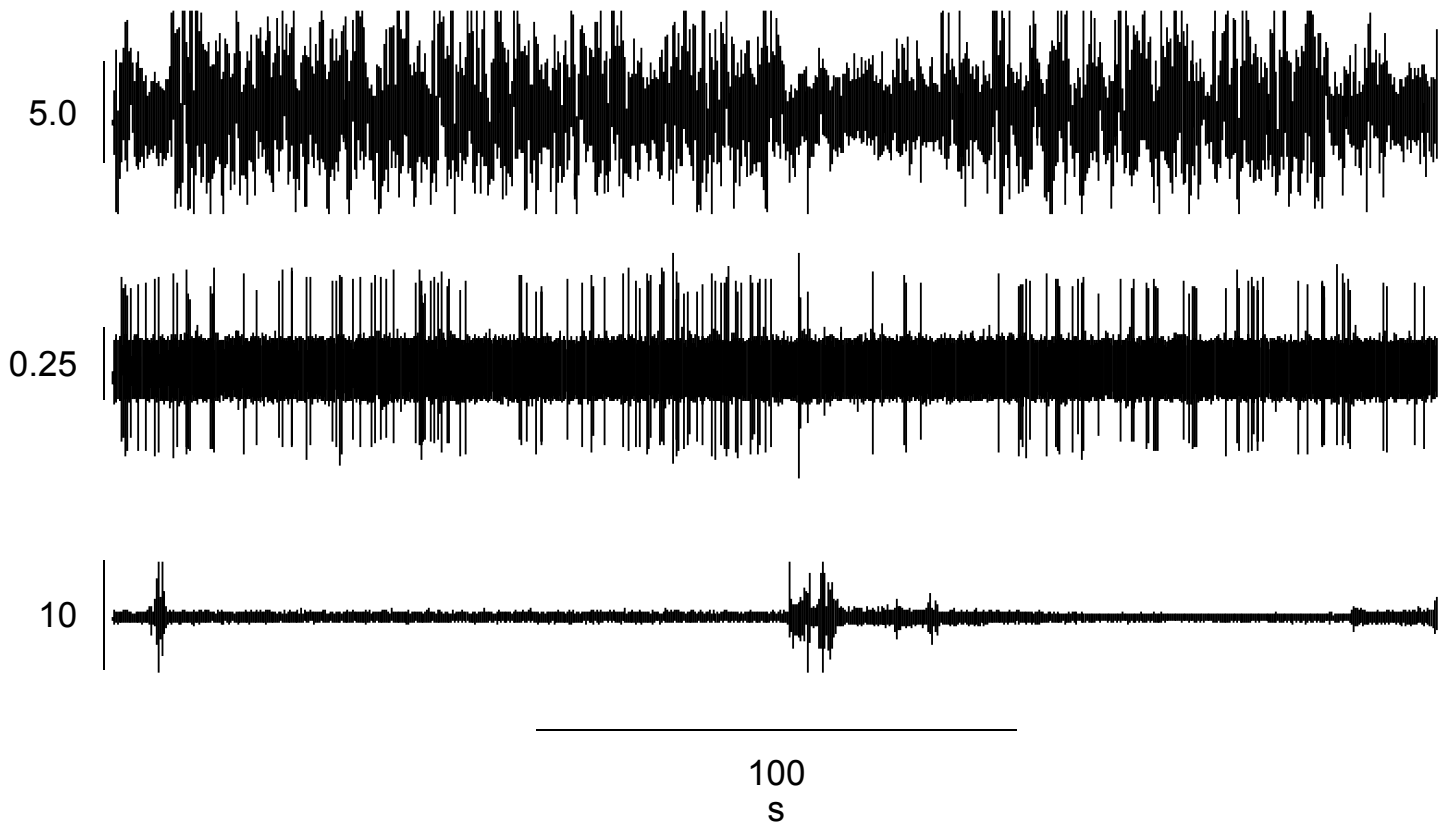

Fig.14. Representative example of the neuronal firing in the dorsal endopiriform nucleus, EPN (middle trace). The upper and the lower signals correspond to EEG of the dorsal CA1 region and EMG respectively. Waking epochs (theta rhythm on the hippocampla EEG and phasic EMG) were associlated with a decrease of firing in the EPN. Maximal discharge was observed during slow-wave sleep.

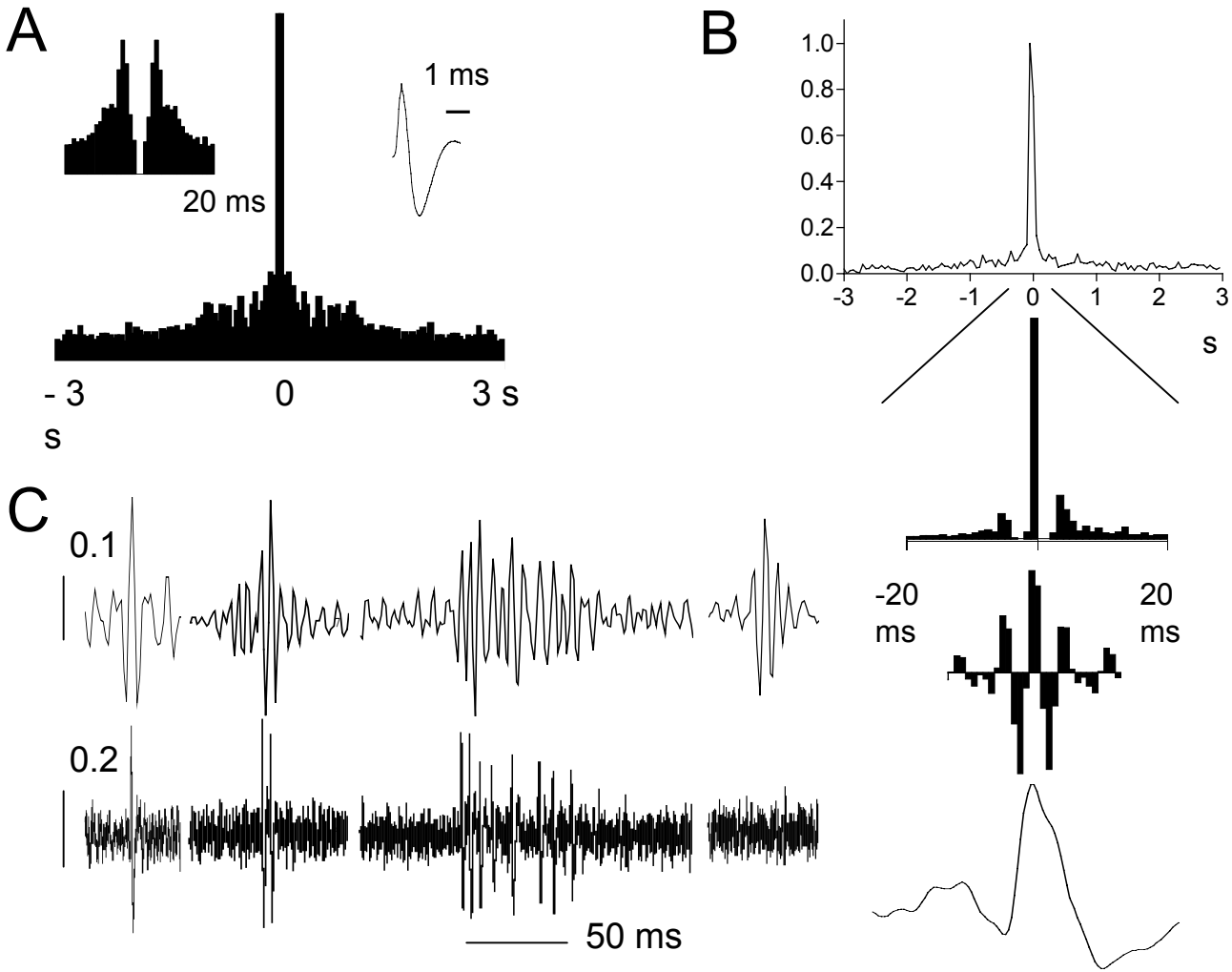

Fig. 15. HFO and neuronal firing in the EPN. **A**. Auto-correlogram of a single unit (bin width 50 ms). Insets show higher resolution autocorrelogram and spike waveform (bin width 0.5 ms, scale 1 ms). Note absence of interspike intervals shorter than 1 ms. **B**. Cross-correlogram between field signal and neuronal firing (n=9) triggered by a peak of HFO (upper trace). Higher resolution cross-correlogram showing phase relationships of unit firing and HFO peaks (middle). Each bin in the HFO waveform histogram has 1 ms width. Averaged waveform in 1-20 Hz band triggered by HFO peak (lower waveform). **C**. Representative examples of correspondence of unit spiking (lower trace) and number of cycles in HFO (upper trace). The last sweeps show an example of oscillatory epoch that was not accompanied by spiking. Bandpass filtered 500 Hz – 10 kHz and 140-250 Hz signals respectively.

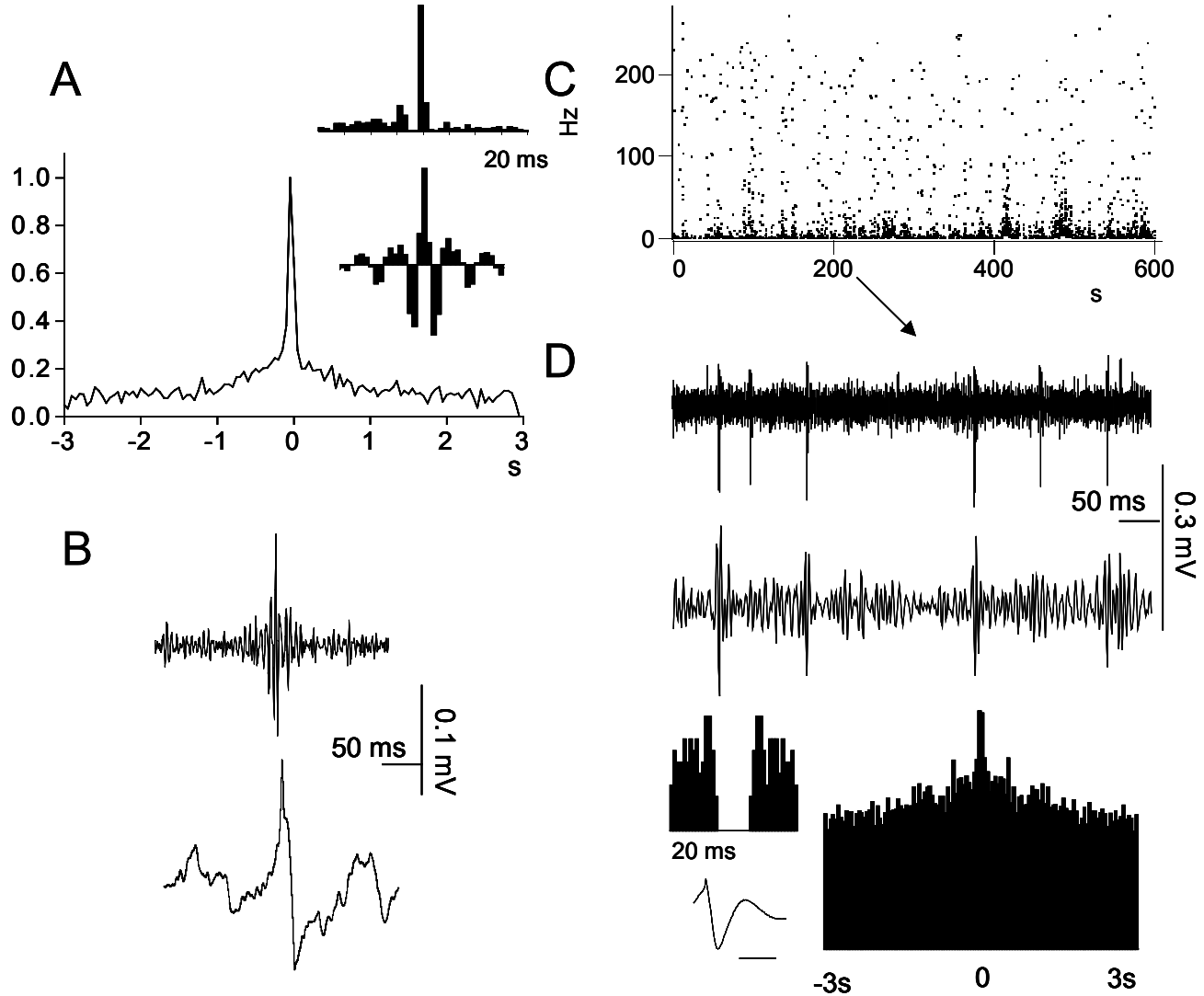

Fig. 16. HFO and neuronal firing in the BL. **A**. Cross-correlogram between the field signal and neuronal firing (n=8) triggered by a peak of HFO. Insets: higher resolution cross-correlogram showing phase relationships of unit firing and HFO peaks (upper) and HFO waveform histogram. Bin width 1 ms. **B**. Averaged waveforms (n=162) of HFO in 140-250 Hz band and an associated sharp potential in 1-20 Hz band triggered by HFO peak. **C**. Representative example of firing pattern of a BL unit (instantaneous frequency). **D**. Corresponding bandpass filtered 500 Hz – 10 kHz (upper) and 140-250 Hz (lower) signals respectively showing occurrence of single spikes during short HFO and sometimes longer HFO as well. Auto-correlogram of the unit (bin width 50 ms) with insets of higher resolution (0.5 ms bin width) and waveform.

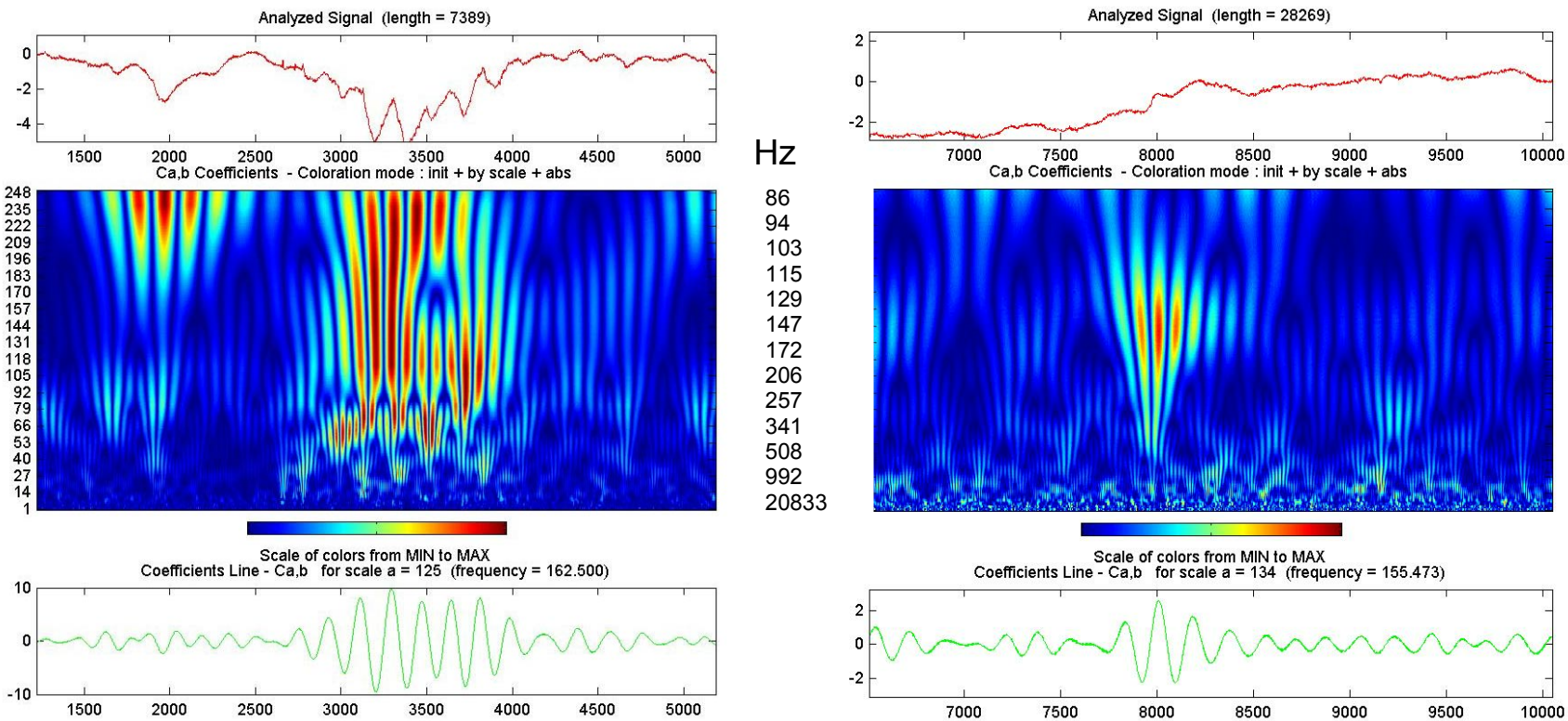

Fig. 17. Spectral features of the hippocampal ripple oscillations (right panels) and HFO in the BL (left panels), representative examples. Spectra (middle panels) represent Morlet wavelet coefficients plotted vs time (1 time unit = 0.04 ms). Median wavelet frequencies for corresponding wavelet transformation scales are plotted between panels. Top panels contain fragments of wide band signal analysed (sampled at 25 kHz) , lower panels represent coefficient lines at 162.5 Hz for hippocampus and at 155.5 Hz for amygdala. Note wide range of frequencies of both hippocampal and amygdaloid HFO and independence of HFO of neuronal activity at higher frequencies (above 992 Hz).

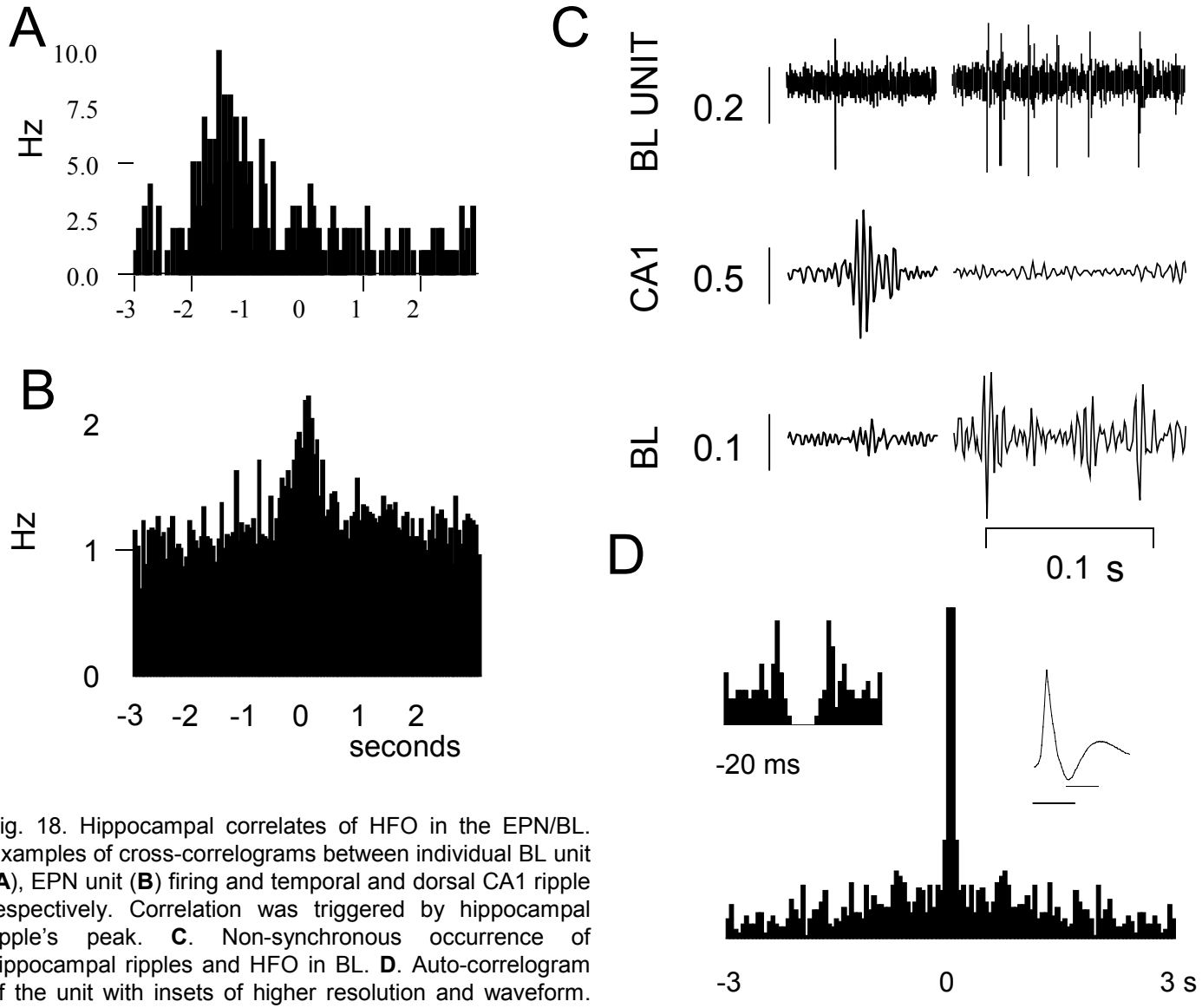

Fig. 18. Hippocampal correlates of HFO in the EPN/BL. Examples of cross-correlograms between individual BL unit (**A**), EPN unit (**B**) firing and temporal and dorsal CA1 ripple respectively. Correlation was triggered by hippocampal ripple's peak. **C**. Non-synchronous occurrence of hippocampal ripples and HFO in BL. **D**. Auto-correlogram of the unit with insets of higher resolution and waveform. Bin width in all correlograms 50 ms with exception of inset (0.5 ms).

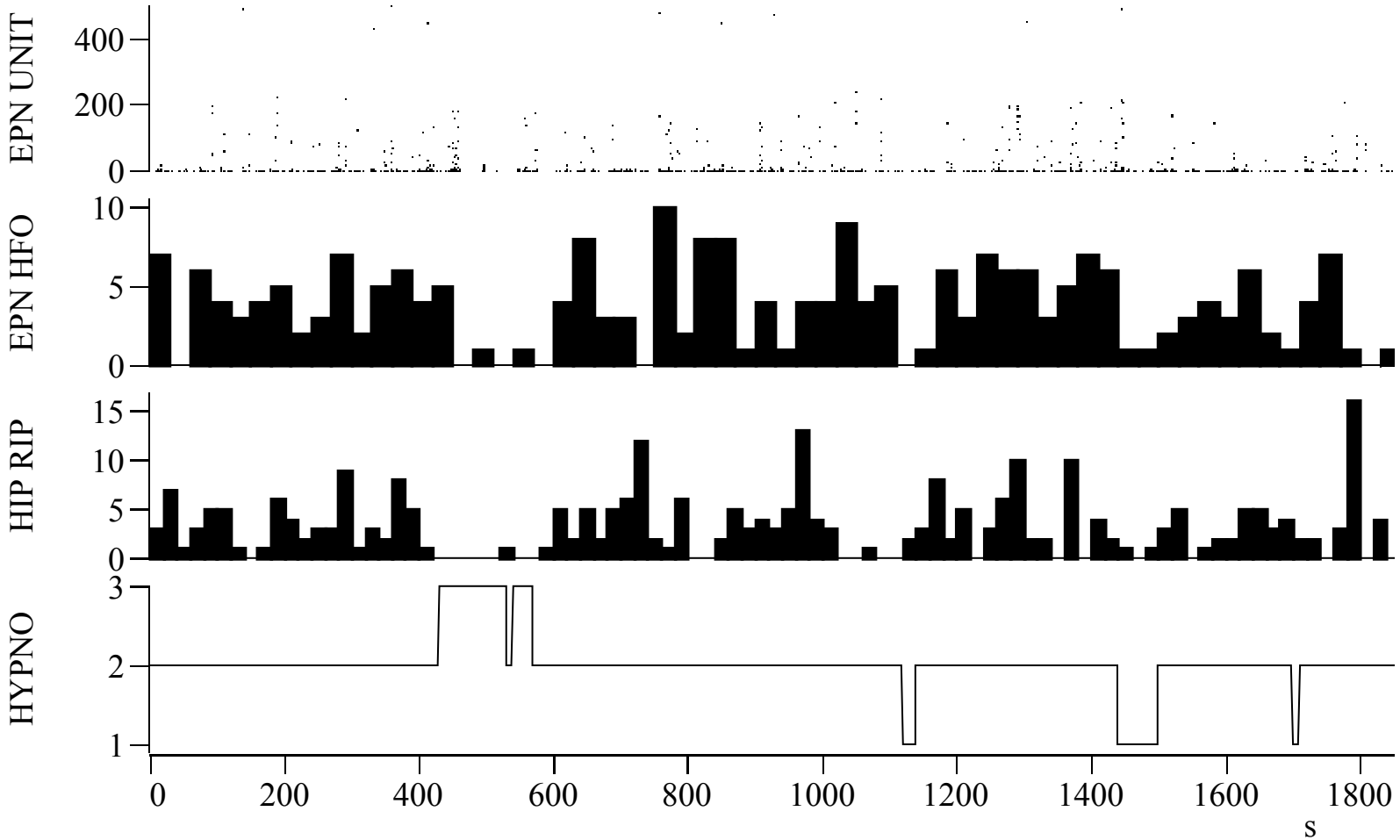

Fig. 19. State dependence of EPN neuronal firing (EPN UNIT), occurrence of HFO in the EPN (EPN HFO) and ripple oscillations in the temporal CA1 (HIP RIP). The number of oscillatory epochs is expressed as events/30 s. Hypnogram (HYPNO): 1 – waking, 2 – SWS, 3 – PS.

DISCUSSION

Methodological considerations.

Hippocampal ripple oscillations are known to display a clear state dependence. Namely their probability of occurrence is inversely correlated with the presence of theta oscillations (Buzsaki, 1986). That is why control of the vigilance state is a necessary condition in a study of ripple regulation to exclude a trivial relationship between ripple modulations and a drug effect on the hippocampal rhythmic state. This control was achieved by both an analysis of the hippocampal EEG spectra in the theta band and assessment of a vigilance state with a reference to neocortical EEG and EMG data. This approach is in agreement with data regarding the dependence of ripple occurrence on specific behaviors (Knoche et al., 2003) that could be explained by its correlation with theta activity.

To prevent possible systematic interactions of different treatments all drug administrations were performed in a randomized order. Three days inter-treatment intervals provided conditions for an effective drug clearance. The number of treatments received by an animal and, especially, the number of neurons recorded in a rat were minimized to avoid possible pharmacodynamic interactions and effects of plasticity (long-term hippocampal circuitry alterations due to down-regulation of receptors, behavioural changes related to conditioning). However the number of experimental manipulations in one animal could not be reduced to a single treatment (recording) due to a complex surgical procedure of electrode implantation. Using this design we successfully reproduced, for instance, the suppression of ripple oscillations by diazepam reported previously by Buzsaki (1986).
Single unit recordings were performed using microwire techniques with a template-based unit isolation. Recording neuronal activity from two microwires in a bundle does not allow capturing as many units at the same time as utilizing the tetrode methodology. Our approach also did not reliably discriminate single units of similar amplitudes. This precluded simultaneous recording of neuronal activity and local field potentials in the hippocampus, where cells are densely packed in layers, producing spikes of similar amplitudes. These data would have been valuable for correlational analysis with amygdaloid activity. On the other hand, the architecture of the amygdala is well suited for neuronal recording with microwires.

Sleep-related dynamics of ripple oscillations.

Our results indicate a dependence of the post-waking “rebound” of ripple occurrence on the duration of waking. Intraripple frequency is elevated following waking regardless of its duration. Recovery of ripple occurrence and frequency from the rebound takes place mostly

during SWS. In contrast, PS differentially modifies ripple occurrence dynamics during and after the recovery period. This clearly indicates that sleep phases regulate the temporal pattern and intrinsic features of ripples (Ponomarenko et al., resubmitted). This complements and extends data from Kudrimoti et al (1999) who have shown the influence of a spatial experience on ripple occurrence during the following SWS.

Although the first SWS following modafinil-induced waking occurred earlier than that after amphetamine treatment, the rebound of ripple occurrence correlated with the waking duration in all treatment groups and across groups. Conversely, a similar duration of waking after both stimulants in the cat resulted in a ripple rebound of similar extent (our unpublished data). There were also no differences in the recovery time course. Similar trends were seen in sleep deprivation experiments. Thus the reinforcing potencies of modafinil and amphetamine (Bizot, 1998;Gold and Balster, 1996;Wisor et al., 2001) did probably not interfere with ripple occurrence rebound. It is likely that the major action that affected ripple occurrence rebound was the theta activity-promoting property of modafinil and amphetamine.

More complex results were obtained regarding rebounds of intraripple frequency and event amplitude. The intraripple frequency was elevated by all treatments but displayed no clear correlation with the waking duration. Remarkably, the largest increase in intraripple frequency was found following sleep deprivation, when the rat was in ongoing contact with the experimenter and novel objects. The fact that the frequency was increased selectively in the population of fast ripples (>140 Hz) suggests an origin of the phenomenon in the CA1 network (Csicsvari et al., 1999a). Slower ripple events, reflecting synchrony in CA3, increased in number but not in frequency.

Treatment with amphetamine evoked a robust elevation of ripple amplitude. This effect was specific for amphetamine, not being observed in other experimental conditions. One explanation for this might be an interference with the depth of SWS during rebound in the delta frequency band, characteristic for amphetamine (Edgar and Seidel, 1997). However, we did not find correlations between power in the delta band and any of the ripples intrinsic features. Another possibility is a differential recruitment of aminergic systems by amphetamine and modafinil or natural waking (Duteil et al., 1990;Jouvet et al., 1991;Wisor et al., 2001). Modulatory actions of amine transmitters upon ripple oscillations in freely behaving rats (Knoche et al., 2003) have been suggested to be mediated via multiple cell type-specific effects of amines (histamine) in the hippocampus and medial septum. The interplay of subcortical aminergic inputs during SWS can at least in part explain the observed rebound of ripple occurrence, frequency and amplitude.

The decay of ripples during SWS might be related to the known fall in adenosine levels during this period in the hippocampus (Huston et al., 1996). A1-receptor activation inhibits pyramidal cells and their excitatory inputs directly while A2 receptor activation excites interneurons in the str. oriens (after priming during waking by histamine (Haas et al., 1997), which are likely involved in the setting of high frequency oscillation patterns (Gerber et al., 1989;Mitchell et al., 1993). However, in preliminary experiments we did not find changes of ripple rebound and its recovery time after caffeine-evoked waking.

Modafinil, unlike amphetamine, does not elicit a PS rebound (Touret et al., 1995). Recovery from ripple rebound after modafinil treatment was in most cases complete within one or two consolidated SWS episodes separated by short waking. Therefore we did not detect any peculiarities associated with PS during the recovery period in modafinil treated rats. With respect to the wake-promoting effect of modafinil our results are in agreement with the known action of the drug in the same rat strain (Edgar and Seidel, 1997).

Reactivation of hippocampal neuronal assemblies during SWS may underly the ripple rebound. It has been shown that cell pairs in the CA1 region with overlapping place fields display an increased synchrony during post-task SWS (Skaggs and McNaughton, 1996;Wilson and McNaughton, 1994) and PS episodes (Hirase et al., 2001;Louie and Wilson, 2001). It is not known whether “new” and “old” firing patterns are expressed within different ripple populations. If this were the case during post-treatment SWS an additional number of ripples of higher frequency and amplitude could contain newly acquired firing patterns. In this scenario the addition of new firing motifs to the hippocampal network activity during PS depends to some extent on the processing of waking-related information during SWS.

The fact that transition sleep took place more often before PS that evoked an increase of ripple occurrence during subsequent SWS might be linked to the suggested role of sleep sequences containing transition sleep in memory processing (Piscopo et al., 2001;Vescia et al., 1996). A systematic analysis of transition sleep combined with an examination of hippocampal firing patterns in different sleep phases is required for further conclusions.

In summary, we suggest that the pattern of ripple occurrence during SWS is a result of interplay of two factors. First, the well-known dependence of ripple occurrence on the depth of SWS and, second, the decay of ripple numbers during SWS reported here. In turn, the initial probability of ripple occurrence at the beginning of a SWS episode is determined by the length and/or nature of the preceding state, waking or PS, and by ripple occurrence at the end of the previous SWS. Results presented in this paper may be pertinent to the temporal dynamics of ripples in humans: after long-term waking during daytime, ripple occurrence and

frequency should be strongly elevated at the beginning of the night sleep. The PS-related dynamics indicate a differential role for PS in hippocampal processing during early vs. late-night sleep.

Benzodiazepine pharmacology of ripple oscillations.

The profound inhibitory action of diazepam, 1 mg/kg, upon occurrence of ripple oscillations is consistent with an earlier report (Buzsaki, 1986). This abolishing of ripples is apparently associated with an increased amplitude of IPSPs on both pyramidal cells and inhibitory interneurons in CA3 and CA1 that would prevent its threshold synchronization (Csicsvari et al., 1999a). Selective ligand for α1 subunit-containing $GABA_A$ receptors (BZ/ω1 site) zolpidem also evoked reduction of ripple occurrence. $GABA_A$ receptor subunits are differentially expressed at the different classes of inhibitory synapses on CA1 pyramidal cells. Fast spiking basket cell inputs appear to utilize α1-containing, high-affinity zolpidem receptors to a greater degree than do regular spiking basket cell- and bistratified cell- inputs (Thomson et al., 2000). Thus the population of regular spiking basket interneurons may be more involved in the generation of oscillatory IPSPs on pyramidal cells during ripples. Another possibility is an involvement of the mentioned classes of interneurons in sharp-wave related synchronization in CA3.

Diazepam, when given 0.1 mg/kg, did not change the probability of rippe occurrence and ripple amplitude, but still reduced ripple duration and frequency. Amplitude of ripples is correlated with a number of CA1 cells involved (Csicsvari et al., 1999a). Thus determinants of ripple amplitude might be the magnitude of sharp wave–related excitatory drive upon CA1 cells (dependent on an inhibition in CA3 area) and interneuronal inhibition in CA1. Ripple duration is related to the duration of a sharp wave and, again, mostly dependent on CA3 inhibition. Intraripple frequency seems to be the only parameter attributable to CA1 network. However, intraripple freqency is also, to some extent, dependent on the magnitude of sharp wave–related excitation in CA1 since ripples of higher amplitude tend to have higher frequency. These two parameters were differentially affected by diazepam, 0.1 mg/kg, indicating reduction of intraripple frequency due to increased duration of IPSPs on CA1 pyramids and/or reduction of firing rated of CA1 interneurons during ripples. Earlier termination of sharp wave-related burst in CA3 probably underlie effect of diazepam upon ripple duration. On the other hand, terminaton of sharp waves was delayed by selective potentiation of IPSPs mediated by BZ/ω1 site containing $GABA_A$ receptors. Possible explanation of this paradoxical finding might be preferential localization of BZ/ω1 sites in

inerneuron-to-interneuron synapses in CA3. This would lead to increased inhibition of the pyramidal cell innervating interneurons as sharp wave burst evolves due to recurrent connectivity and might result in the second wave of poplation synchronization in CA3 and double-peak ripple in CA1. Thus shunting (perisomatic) inhibition of CA3 pyramids by certain subclass of basket interneurons (expressing BZ/ω1 sites) could terminate sharp wave burst. In this scenario, coordinated desinhibition of CA3 pyramidal cells by another subclass of interneurons (for instance, regular spiking basket cells) would result in initiation of a sharp wave. The later synapses could also utilize BZ/ω1 site containing $GABA_A$ receptors, explaining reduction of ripple amplitude and probability of occurrence by zolpidem. Recent findings by Klausberger et al. (2003) support the differential involvement of interneuronal classes in the orchestration of pyramidal cell discharge during hippocampal oscillations.

The low-efficacy partial agonist (antagonist) flumazenil blocks benzodiazepine actions at receptors containing the α1, α2/3 or α5 subunits, but is an agonist at receptors containing the α4 subunit (Whittemore et al., 1996). Flumazenil alone decreases the amplitude of IPSPs evoked by basket cells, suggesting an antagonism at an endogenous BZ-site ligand (Izquierdo and Medina, 1991; Thomson et al., 2000). Thus one explanation for the suppression of ripples by flumazenil is the prevention of an endogenous modulation of the BZ-site that might facilitate oscillatory IPSPs during ripples. Another possibility is an enhanced cholinergic stimulation of the hippocampus due to disinhibition of the medial septum by flumazenil (Moor et al., 1998). This is known to shift the oscillatory state of the hippocampus towards theta. However it would not explain the observed light SWS along with the large irregular hippocampal activity during most periods of ripple suppression following flumazenil treatment. More detailed dose-response information for flumazenil would help to defferentiate between mentioned possibilities.

Histaminergic modulation of synchronization in the hippocampus.

We have confirmed an increase of ripple occurrence by H_1-receptor antagonists (Knoche et al., 2003) using the systemic route of drug administration and have now detected a new consequence of H_2-receptor antagonism – a transient suppression of ripple oscillatory activity (Ponomarenko et al, submitted).

I.c.v. pyrilamine and ketotifen (H_1-antagonists) increase an occurrence of ripple oscillatory epochs and i.c.v. histamine decreases ripple numbers (Knoche et al., 2003) independent of the known behavioural actions of H_1-antagonists. On the basis of the regional

distribution of drugs after i.c.v. injection these effects were attributed predominatly to blockage of tonic histaminergic excitation of the medial septal cholinergic neurons (Gorelova and Reiner, 1997). This would reduce tonic cholinergic excitation of hippocampal pyramidal cells and interneurons that is known to facilitate theta-synchronization. The present results show a similar pattern of ripple modulation when an H_1-antagonist affected the hippocampus and the medial septum simultaneously. H1-receptor activation inhibits hippocampal pyramidal cells (Selbach et al., 1997). In addition H1-antihistaminics are potentially epileptogenic while H3- receptor antagonists display an anticonvulsant effect (Yokoyama et al., 1992;Yokoyama et al., 1993). Thus a tonic inhibitory action of histamine upon ripple oscillations via H_1-receptors is coordinated at different levels of the septo-hippocampal network.

The blockade of H1-receptors has been reported to disinhibit cognitive processes (Alvarez and Banzan, 1996) and to increase learning ability (Frisch et al., 1997). These findings and the increase of ripple occurrence after icv. injection of H1-antagonists described here are in keeping with Buzsaki´s hypothesis of a ripple-related memory forming process (Buzsaki, 1989).

Along with the modulation of the oscillatory state, the histaminergic system can adaptively improve the precision of spatial encoding by the hippocampal networks. Representation of space by activity of pyramidal neurons is achieved both by increased firing rate within place field and by precise timing of the discharge in relation to phase of the field theta-rhythm (O'Keefe, 1976;O'Keefe and Recce, 1993). The later phenomenon is refered as theta-phase precession. Computer simulation based on the somato-dendritic interference model of the theta phase-precession (Harris et al., 2002) has shown that speed of the phase advancement depends on the suppression of the Ca^{2+}-dependent K^+-channel activity responsible for the slow afterhyperpolirazation (AHP) in the model pyramidal cells. Inhibition of the AHP by histamine is obviously determined by the histaminergic system activity in sleep-waking cycle. It is maximal during active waking and virtually absent during PS (Vanni Mercier et al., 1984). At the same time locomotion differs from PS in 10-20-fold compressed “spatial” firing of place cells during the later state. It would require a faster theta-phase precession during PS. I suggest that state-dependent activity of the histaminergic system (along with other aminergic systems) adjusts hippocampal encoding precission to a global network state via adaptive regulation of ionic conductances.

The H_2-receptor dependent actions of histamine described in vitro can partially explain the transient inhibitory action of systemic zolantidine on ripple occurrence. H_2-receptor

activation blocks pyramidal cell accommodation (Haas and Konnerth, 1983) and strongly excites interneurons (Haas et al., 1997). On the other hand it lowers the maximum firing frequency of inhibitory neurons, which in turn negatively modulates high-frequency population oscillations recorded in principal cell layers of CA3 in vitro (Atzori et al., 2000).

Why do different receptor subtypes of the same transmitter not provide for a coordinated modulation of ripple occurrence? I suggest that a given monoamine does not unidirectionally modulate patterns of population synchrony. Its action might be dependent on the tone of other modulatory systems and cross-talk of intracellular signal pathways (Wang et al., 1999).

High-frequency oscillations in the BL and EPN.

I have reported here the first evidence of high-frequency (200 Hz) field oscillations phase-locked with neuronal discharge in BL and the adjacent EPN (Ponomarenko et al., 2003). These HFO are independent of the fast synchronous population patterns in the CA3-CA1 axis and most likely also from those in the parahippocampal cortices downstream from CA1 (Buzsaki, 1986;Buzsaki et al., 1992; Chrobak and Buzsaki, 1996). Thus temporal CA1/subicular afferents to BL (van Groen and Wyss, 1990) are probably not responsible for synchronizing BL neurons at the scale of tens of milliseconds. Another major finding is the similarity of neuronal firing and associated EEG events of EPN and BL that provides further support for the functional resemblance of these nuclei.

The firing behaviour of a majority of the recorded units in the amygdala corresponds to the class of bursting projection neurons of BL (Pare and Gaudreau, 1996;Rainnie et al., 1993; Rosenkranz and Grace, 2001;Washburn and Moises, 1992). Results on state dependent modulation of BL neuron firing complement previously published data in the behaving rats (Bordi et al., 1993). In the cat, activity of these BL cells is believed to initiate the generation of sharp potentials in the entorhinal cortex and does not correlate with population events beyond the dentate gyrus (Pare et al., 1995a). We found no reliable link between HFO in BL or EPN with CA1 ripples in the rat.

The burst firing superimposed on field HFO is in keeping with in vitro findings of populational discharge in the EPN (Tseng and Haberly, 1989). Bursting of principal cells in the EPN depends on low and high-voltage-activated Ca^{2+} currents with fast inactivation kinetics (de Curtis et al., 1991). In light of the extensive collateral connections between EPN principal neurons (Behan and Haberly, 1999) this bursting can entrain a large number of cells in population synchrony.

The presence of sharp field potentials superimposed on HFO suggests a mechanism analogous to the known interplay of sharp wave-associated dendritic depolarization and oscillatory somatic inhibition in CA1 (Ylinen et al., 1995a). The basolateral amygdaloid circuitry (L) displays $GABA_B$ -receptor dependent attenuation of interneuronal IPSCs in the principal cells under the conditions of paired pulse stimulation of putative cortical and thalamic afferents (Szinyei et al., 2000). Furthermore, specific subsets of BL principal neurons generate repetitive or single spike bursts in response to prolonged depolarization (Pare et al., 1995b). Short-scale synchronous firing of BL projection neurons receiving different inputs may organize the precise timing of multimodal information outflow to other amygdaloid nuclei and extraamygdaloid regions.

It is assumed that the population discharge of EPN neurons depolarizes target pyramidal cells throughout the olfactory cortices. The EPN and basolateral amygdaloid complex might constitute part of the subplate layer of the temporal and piriform cortices; these regions are among the (peri)amygdaloid nuclei that give rise to an excitatory output (Swanson and Petrovich, 1998). They use the common principles of efferent temporal coding via focal or global population synchrony though they convey signals of different modalities.

CONCLUSIONS

1. Waking in the rat elevates occurrence of hippocampal ripple oscillations during the following SWS episode in relation to the preceding one.
2. Ripple occurrence progressively decays during SWS episodes.
3. PS acts to reduce elevated ripple numbers but evokes an increase of ripple occurrence from baseline, similar to waking.
4. The non-selective benzodiazepine agonist diazepam reduces occurrence, frequency, amplitude and duration of ripple oscillations.
5. The ω1 site–selective benzodiazepine agonist zolpidem decreases occurence, amplitude and frequency but elevates duration of ripples.
6. The benzodiazepine antagonist flumazenil reduces number of ripples.
7. The histaminergic system exerts divergent effects upon ripple oscillations: systemic administration of an antagonist of H_1-receptors elevates the number of ripples, whilst an antagonist of H_2-receptors produces a transient suppression.
8. Populational neuronal activity in the basolateral nucleus (BL) of the amygdala and the dorsal endopiriform nucleus (EPN) displays state-dependent ~200 Hz synchronization.
9. High-frequency oscillations and associated neuronal firing in the BL and EPN are independent from ripple oscillations in both temporal and septal CA1 fields of the hippocampus.
10. Neuronal firing and EEG patterns are similar in the EPN and BL.

REFERENCE LIST

Aggleton J.P. (2000) The amygdala. Oxford: Oxford University Press.

Aggleton JP (1993) The contribution of the amygdala to normal and abnormal emotional states. Trends Neurosci 16: 328-333.

Akaoka H, Roussel B, Lin JS, Chouvet G, Jouvet M (1991) Effect of modafinil and amphetamine on the rat catecholaminergic neuron activity. Neurosci Lett 123: 20-22.

Aleksanov SN (1983) [Coherent functions of the electrical activity of the hippocampus, amygdala and frontal cortex during alimentary instrumental reflexes in the dog]. Zh Vyssh Nerv Deiat Im I P Pavlova 33: 694-699.

Alvarez EO, Banzan AM (1995) Effects of localized histamine microinjections into the hippocampal formation on the retrieval of a one-way active avoidance response in rats. J Neural Transm Gen Sect 101: 201-211.

Alvarez EO, Banzan AM (1996) Hippocampal histamine receptors: possible role on the mechanisms of memory in the rat, II. J Neural Transm 103: 147-156.

Alvarez XA, Franco A, Fernandez Novoa L, Cacabelos R (1994) Effects of neurotoxic lesions in histaminergic neurons on brain tumor necrosis factor levels. Agents Actions 41 Spec No: C70-2.

Amaral DG, Dolorfo C, Alvarez-Royo P (1991) Organization of CA1 projections to the subiculum: a PHA-L analysis in the rat. Hippocampus 1: 415-435.

Amaral DG, Witter MP (1989) The three-dimensional organization of the hippocampal formation: a review of anatomical data. Neuroscience 31: 571-591.

Arrang J-M, Garbarg M, Schwartz J-C (1983) Auto-inhibition of brain histamine release mediated by a novel class (H_3) of histamine receptor. Nature 302: 832-837.

Atzori M, Lau D, Tansey EP, Chow A, Ozaita A, Rudy B, McBain CJ (2000) H2 histamine receptor-phosphorylation of Kv3.2 modulates interneuron fast spiking. Nat Neurosci 3: 791-798.

Baudry M, Martres MP, Schwartz JC (1975) H1 and H2 receptors in the histamine-induced accumulation of cyclic AMP in guinea pig brain slices. Nature 253: 362-364.

Behan M, Haberly LB (1999) Intrinsic and efferent connections of the endopiriform nucleus in rat. J Comp Neurol 408: 532-548.

Bekkers JM, Stevens CF (1993) NMDA receptors at excitatory synapses in the hippocampus: test of a theory of magnesium block. Neurosci Lett 156: 73-77.

Bizot JC (1998) Effects of various drugs including organophosphorus compounds (OPC) and therapeutic compounds against OPC on DRL responding. Pharmacol Biochem Behav 59: 1069-1080.

Bland BH (1986) The physiology and pharmacology of hippocampal formation theta rhythms. Prog Neurobiol 26: 1-54.

Blandina P, Giorgetti M, Bartolini L, Cecchi M, Timmerman H, Leurs R, Pepeu G, Giovannini MG (1996) Inhibition of cortical acetylcholine release and cognitive performance by histamine H3 receptor activation in rats. Br J Pharmacol 119: 1656-1664.

Blasco-Ibanez JM, Freund TF (1995) Synaptic input of horizontal interneurons in stratum oriens of the hippocampal CA1 subfield: structural basis of feed-back activation. Eur J Neurosci 7: 2170-2180.

Bliss TV, Collingridge GL (1993) A synaptic model of memory: long-term potentiation in the hippocampus. Nature 361: 31-39.

Bordi F, LeDoux J, Clugnet MC, Pavlides C (1993) Single-unit activity in the lateral nucleus of the amygdala and overlying areas of the striatum in freely behaving rats: rates, discharge patterns, and responses to acoustic stimuli. Behav Neurosci 107: 757-769.

Borhegyi Z, Magloczky Z, Acsady L, Freund TF (1998) The supramammillary nucleus innervates cholinergic and GABAergic neurons in the medial septum-diagonal band of Broca complex. Neuroscience 82: 1053-1065.

Bragin A, Engel J, Jr., Wilson CL, Fried I, Buzsaki G (1999a) High-frequency oscillations in human brain. Hippocampus 9: 137-142.

Bragin A, Engel J, Jr., Wilson CL, Vizentin E, Mathern GW (1999b) Electrophysiologic analysis of a chronic seizure model after unilateral hippocampal KA injection. Epilepsia 40: 1210-1221.

Bragin A, Jando G, Nadasdy Z, Hetke J, Wise K, Buzsaki G (1995a) Gamma (40-100 Hz) oscillation in the hippocampus of the behaving rat. J Neurosci 15: 47-60.

Bragin A, Jando G, Nadasdy Z, van Landeghem M, Buzsaki G (1995b) Dentate EEG spikes and associated interneuronal population bursts in the hippocampal hilar region of the rat. J Neurophysiol 73: 1691-1705.

Braun AR, Balkin TJ, Wesenten NJ, Carson RE, Varga M, Baldwin P, Selbie S, Belenky G, Herscovitch P (1997) Regional cerebral blood flow throughout the sleep-wake cycle. An H2(15)O PET study. Brain 120 (Pt 7): 1173-1197.

Brazhnik ES, Fox SE (1999) Action potentials and relations to the theta rhythm of medial septal neurons in vivo. Exp Brain Res 127: 244-258.

Brown, R. E. Histaminergic modulation of synaptic transmission and plasticity in the hippocampus of the rat. 1996. Otto-von-Guericke University, Magdeburg, Germany. 1996. Ref Type: Thesis/Dissertation

Brown RE, Fedorov NB, Haas HL, Reymann KG (1995) Histaminergic modulation of synaptic plasticity in area CA1 of rat hippocampal slices. Neuropharmacology 34: 181-190.

Brown RE, Reymann KG (1996) Histamine H_3 receptor-mediated depression of synaptic transmission in the dentate gyrus of the rat *in vitro*. J Physiol Lond 496: 175-184.

Buhl EH, Szilagyi T, Halasy K, Somogyi P (1996) Physiological properties of anatomically identified basket and bistratified cells in the CA1 area of the rat hippocampus in vitro. Hippocampus 6: 294-305.

Bullock TH, Buzsaki G, McClune MC (1990) Coherence of compound field potentials reveals discontinuities in the CA1-subiculum of the hippocampus in freely-moving rats. Neuroscience 38: 609-619.

Buzsaki G (1986) Hippocampal sharp waves: their origin and significance. Brain Res 398: 242-252.

Buzsaki G (1989) Two-stage model of memory trace formation: a role for "noisy" brain states. Neuroscience 31: 551-570.

Buzsaki G (1996) The hippocampo-neocortical dialogue. Cereb Cortex 6: 81-92.

Buzsaki G (2002) Theta oscillations in the hippocampus. Neuron 33: 325-340.

Buzsaki G, Eidelberg E (1981) Commissural projection to the dentate gyrus of the rat: evidence for feed-forward inhibition. Brain Res 230: 346-350.

Buzsaki G, Freund TF, Bayardo F, Somogyi P (1989) Ischemia-induced changes in the electrical activity of the hippocampus. Exp Brain Res 78: 268-278.

Buzsaki G, Haas HL, Anderson EG (1987a) Long-term potentiation induced by physiologically relevant stimulus patterns. Brain Res 435: 331-333.

Buzsaki G, Gage FH, Czopf J, Bjorklund A (1987b) Restoration of rhythmic slow activity (theta) in the subcortically denervated hippocampus by fetal CNS transplants. Brain Res 400: 334-347.

Buzsaki G, Horvath Z, Urioste R, Hetke J, Wise K (1992) High-frequency network oscillation in the hippocampus. Science 256: 1025-1027.

Buzsaki G, Leung LW, Vanderwolf CH (1983) Cellular bases of hippocampal EEG in the behaving rat. Brain Res 287: 139-171.

Cahill L, McGaugh JL (1998) Mechanisms of emotional arousal and lasting declarative memory. Trends Neurosci 21: 294-299.

Canteras NS, Simerly RB, Swanson LW (1992) Connections of the posterior nucleus of the amygdala. J Comp Neurol 324: 143-179.

Canteras NS, Simerly RB, Swanson LW (1995) Organization of projections from the medial nucleus of the amygdala: a PHAL study in the rat. J Comp Neurol 360: 213-245.

Cesare CM, Smith KL, Rice FL, Swann JW (1996) Anatomical properties of fast spiking cells that initiate synchronized population discharges in immature hippocampus. Neuroscience 75: 83-97.

Chang RS, Tran VT, Snyder SH (1979) Heterogeneity of histamine H1-receptors: species variations in [3H]mepyramine binding of brain membranes. J Neurochem 32: 1653-1663.

Chapman CA, Lacaille JC (1999) Cholinergic induction of theta-frequency oscillations in hippocampal inhibitory interneurons and pacing of pyramidal cell firing. J Neurosci 19: 8637-8645.

Charpak S, Pare D, Llinas R (1995) The entorhinal cortex entrains fast CA1 hippocampal oscillations in the anaesthetized guinea-pig: role of the monosynaptic component of the perforant path. Eur J Neurosci 7: 1548-1557.

Chemelli RM, Willie JT, Sinton CM, Elmquist JK, Scammell T, Lee C, Richardson JA, Williams SC, Xiong Y, Kisanuki Y, Fitch TE, Nakazato M, Hammer RE, Saper CB, Yanagisawa M (1999) Narcolepsy in orexin knockout mice: molecular genetics of sleep regulation. Cell 98: 437-451.

Chepurnov, S. A. and Chepurnova, N. E. Amygdaloid complex of the brain. 1981. Moscow, Moscow University Press.

Chrobak JJ, Buzsaki G (1994) Selective activation of deep layer (V-VI) retrohippocampal cortical neurons during hippocampal sharp waves in the behaving rat. J Neurosci 14: 6160-6170.

Chrobak JJ, Buzsaki G (1996) High-frequency oscillations in the output networks of the hippocampal- entorhinal axis of the freely behaving rat. J Neurosci 16: 3056-3066.

Chrobak JJ, Buzsaki G (1998) Gamma oscillations in the entorhinal cortex of the freely behaving rat. J Neurosci 18: 388-398.

Chrobak JJ, Lorincz A, Buzsaki G (2000) Physiological patterns in the hippocampo-entorhinal cortex system. Hippocampus 10: 457-465.

Cohn CK, Ball GG, Hirsch J (1973) Histamine: effect on self-stimulation. Science 180: 757-758.

Collins DR, Lang EJ, Pare D (1999) Spontaneous activity of the perirhinal cortex in behaving cats. Neuroscience 89: 1025-1039.

Collins DR, Pelletier JG, Pare D (2001) Slow and fast (gamma) neuronal oscillations in the perirhinal cortex and lateral amygdala. J Neurophysiol 85: 1661-1672.

Cote NK, Harrington ME (1993) Histamine phase shifts the circadian clock in a manner similar to light. Brain Res 613: 149-151.

Csicsvari J, Hirase H, Czurko A, Buzsaki G (1998) Reliability and state dependence of pyramidal cell-interneuron synapses in the hippocampus: an ensemble approach in the behaving rat. Neuron 21: 179-189.

Csicsvari J, Hirase H, Czurko A, Mamiya A, Buzsaki G (1999a) Fast network oscillations in the hippocampal CA1 region of the behaving rat. J Neurosci 19: RC20.

Csicsvari J, Hirase H, Czurko A, Mamiya A, Buzsaki G (1999b) Oscillatory coupling of hippocampal pyramidal cells and interneurons in the behaving Rat. J Neurosci 19: 274-287.

Datta S (2000) Avoidance task training potentiates phasic pontine-wave density in the rat: A mechanism for sleep-dependent plasticity. J Neurosci 20: 8607-8613.

Dave AS, Margoliash D (2000) Song replay during sleep and computational rules for sensorimotor vocal learning. Science 290: 812-816.

de Curtis M, Pare D, Llinas RR (1991) The electrophysiology of the hippocampal circuit in the isolated and perfused adult mammalian brain in vitro. Hippocampus 1: 341-354.

De Koninck J, Lorrain D, Christ G, Proulx G, Coulombe D (1989) Intensive language learning and increases in rapid eye movement sleep: evidence of a performance factor. Int J Psychophysiol 8: 43-47.

Denham MJ, Borisyuk RM (2000) A model of theta rhythm production in the septal-hippocampal system and its modulation by ascending brain stem pathways. Hippocampus 10: 698-716.

Deuchars J, Thomson AM (1996) CA1 pyramid-pyramid connections in rat hippocampus in vitro: dual intracellular recordings with biocytin filling. Neuroscience 74: 1009-1018.

Dichter M, Spencer WA (1969) Penicillin-induced interictal discharges from the cat hippocampus. II. Mechanisms underlying origin and restriction. J Neurophysiol 32: 663-687.

Diewald L, Heimrich B, Busselberg D, Watanabe T, Haas HL (1997) Histaminergic system in co-cultures of hippocampus and posterior hypothalamus: a morphological and electrophysiological study in the rat. Eur J Neurosci 9: 2406-2413.

Dragoi G, Carpi D, Recce M, Csicsvari J, Buzsaki G (1999) Interactions between hippocampus and medial septum during sharp waves and theta oscillation in the behaving rat. J Neurosci 19: 6191-6199.

Draguhn A, Traub RD, Schmitz D, Jefferys JG (1998) Electrical coupling underlies high-frequency oscillations in the hippocampus in vitro. Nature 394: 189-192.

Duteil J, Rambert FA, Pessonnier J, Hermant JF, Gombert R, Assous E (1990) Central alpha 1-adrenergic stimulation in relation to the behaviour stimulating effect of modafinil; studies with experimental animals. Eur J Pharmacol 180: 49-58.

Eaton SJ, Cote NK, Harrington ME (1995) Histamine synthesis inhibition reduces light-induced phase shifts of circadian rhythms. Brain Res 695: 227-230.

Edgar DM, Seidel WF (1997) Modafinil induces wakefulness without intensifying motor activity or subsequent rebound hypersomnolence in the rat. J Pharmacol Exp Ther 283: 757-769.

Engel J, Jr., Henry TR, Risinger MW, Mazziotta JC, Sutherling WW, Levesque MF, Phelps ME (1990) Presurgical evaluation for partial epilepsy: relative contributions of chronic depth-electrode recordings versus FDG-PET and scalp-sphenoidal ictal EEG. Neurology 40: 1670-1677.

Ericson H, Köhler C, Blomqvist A (1991) GABA-like immunoreactivity in the tuberomammillary nucleus: an electron microscopic study in the rat. J Comp Neurol 305: 462-469.

Ericson H, Watanabe T, Köhler C (1987) Morphological analysis of the tuberomammillary nucleus in the rat brain: delineation of subgroups with antibody against L- histidine decarboxylase as a marker. J Comp Neurol 263: 1-24.

Eriksson KS, Peitsaro N, Karlstedt K, Kaslin J, Panula P (1998) Development of the histaminergic neurons and expression of histidine decarboxylase mRNA in the zebrafish brain in the absence of all peripheral histaminergic systems. Eur J Neurosci 10: 3799-3812.

Ferraro L, Tanganelli S, O'Connor WT, Antonelli T, Rambert F, Fuxe K (1996) The vigilance promoting drug modafinil increases dopamine release in the rat nucleus accumbens via the involvement of a local GABAergic mechanism. Eur J Pharmacol 306: 33-39.

Flood JF, Uezu K, Morley JE (1998) Effect of histamine H2 and H3 receptor modulation in the septum on post-training memory processing. Psychopharmacology Berl 140: 279-284.

Forslid A, Andersson B, Johansson S (1986) Observations on normal EEG activity in different brain regions of the unrestrained swine. Acta Physiol Scand 128: 389-396.

Fox SE, Wolfson S, Ranck JB, Jr. (1986) Hippocampal theta rhythm and the firing of neurons in walking and urethane anesthetized rats. Exp Brain Res 62: 495-508.

Frank MG, Issa NP, Stryker MP (2001) Sleep enhances plasticity in the developing visual cortex. Neuron 30: 275-287.

Freund TF, Antal M (1988) GABA-containing neurons in the septum control inhibitory interneurons in the hippocampus. Nature 336: 170-173.

Freund TF, Buzsaki G (1996) Interneurons of the hippocampus. Hippocampus 6: 347-470.

Friedman AH, Walker CA (1968) Circadian rhythms in rat mid-brain and caudate nucleus biogenic amine levels. J Physiol Lond 197: 77-85.

Frisch C, Hasenohrl RU, Haas HL, Weiler HT, Steinbusch HW, Huston JP (1998) Facilitation of learning after lesions of the tuberomammillary nucleus region in adult and aged rats. Exp Brain Res 118: 447-456.

Frisch C, Hasenohrl RU, Huston JP (1997) The histamine H1-antagonist chlorpheniramine facilitates learning in aged rats. Neurosci Lett 229: 89-92.

Galarreta M, Hestrin S (1999) A network of fast-spiking cells in the neocortex connected by electrical synapses. Nature 402: 72-75.

Gerber U, Greene RW, Haas HL, Stevens DR (1989) Characterization of inhibition mediated by adenosine in the hippocampus of the rat in vitro. J Physiol Lond 417: 567-578.

Giuditta A, Ambrosini MV, Montagnese P, Mandile P, Cotugno M, Grassi ZG, Vescia S (1995) The sequential hypothesis of the function of sleep. Behav Brain Res 69: 157-166.

Gold LH, Balster RL (1996) Evaluation of the cocaine-like discriminative stimulus effects and reinforcing effects of modafinil. Psychopharmacology (Berl) 126: 286-292.

Goldman-Rakic PS (1996) The prefrontal landscape: implications of functional architecture for understanding human mentation and the central executive. Philos Trans R Soc Lond B Biol Sci 351: 1445-1453.

Gorelova N, Reiner PB (1997) Histamine depolarizes cholinergic septal neurons. J Neurophysiol 75: 707-714.

Goto Y, O'Donnell P (2001) Synchronous activity in the hippocampus and nucleus accumbens in vivo. J Neurosci 21: RC131.

Graves L, Pack A, Abel T (2001) Sleep and memory: a molecular perspective. Trends Neurosci 24: 237-243.

Gray TS (1999) Functional and anatomical relationships among the amygdala, basal forebrain, ventral striatum, and cortex.An integrative discussion. Ann N Y Acad Sci 877: 439-444.

Greene RW, Haas HL (1990) Effects of histamine on dentate granule cells in vitro. Neuroscience 34: 299-303.

Gutwein BM, Shiromani PJ, Fishbein W (1980) Paradoxical sleep and memory: long-term disruptive effects of Anisomycin. Pharmacol Biochem Behav 12: 377-384.

Haas HL (1984) Histamine potentiates neuronal excitation by blocking a calcium- dependent potassium conductance. Agents Actions 14: 534-537.

Haas HL, Greene RW (1986) Effects of histamine on hippocampal pyramidal cells of the rat in vitro. Exp Brain Res 62: 123-130.

Haas HL, Konnerth A (1983) Histamine and noradrenaline decrease calcium-activated potassium conductance in hippocampal pyramidal cells. Nature 302: 432-434.

Haas HL, Sergueeva OA, Vorobjev VS, Sharonova IN (1995) Subcortical modulation of synaptic plasticity in the hippocampus. Behav Brain Res 66: 41-44.

Haas HL, Yanovsky Y, Greene RW (1997) Action of histamine and adenosine on hippocampal interneurons. Pflugers Arch 433: R72.

Harris KD, Henze DA, Csicsvari J, Hirase H, Buzsaki G (2000) Accuracy of tetrode spike separation as determined by simultaneous intracellular and extracellular measurements. J Neurophysiol 84: 401-414.

Harris KD, Henze DA, Hirase H, Leinekugel X, Dragoi G, Czurko A, Buzsaki G (2002) Spike train dynamics predicts theta-related phase precession in hippocampal pyramidal cells. Nature 417: 738-741.

Henze DA, Borhegyi Z, Csicsvari J, Mamiya A, Harris KD, Buzsaki G (2000) Intracellular features predicted by extracellular recordings in the hippocampus in vivo. J Neurophysiol 84: 390-400.

Hill SJ, Ganellin CR, Timmerman H, Schwartz JC, Shankley NP, Young JM, Schunack W, Levi R, Haas HL (1997) International Union of Pharmacology. XIII. Classification of histamine receptors. Pharmacol Rev 49: 253-278.

Hinton GE, Dayan P, Frey BJ, Neal RM (1995) The "wake-sleep" algorithm for unsupervised neural networks. Science 268: 1158-1161.

Hirase H, Leinekugel X, Czurko A, Csicsvari J, Buzsaki G (2001) Firing rates of hippocampal neurons are preserved during subsequent sleep episodes and modified by novel awake experience. Proc Natl Acad Sci U S A 98: 9386-9390.

Hobson JA, McCarley RW (1977) The brain as a dream state generator: an activation-synthesis hypothesis of the dream process. Am J Psychiatry 134: 1335-1348.

Hobson JA, McCarley RW, Wyzinski PW (1975) Sleep cycle oscillation: reciprocal discharge by two brainstem neuronal groups. Science 189: 55-58.

Hobson JA, Pace-Schott EF, Stickgold R, Kahn D (1998) To dream or not to dream? Relevant data from new neuroimaging and electrophysiological studies. Curr Opin Neurobiol 8: 239-244.

Hoffman A, Afargan M, Backon J, Perlstein I (1997) The anticonvulsant effect of deprenyl on pentylenetetrazol-induced seizures in Lewis rats. Int J Neurosci 90: 223-232.

Horne JA (2000) REM sl. Neurosci Biobehav Rev 24: 777-797.

Huerta R, Mena A, Malacara JM, de Leon JD (1995) Symptoms at the menopausal and premenopausal years: their relationship with insulin, glucose, cortisol, FSH, prolactin, obesity and attitudes towards sexuality. Psychoneuroendocrinology 20: 851-864.

Huston JP, Haas HL, Boix F, Pfister M, Decking U, Schrader J, Schwarting RK (1996) Extracellular adenosine levels in neostriatum and hippocampus during rest and activity periods of rats. Neuroscience 73: 99-107.

Huston JP, Wagner U, Hasenohrl RU (1997) The tuberomammillary nucleus projections in the control of learning, memory and reinforcement processes: evidence for an inhibitory role. Behav Brain Res 83: 97-105.

Inagaki N, Yamatodani A, Ando-Yamamoto M, Tohyama M, Watanabe T, Wada H (1988) Organization of histaminergic fibers in the rat brain. J Comp Neurol 273: 283-300.

Itowi N, Yamatodani A, Mochizuki T, Wada H (1991) Effects of intracerebroventricular histamine injection on circadian activity phase entrainment during rapid illumination changes. Neurosci Lett 123: 53-56.

Izquierdo I, Medina JH (1991) GABAA receptor modulation of memory: the role of endogenous benzodiazepines. Trends Pharmacol Sci 12: 260-265.

Jefferys JG, Haas HL (1982) Synchronized bursting of CA1 hippocampal pyramidal cells in the absence of synaptic transmission. Nature 300: 448-450.

Ji D, Dani JA (2000) Inhibition and disinhibition of pyramidal neurons by activation of nicotinic receptors on hippocampal interneurons. J Neurophysiol 83: 2682-2690.

Jones BE, Harper ST, Halaris AE (1977) Effects of locus coeruleus lesions upon cerebral monoamine content, sleep-wakefulness states and the response to amphetamine in the cat. Brain Res 124: 473-496.

Jouvet M (1969) Biogenic amines and the states of sleep. Science 163: 32-41.

Jouvet M, Albarede JL, Lubin S, Meyrignac C (1991) [Noradrenaline and cerebral aging]. Encephale 17: 187-195.

Kahana MJ, Caplan JB, Sekuler R, Madsen JR (1999) Using intracranial recordings to study thetaResponse to J. O'Keefe and N. Burgess (1999). Trends Cogn Sci 3: 406-407.

Kametani H, Kawamura H (1990) Alterations in acetylcholine release in the rat hippocampus during sleep-wakefulness detected by intracerebral dialysis. Life Sci 47: 421-426.

Kamondi A, Acsady L, Wang XJ, Buzsaki G (1998) Theta oscillations in somata and dendrites of hippocampal pyramidal cells in vivo: activity-dependent phase-precession of action potentials. Hippocampus 8: 244-261.

Karni A, Tanne D, Rubenstein BS, Askenasy JJ, Sagi D (1994) Dependence on REM sleep of overnight improvement of a perceptual skill. Science 265: 679-682.

Katz JL, Goldberg SR (1986) Effects of H1-receptor antagonists on responding punished by histamine injection or electric shock presentation in squirrel monkeys. Psychopharmacology Berl 90: 461-467.

Kemppainen S, Pitkanen A (2000) Distribution of parvalbumin, calretinin, and calbindin-D(28k) immunoreactivity in the rat amygdaloid complex and colocalization with gamma-aminobutyric acid. J Comp Neurol 426: 441-467.

Klapdor K, Hasenohrl RU, Huston JP (1994) Facilitation of learning in adult and aged rats following bilateral lesions of the tuberomammillary nucleus region. Behav Brain Res 61: 113-116.

Klausberger T, Magill PJ, Marton LF, Roberts JD, Cobden PM, Buzsaki G, Somogyi P (2003) Brain-s. Nature 421: 844-848.

Knoche A, Yokoyama H, Ponomarenko A, Frisch C, Huston JP, Haas HL (2003) High-frequency oscillation in the hippocampus of the behaving rat and its modulation by the histaminergic systemhistaminergic system. Hippocampus 13: 273-280.

Kocsis B, Bragin A, Buzsaki G (1999) Interdependence of multiple theta generators in the hippocampus: a partial coherence analysis. J Neurosci 19: 6200-6212.

Kohler C, Ericson H, Watanabe T, Polak J, Palay SL, Palay V, Chan Palay V (1986) Galanin immunoreactivity in hypothalamic neurons: further evidence for multiple chemical messengers in the tuberomammillary nucleus. J Comp Neurol 250: 58-64.

Konopacki J, MacIver MB, Bland BH, Roth SH (1987) Carbachol-induced EEG 'theta' activity in hippocampal brain slices. Brain Res 405: 196-198.

Kramis R, Vanderwolf CH, Bland BH (1975) Two types of hippocampal rhythmical slow activity in both the rabbit and the rat: relations to behavior and effects of atropine, diethyl ether, urethane, and pentobarbital. Exp Neurol 49: 58-85.

Kruger, L., Saporta, S., and Swanson, L. W. Photographic Atlas of the rat brain cell and fibre architecture illustrated in three planes with stereotaxic coordinates. 1995. Cambridge University Press.

Kudrimoti HS, Barnes CA, McNaughton BL (1999) Reactivation of hippocampal cell assemblies: effects of behavioral state, experience, and EEG dynamics. J Neurosci 19: 4090-4101.

Kupfer DJ, Foster FG (1972) Interval between onset of sleep and rapid-eye-movement sleep as an indicator of depression. Lancet 2: 684-686.

Lauer C, Riemann D, Lund R, Berger M (1987) Shortened REM latency: a consequence of psychological strain? Psychophysiology 24: 263-271.

Le Coniat M, Traiffort E, Ruat M, Arrang J-M, Berger R (1994) Chromosomal location of the human histamine H1-receptor gene. Hum Genet 94: 186-188.

Lee AK, Wilson MA (2002) Memory of sequential experience in the hippocampus during slow wave sleep. Neuron 36: 1183-1194.

Lee MG, Chrobak JJ, Sik A, Wiley RG, Buzsaki G (1994) Hippocampal theta activity following selective lesion of the septal cholinergic system. Neuroscience 62: 1033-1047.

Leinekugel X, Khazipov R, Cannon R, Hirase H, Ben Ari Y, Buzsaki G (2002) Correlated bursts of activity in the neonatal hippocampus in vivo. Science 296: 2049-2052.

Leung LS, Yim CY (1986) Intracellular records of theta rhythm in hippocampal CA1 cells of the rat. Brain Res 367: 323-327.

Leung LW, Buzsaki G (1983) Spectral analysis of hippocampal unit train in relation to hippocampal EEG. Electroencephalogr Clin Neurophysiol 56: 668-671.

Leurs R, Smit MJ, Menge WM, Timmerman H (1994) Pharmacological characterization of the human histamine H2 receptor stably expressed in Chinese hamster ovary cells. Br J Pharmacol 112: 847-854.

Leviel V, Cheramy A, Glowinski J (1979) Role of the dendritic release of dopamine in the reciprocal control of the two nigro-striatal dopaminergic pathways. Nature 280: 236-239.

Lin JS, Hou Y, Sakai K, Jouvet M (1996) Histaminergic descending inputs to the mesopontine tegmentum and their role in the control of cortical activation and wakefulness in the cat. J Neurosci 16: 1523-1537.

Lin JS, Roussel B, Akaoka H, Fort P, Debilly G, Jouvet M (1992) Role of catecholamines in the modafinil and amphetamine induced wakefulness, a comparative pharmacological study in the cat. Brain Res 591: 319-326.

Lin JS, Sakai K, Jouvet M (1988) Evidence for histaminergic arousal mechanisms in the hypothalamus of cat. Neuropharmacology 27: 111-122.

Lin JS, Sakai K, Jouvet M (1994) Hypothalamo-preoptic histaminergic projections in sleep-wake control in the cat. Eur J Neurosci 6: 618-625.

Lin JS, Sakai K, Vanni Mercier G, Arrang JM, Garbarg M, Schwartz JC, Jouvet M (1990) Involvement of histaminergic neurons in arousal mechanisms demonstrated with H3-receptor ligands in the cat. Brain Res 523: 325-330.

Lin JS, Sakai K, Vanni MG, Jouvet M (1989) A critical role of the posterior hypothalamus in the mechanisms of wakefulness determined by microinjection of muscimol in freely moving cats. Brain Res 479: 225-240.

Lingenhohl K, Finch DM (1991) Morphological characterization of rat entorhinal neurons in vivo: soma- dendritic structure and axonal domains. Exp Brain Res 84: 57-74.

Lisman JE, Idiart MA (1995) Storage of 7 +/- 2 short-term memories in oscillatory subcycles. Science 267: 1512-1515.

Lockery SR, Sejnowski TJ (1992) Distributed processing of sensory information in the leech. III. A dynamical neural network model of the local bending reflex. J Neurosci 12: 3877-3895.

Lorincz A, Buzsaki G (2000) Two-phase computational model training long-term memories in the entorhinal-hippocampal region. Ann N Y Acad Sci 911: 83-111.

Louie K, Wilson MA (2001b) Temporally structured replay of awake hippocampal ensemble activity during rapid eye movement sleep. Neuron 29: 145-156.

Lovenberg TW, Roland BL, Wilson SW, Jiang X, Pyati J, Huvar A, Jackson MR, Erlander MG (1999) Cloning and functional expression of the human histamine H_3 receptor. Mol Pharmacol 55: 1101-1107.

Luskin MB, Price JL (1983) The topographic organization of associational fibers of the olfactory system in the rat, including centrifugal fibers to the olfactory bulb. J Comp Neurol 216: 264-291.

MacVicar BA, Dudek FE (1982) Electrotonic coupling between granule cells of rat dentate gyrus: physiological and anatomical evidence. J Neurophysiol 47: 579-592.

Madison DV, Lancaster B, Nicoll RA (1987) Voltage clamp analysis of cholinergic action in the hippocampus. J Neurosci 7: 733-741.

Maier N, Guldenagel M, Sohl G, Siegmund H, Willecke K, Draguhn A (2002) Reduction of high-frequency network oscillations (ripples) and pathological network discharges in hippocampal slices from connexin 36- deficient mice. J Physiol 541: 521-528.

Majak K, Pikkarainen M, Kemppainen S, Jolkkonen E, Pitkanen A (2002) Projections from the amygdaloid complex to the claustrum and the endopiriform nucleus: a Phaseolus vulgaris leucoagglutinin study in the rat. J Comp Neurol 451: 236-249.

Manahan-Vaughan D, Reymann KG, Brown RE (1998) In vivo electrophysiological investigations into the role of histamine in the dentate gyrus of the rat. Neuroscience 84: 783-790.

Mandile P, Vescia S, Montagnese P, Romano F, Onio GA (1996) Characterization of transition sleep episodes in baseline EEG recordings of adult rats. Physiol Behav 60: 1435-1439.

Maquet P, Degueldre C, Delfiore G, Aerts J, Peters JM, Luxen A, Franck G (1997) Functional neuroanatomy of human slow wave sleep. J Neurosci 17: 2807-2812.

Maquet P, Peters J, Aerts J, Delfiore G, Degueldre C, Luxen A, Franck G (1996) Functional neuroanatomy of human rapid-eye-movement sleep and dreaming. Nature 383: 163-166.

Martinez Mir MI, Pollard H, Moreau J, Arrang JM, Ruat M, Traiffort E, Schwartz JC, Palacios JM (1990) Three histamine receptors (H1, H2 and H3) visualized in the brain of human and non-human primates. Brain Res 526: 322-327.

McDonald AJ (1998) Cortical pathways to the mammalian amygdala. Prog Neurobiol 55: 257-332.

McKearney JW (1982b) Effects of tricyclic antidepressant and anticholinergic drugs on fixed-interval responding in the squirrel monkey. J Pharmacol Exp Ther 222: 215-219.

McKearney JW (1982a) Stimulant actions of histamine H1 antagonists on operant behavior in the squirrel monkey. Psychopharmacology Berl 77: 156-158.

Meguro K, Yanai K, Sakai N, Sakurai E, Maeyama K, Sasaki H, Watanabe T (1995) Effects of thioperamide, a histamine H3 antagonist, on the step-through passive avoidance response and histidine decarboxylase activity in senescence-accelerated mice. Pharmacol Biochem Behav 50: 321-325.

Meyer JL, Hall AC, Harrington ME (1998) Histamine phase shifts the hamster circadian pacemaker via an NMDA dependent mechanism. J Biol Rhythms 13: 288-295.

Mignot E, Nishino S, Guilleminault C, Dement WC (1994) Modafinil binds to the dopamine uptake carrier site with low affinity. Sleep 17: 436-437.

Miles R, Wong RK (1986) Excitatory synaptic interactions between CA3 neurones in the guinea-pig hippocampus. J Physiol 373: 397-418.

Mitchell JB, Miller K, Dunwiddie TV (1993) Adenosine-induced suppression of synaptic responses and the initiation and expression of long-term potentiation in the CA1 region of the hippocampus. Hippocampus 3: 77-86.

Mitzdorf U (1985) Current source-density method and application in cat cerebral cortex: investigation of evoked potentials and EEG phenomena. Physiol Rev 65: 37-100.

Miyazaki S, Imaizumi M, Onodera K (1995) Ameliorating effects of histidine on learning deficits in an elevated plus-maze test in mice and the contribution of cholinergic neuronal systems. Methods Find Exp Clin Pharmacol 17 Suppl C: 57-63.

Mizumori SJ, Barnes CA, McNaughton BL (1990) Behavioral correlates of theta-on and theta-off cells recorded from hippocampal formation of mature young and aged rats. Exp Brain Res 80: 365-373.

Monmaur P, Thomson MA, M'Harzi M (1986) Temporal changes in hippocampal theta activity following twenty minutes of forebrain ischemia in the chronic rat. Brain Res 378: 262-273.

Monnier M, Hatt AM (1969) Afferent and central activating effects of histamine on the brain. Experientia 25: 1297-1298.

Monti JM (1993) Involvement of histamine in the control of the waking state. Life Sci 53: 1331-1338.

Monti JM, D'Angelo L, Jantos H, Pazos S (1988) Effects of a-fluoromethylhistidine on sleep and wakefulness in the rat. Short note. J Neural Transm 72: 141-145.

Monti JM, Jantos H, Boussard M, Altier H, Orellana C, Olivera S (1991) Effects of selective activation or blockade of the histamine H3 receptor on sleep and wakefulness. Eur J Pharmacol 205: 283-287.

Moor E, DeBoer P, Westerink BH (1998) GABA receptors and benzodiazepine binding sites modulate hippocampal acetylcholine release in vivo. Eur J Pharmacol 359: 119-126.

Nadasdy Z, Hirase H, Czurko A, Csicsvari J, Buzsaki G (1999) Replay and time compression of recurring spike sequences in the hippocampus. J Neurosci 19: 9497-9507.

Nauta WJH (1946) Hypothalamic regulation of sleep in rats. An experimental study. J Neurophysiol 9: 285-361.

Nishino S, Mignot E (1997) Pharmacological aspects of human and canine narcolepsy. Prog Neurobiol 52: 27-78.

Nofzinger EA, Mintun MA, Price J, Meltzer CC, Townsend D, Buysse DJ, Reynolds CF, III, Dachille M, Matzzie J, Kupfer DJ, Moore RY (1998) A method for the assessment of the functional neuroanatomy of human sleep using FDG PET. Brain Res Brain Res Protoc 2: 191-198.

O'Keefe J (1976) Place units in the hippocampus of the freely moving rat. Exp Neurol 51: 78-109.

O'Keefe J, Recce ML (1993) Phase relationship between hippocampal place units and the EEG theta rhythm. Hippocampus 3: 317-330.

Ottersen OP (1982) Connections of the amygdala of the rat. IV: Corticoamygdaloid and intraamygdaloid connections as studied with axonal transport of horseradish peroxidase. J Comp Neurol 205: 30-48.

Otto MP (1991) Watchful nursing staff helps improve quality of sleep. Provider 17: 55.

Otto T, Eichenbaum H, Wiener SI, Wible CG (1991) Learning-related patterns of CA1 spike trains parallel stimulation parameters optimal for inducing hippocampal long-term potentiation. Hippocampus 1: 181-192.

Panula P, Pirvola U, Auvinen S, Airaksinen MS (1989) Histamine-immunoreactive nerve fibres in the rat brain. Neuroscience 28: 585-610.

Panula P, Yang HY, Costa E (1984) Histamine-containing neurons in the rat hypothalamus. Proc Natl Acad Sci U S A 81: 2572-2576.

Pare D, Collins DR (2000) Neuronal correlates of fear in the lateral amygdala: multiple extracellular recordings in conscious cats. J Neurosci 20: 2701-2710.

Pare D, Collins DR, Pelletier JG (2002) Amygdala oscillations and the consolidation of emotional memories. Trends Cogn Sci 6: 306-314.

Pare D, Dong J, Gaudreau H (1995a) Amygdalo-entorhinal relations and their reflection in the hippocampal formation: generation of sharp sleep potentials. J Neurosci 15: 2482-2503.

Pare D, Gaudreau H (1996) Projection cells and interneurons of the lateral and basolateral amygdala: distinct firing patterns and differential relation to theta and delta rhythms in conscious cats. J Neurosci 16: 3334-3350.

Pare D, Pape HC, Dong J (1995b) Bursting and oscillating neurons of the cat basolateral amygdaloid complex in vivo: electrophysiological properties and morphological features. J Neurophysiol 74: 1179-1191.

Pare D, Steriade M, Deschenes M, Oakson G (1987) Physiological characteristics of anterior thalamic nuclei, a group devoid of inputs from reticular thalamic nucleus. J Neurophysiol 57: 1669-1685.

Parent A, Pare D, Smith Y, Steriade M (1988) Basal forebrain cholinergic and noncholinergic projections to the thalamus and brainstem in cats and monkeys. J Comp Neurol 277: 281-301.

Pavlides C, Winson J (1989) Influences of hippocampal place cell firing in the awake state on the activity of these cells during subsequent sleep episodes. J Neurosci 9: 2907-2918.

Pedarzani P, Storm JF (1995) Protein kinase A-independent modulation of ion channels in the brain by cyclic AMP. Proc Natl Acad Sci U S A 92: 11716-11720.

Pelletier JG, Pare D (2002) Uniform range of conduction times from the lateral amygdala to distributed perirhinal sites. J Neurophysiol 87: 1213-1221.

Penttonen M, Kamondi A, Sik A, Acsady L, Buzsaki G (1997) Feed-forward and feed-back activation of the dentate gyrus in vivo during dentate spikes and sharp wave bursts. Hippocampus 7: 437-450.

Perez Velazquez JL, Carlen PL (2000) Gap junctions, synchrony and seizures. Trends Neurosci 23: 68-74.

Pikkarainen M, Ronkko S, Savander V, Insausti R, Pitkanen A (1999) Projections from the lateral, basal, and accessory basal nuclei of the amygdala to the hippocampal formation in rat. J Comp Neurol 403: 229-260.

Piscopo S, Mandile P, Montagnese P, Cotugno M, Giuditta A, Vescia S (2001) Trains of sleep sequences are indices of learning capacity in rats. Behav Brain Res 120: 13-21.

Pitkanen A, Pikkarainen M, Nurminen N, Ylinen A (2000) Reciprocal connections between the amygdala and the hippocampal formation, perirhinal cortex, and postrhinal cortex in rat. A review. Ann N Y Acad Sci 911: 369-391.

Plihal W, Born J (1999) Effects of early and late nocturnal sleep on priming and spatial memory. Psychophysiology 36: 571-582.

Poe GR, Nitz DA, McNaughton BL, Barnes CA (2000) Experience-dependent phase-reversal of hippocampal neuron firing during REM sleep. Brain Res 855: 176-180.

Pollard H, Moreau J, Arrang JM, Schwartz JC (1993) A detailed autoradiographic mapping of histamine H3 receptors in rat brain areas. Neuroscience 52: 169-189.

Ponomarenko AA, Korotkova TM, Haas HL (2003) High frequency (200 Hz) oscillations and firing patterns in the basolateral amygdala and dorsal endopiriform nucleus of the behaving rat. Behav Brain Res 141: 123-129.

Ponomarenko AA., Lin JS., Selbach O, Haas HL. Temporal pattern of hippocampal high-frequency oscillations during sleep after stimulant-evoked waking. Neuroscience (in press).

Ponomarenko AA., Knoche A, Korotkova TM, Haas HL. Monoaminergic control of high-frequency (~200 Hz) oscillations in the hippocampus of the behaving rat. Neurosci. Lett. (resubmitted).

Prast H, Argyriou A, Philippu A (1996) Histaminergic neurons facilitate social memory in rats. Brain Res 734: 316-318.

Privou C, Knoche A, Hasenohrl RU, Huston JP (1998) The H1- and H2-histamine blockers chlorpheniramine and ranitidine applied to the nucleus basalis magnocellularis region modulate anxiety and reinforcement related processes. Neuropharmacology 37: 1019-1032.

Pyapali GK, Sik A, Penttonen M, Buzsaki G, Turner DA (1998) Dendritic properties of hippocampal CA1 pyramidal neurons in the rat: intracellular staining in vivo and in vitro. J Comp Neurol 391: 335-352.

Rainnie DG, Asprodini EK, Shinnick-Gallagher P (1993) Intracellular recordings from morphologically identified neurons of the basolateral amygdala. J Neurophysiol 69: 1350-1362.

Richelson E (1978) Histamine H1 receptor-mediated guanosine 3',5'-monophosphate formation by cultured mouse neuroblastoma cells. Science 201: 69-71.

Room P, Groenewegen HJ (1986) Connections of the parahippocampal cortex in the cat. II. Subcortical afferents. J Comp Neurol 251: 451-473.

Rosenkranz JA, Grace AA (2001) Dopamine attenuates prefrontal cortical suppression of sensory inputs to the basolateral amygdala of rats. J Neurosci 21: 4090-4103.

Sakai K, El Mansari M, Lin JS, Zhang JG, Vanni Mercier G (1990) The posterior hypothalamus in the regulation of wakefulness and paradoxical sleep. In: The Diencephalon and Sleep (Mancia, Marini, eds), pp 171-198. New York: Raven Press.

Savander V, LeDoux JE, Pitkanen A (1997) Interamygdaloid projections of the basal and accessory basal nuclei of the rat amygdaloid complex. Neuroscience 76: 725-735.

Schmalbruch H, Jahnsen H (1981) Gap junctions on CA3 pyramidal cells of guinea pig hippocampus shown by freeze-fracture. Brain Res 217: 175-178.

Schwartz J-C, Arrang J-M, Garbarg M, Pollard H, Ruat M (1991) Histaminergic transmission in the mammalian brain. Physiol Rev 71: 1-51.

Segal M (1981) Histamine modulates reactivity of hippocampal CA3 neurons to afferent stimulation in vitro. Brain Res 213: 443-448.

Segal M, Barker JL (1984) Rat hippocampal neurons in culture: potassium conductances. J Neurophysiol 51: 1409-1433.

Segal M, Bjorklund A, Gage FH (1985) Transplanted septal neurons make viable cholinergic synapses with a host hippocampus. Brain Res 336: 302-307.

Seiden LS, Sabol KE, Ricaurte GA (1993) Amphetamine: effects on catecholamine systems and behavior. Annu Rev Pharmacol Toxicol 33: 639-677.

Sejnowski TJ, Destexhe A (2000) Why do we sleep? Brain Res 886: 208-223.

Selbach O, Brown RE, Haas HL (1997) Long-term increase of hippocampal excitability by histamine and cyclic AMP. Neuropharmacology 36: 1539-1548.

Sheng M, Thompson MA, Greenberg ME (1991) CREB: a Ca(2+)-regulated transcription factor phosphorylated by calmodulin-dependent kinases. Science 252: 1427-1430.

Siapas AG, Wilson MA (1998) Coordinated interactions between hippocampal ripples and cortical spindles during slow-wave sleep. Neuron 21: 1123-1128.

Sik A, Penttonen M, Buzsaki G (1997) Interneurons in the hippocampal dentate gyrus: an in vivo intracellular study. Eur J Neurosci 9: 573-588.

Sik A, Penttonen M, Ylinen A, Buzsaki G (1995) Hippocampal CA1 interneurons: an in vivo intracellular labeling study. J Neurosci 15: 6651-6665.

Skaggs WE, McNaughton BL (1996) Replay of neuronal firing sequences in rat hippocampus during sleep following spatial experience. Science 271: 1870-1873.

Smith C (1985) Sleep states and learning: a review of the animal literature. Neurosci Biobehav Rev 9: 157-168.

Smith C, Butler S (1982) Paradoxical sleep at selective times following training is necessary for learning. Physiol Behav 29: 469-473.

Soltesz I, Deschenes M (1993) Low- and high-frequency membrane potential oscillations during theta activity in CA1 and CA3 pyramidal neurons of the rat hippocampus under ketamine-xylazine anesthesia. J Neurophysiol 70: 97-116.

Steriade M (2000) Corticothalamic resonance, states of vigilance and mentation. Neuroscience 101: 243-276.

Steriade M, Nunez A, Amzica F (1993) A novel slow (< 1 Hz) oscillation of neocortical neurons in vivo: depolarizing and hyperpolarizing components. J Neurosci 13: 3252-3265.

Stewart M, Fox SE (1990) Do septal neurons pace the hippocampal theta rhythm? Trends Neurosci 13: 163-168.

Stickgold R, James L, Hobson JA (2000) Visual discrimination learning requires sleep after training. Nat Neurosci 3: 1237-1238.

Stickgold R, Scott L, Rittenhouse C, Hobson JA (1999) Sleep-induced changes in associative memory. J Cogn Neurosci 11: 182-193.

Stone EA, Cotecchia S, Lin Y, Quartermain D (2002) Role of brain alpha 1B-adrenoceptors in modafinil-induced behavioral activity. Synapse 46: 269-270.

Swanson LW, Petrovich GD (1998) What is the amygdala? Trends Neurosci 21: 323-331.

Szinyei C, Heinbockel T, Montagne J, Pape HC (2000) Putative cortical and thalamic inputs elicit convergent excitation in a population of GABAergic interneurons of the lateral amygdala. J Neurosci 20: 8909-8915.

Takagi H, Morishima Y, Matsuyama T, Hayashi H, Watanabe T, Wada H (1986) Histaminergic axons in the neostriatum and cerebral cortex of the rat: a correlated light and electron microscopic immunocytochemical study using histidine decarboxylase as a marker. Brain Res 364: 114-123.

Tasaka K, Kamei C, Akahori H, Kitazumi K (1985) The effects of histamine and some related compounds on conditioned avoidance response in rats. Life Sci 37: 2005-2014.

Thomson AM, Bannister AP, Hughes DI, Pawelzik H (2000) Differential sensitivity to Zolpidem of IPSPs activated by morphologically identified CA1 interneurons in slices of rat hippocampus. Eur J Neurosci 12: 425-436.

Timofeev I, Grenier F, Bazhenov M, Sejnowski TJ, Steriade M (2000) Origin of slow cortical oscillations in deafferented cortical slabs. Cereb Cortex 10: 1185-1199.

Toth M, Grimsby J, Buzsaki G, Donovan GP (1995) Epileptic seizures caused by inactivation of a novel gene, jerky, related to centromere binding protein-B in transgenic mice. Nat Genet 11: 71-75.

Touret M, Sallanon-Moulin M, Jouvet M (1995) Awakening properties of modafinil without paradoxical sleep rebound: comparative study with amphetamine in the rat. Neurosci Lett 189: 43-46.

Traiffort E, Vizuete ML, Tardivel Lacombe J, Souil E, Schwartz JC, Ruat M (1995) The guinea pig histamine H2 receptor: gene cloning, tissue expression and chromosomal localization of its human counterpart. Biochem Biophys Res Commun 211: 570-577.

Traub RD (1995) Model of synchronized population bursts in electrically coupled interneurons containing active dendritic conductances. J Comput Neurosci 2: 283-289.

Traub RD, Bibbig A (2000) A model of high-frequency ripples in the hippocampus based on synaptic coupling plus axon-axon gap junctions between pyramidal neurons. J Neurosci 20: 2086-2093.

Traub RD, Colling SB, Jefferys JG (1995) Cellular mechanisms of 4-aminopyridine-induced synchronized after- discharges in the rat hippocampal slice. J Physiol 489 (Pt 1): 127-140.

Traub RD, Miles R, Buzsaki G (1992) Computer simulation of carbachol-driven rhythmic population oscillations in the CA3 region of the in vitro rat hippocampus. J Physiol 451: 653-672.

Traub RD, Schmitz D, Jefferys JG, Draguhn A (1999a) High-frequency population oscillations are predicted to occur in hippocampal pyramidal neuronal networks interconnected by axoaxonal gap junctions. Neuroscience 92: 407-426.

Traub RD, Whittington MA, Buhl EH, Jefferys JG, Faulkner HJ (1999b) On the mechanism of the gamma --> beta frequency shift in neuronal oscillations induced in rat hippocampal slices by tetanic stimulation. J Neurosci 19: 1088-1105.

Traub RD, Whittington MA, Colling SB, Buzsaki G, Jefferys JG (1996a) Analysis of gamma rhythms in the rat hippocampus in vitro and in vivo. J Physiol 493 (Pt 2): 471-484.

Traub RD, Whittington MA, Stanford IM, Jefferys JG (1996b) A mechanism for generation of long-range synchronous fast oscillations in the cortex. Nature 383: 621-624.

Tseng GF, Haberly LB (1989) Deep neurons in piriform cortex. I. Morphology and synaptically evoked responses including a unique high-amplitude paired shock facilitation. J Neurophysiol 62: 369-385.

Turner BH, Herkenham M (1991) Thalamoamygdaloid projections in the rat: a test of the amygdala's role in sensory processing. J Comp Neurol 313: 295-325.

Valiante TA, Perez Velazquez JL, Jahromi SS, Carlen PL (1995) Coupling potentials in CA1 neurons during calcium-free-induced field burst activity. J Neurosci 15: 6946-6956.

van Der LS, Panzica F, de Curtis M (1999) Carbachol induces fast oscillations in the medial but not in the lateral entorhinal cortex of the isolated guinea pig brain. J Neurophysiol 82: 2441-2450.

van Groen T, Wyss JM (1990) Extrinsic projections from area CA1 of the rat hippocampus: olfactory, cortical, subcortical, and bilateral hippocampal formation projections. J Comp Neurol 302: 515-528.

van Haeften T, Wouterlood FG, Witter MP (2000) Presubicular input to the dendrites of layer-V entorhinal neurons in the rat. Ann N Y Acad Sci 911: 471-473.

Vanderwolf CH (1969) Hippocampal electrical activity and voluntary movement in the rat. Electroencephalogr Clin Neurophysiol 26: 407-418.

Vanderwolf CH (1988) Cerebral activity and behavior: control by central cholinergic and serotonergic systems. Int Rev Neurobiol 30: 225-340.

Vaney DI (1993) The coupling pattern of axon-bearing horizontal cells in the mammalian retina. Proc R Soc Lond B Biol Sci 252: 93-101.

Vanni Mercier G, Sakai K, Jouvet M (1984) [Specific neurons for wakefulness in the posterior hypothalamus in the cat]. C R Acad Sci III 298: 195-200.

Vertes RP, Kocsis B (1997) Brainstem-diencephalo-septohippocampal systems controlling the theta rhythm of the hippocampus. Neuroscience 81: 893-926.

Vescia S, Mandile P, Montagnese P, Romano F, Cataldo G, Cotugno M, Giuditta A (1996) Baseline transition sleep and associated sleep episodes are related to the learning ability of rats. Physiol Behav 60: 1513-1525.

Vorobjev VS, Sharonova IN, Walsh IB, Haas HL (1993) Histamine potentiates N-methyl-D-aspartate responses in acutely isolated hippocampal neurons. Neuron 11: 837-844.

Wada H, Inagaki N, Yamatodani A, Watanabe T (1991) Is the histaminergic neuron system a regulatory center for whole- brain activity? Trends Neurosci 14: 415-418.

Wagner JJ, Terman GW, Chavkin C (1993) Endogenous dynorphins inhibit excitatory neurotransmission and block LTP induction in the hippocampus. Nature 363: 451-454.

Wagner U, Gais S, Born J (2001) Emotional memory formation is enhanced across sleep intervals with high amounts of rapid eye movement sleep. Learn Mem 8: 112-119.

Wang SJ, Cheng LL, Gean PW (1999) Cross-modulation of synaptic plasticity by beta-adrenergic and 5-HT1A receptors in the rat basolateral amygdala. J Neurosci 19: 570-577.

Wang XJ, Buzsaki G (1996) Gamma oscillation by synaptic inhibition in a hippocampal interneuronal network model. J Neurosci 16: 6402-6413.

Washburn MS, Moises HC (1992) Electrophysiological and morphological properties of rat basolateral amygdaloid neurons in vitro. J Neurosci 12: 4066-4079.

Watanabe T, Taguchi Y, Shiosaka S, Tanaka J, Kubota H, Terano Y, Tohyama M, Wada H (1984) Distribution of the histaminergic neuron system in the central nervous system of rats: a fluorescent immunohistochemical analysis with histidine decarboxylase as a marker. Brain Res 295: 13-25.

Weiler HT, Hasenohrl RU, van Landeghem AA, van Landeghem M, Brankack J, Huston JP, Haas HL (1998) Differential modulation of hippocampal signal transfer by tuberomammillary nucleus stimulation in freely moving rats dependent on behavioral state. Synapse 28: 294-301.

White JM, Rumbold GR (1988) Behavioural effects of histamine and its antagonists: a review. Psychopharmacology Berl 95: 1-14.

Whittemore ER, Yang W, Drewe JA, Woodward RM (1996) Pharmacology of the human gamma-aminobutyric acidA receptor alpha 4 subunit expressed in Xenopus laevis oocytes. Mol Pharmacol 50: 1364-1375.

Whittington MA, Jefferys JG, Traub RD (1996) Effects of intravenous anaesthetic agents on fast inhibitory oscillations in the rat hippocampus in vitro. Br J Pharmacol 118: 1977-1986.

Whittington MA, Stanford IM, Colling SB, Jefferys JG, Traub RD (1997) Spatiotemporal patterns of gamma frequency oscillations tetanically induced in the rat hippocampal slice. J Physiol 502 (Pt 3): 591-607.

Whittington MA, Traub RD, Jefferys JG (1995) Synchronized oscillations in interneuron networks driven by metabotropic glutamate receptor activation. Nature 373: 612-615.

Wilson MA, McNaughton BL (1994) Reactivation of hippocampal ensemble memories during sleep. Science 265: 676-679.

Winson J (1974) Patterns of hippocampal theta rhythm in the freely moving rat. Electroencephalogr Clin Neurophysiol 36: 291-301.

Wisor JP, Nishino S, Sora I, Uhl GH, Mignot E, Edgar DM (2001a) Dopaminergic role in stimulant-induced wakefulness. J Neurosci 21: 1787-1794.

Witter MP, Amaral DG (1991) Entorhinal cortex of the monkey: V. Projections to the dentate gyrus, hippocampus, and subicular complex. J Comp Neurol 307: 437-459.

Wouterlood FG, Sauren YM, Steinbusch HW (1986) Histaminergic neurons in the rat brain: correlative immunocytochemistry, Golgi impregnation, and electron microscopy. J Comp Neurol 252: 227-244.

Yanovsky Y, Haas HL (1998) Histamine increases the bursting activity of pyramidal cells in the CA3 region of mouse hippocampus. Neurosci Lett 240: 110-112.

Ylinen A, Bragin A, Nadasdy Z, Jando G, Szabo I, Sik A, Buzsaki G (1995a) Sharp wave-associated high-frequency oscillation (200 Hz) in the intact hippocampus: network and intracellular mechanisms. J Neurosci 15: 30-46.

Ylinen A, Soltesz I, Bragin A, Penttonen M, Sik A, Buzsaki G (1995b) Intracellular correlates of hippocampal theta rhythm in identified pyramidal cells, granule cells, and basket cells. Hippocampus 5: 78-90.

Yokoyama H, Iinuma K, Yanai K, Watanabe T, Sakurai E, Onodera K (1993) Proconvulsant effect of ketotifen, a histamine H1 antagonist, confirmed by the use of d-chlorpheniramine with monitoring electroencephalography. Methods Find Exp Clin Pharmacol 15: 183-188.

Yokoyama H, Onodera K, Maeyama K, Yanai K, Iinuma K, Tuomisto L, Watanabe T (1992) Histamine levels and clonic convulsions of electrically-induced seizure in mice: the effects of alpha-fluoromethylhistidine and metoprine. Naunyn Schmiedebergs Arch Pharmacol 346: 40-45.

APPENDIX. Table 1. Numbers of sleep and waking episodes.

Sleep phase – treatment / time, h	*1*	*2*	*3*	*4*	*5*	*6*
SWS						
Vehicle n=6	8.2 ± 2.0	0	0	4.2 ± 2.0	4.8 ± 1.4	4.5 ± 0.5
Amph n=5	7.7 ± 0.7	2.7 ± 1.4	10.7 ± 2.4	12.0 ± 2.7	12.0 ± 1.0	13.7 ± 2.9
Mod 128 n=6	9.6 ± 1.6	7.0 ± 1.1	10.0 ± 1.6	12.7 ± 0.7	9.8 ± 0.9	11.8 ± 1.1
Mod 64 n=4	9.0 ± 2.0	0	0	0	4.0 ± 0.0	6.0 ± 0.0
Sleep dep. n=2	8.5 ± 1.6	10.0 ± 1.8	11.5 ± 2.6	11.3 ± 2.3	11.0 ± 1.6	11.0 ± 2.9
PS						
amph	4.2 ± 1.9	0	0	0	1.2 ± 0.6	2.5 ± 0.3
mod 64	2.0 ± 0.6	1.0 ± 0.6	2.0 ± 1.2	2.0 ± 1.2	6.7 ± 1.3	2.7 ± 0.9
mod 128	2.8 ± 1.0	1.0 ± 1.0	0.7 ± 0.7	1.4 ± 0.9	4.0 ± 2.2	3.0 ± 0.8
sleep dep	2.0 ± 2.0	0	0	0	2.5 ± 1.5	2.5 ± 0.5
vehicle	1.5 ± 1.2	2.3 ± 1.7	3.3 ± 2.1	3.8 ± 0.8	4.7 ± 1.3	6.4 ± 2.1
W						
amph	7.1 ± 1.0	1.0 ± 0.0	1.0 ± 0.0	4.4 ± 1.7	3.6 ± 0.9	2.4 ± 0.3
mod 64	7.0 ± 0.6	2.7 ± 0.9	8.0 ±1.6	11.4 ± 3.0	8.7 ± 0.9	9.4 ± 4.3
mod 128	7.8 ± 1.3	5.5 ± 2.7	9.7 ± 1.5	11.0 ± 1.2	6.8 ± 0.9	10.0 ± 2.0
sleep dep	7.0 ± 3.0	1.0 ± 0.0	1.0 ± 0.0	1.0 ± 0.0	4.5 ± 0.5	3.0 ± 0.0
vehicle	7.8 ± 1.5	8.3 ± 1.9	8.8 ± 3.2	8.8 ± 2.4	7.4 ± 1.9	7.0 ± 0.6

Table 2. Duration of sleep and waking episodes.

Sleep phase –treatment / time, h	*1*	*2*	*3*	*4*	*5*	*6*
SWS						
Vehicle n=6	3.8 ± 0.5	0	0	5.3 ± 1.7	6.1 ± 1.0	9.4 ± 1.8
Amph n=5	4.9 ± 1.0	3.6 ± 1.1	2.9 ± 0.6	3.0 ± 0.5	3 ± 0.5	2.3 ± 0.3
Mod 128 n=6	3.2 ± 0.5	2.0 ± 0.5	2.5 ± 0.5	3.2 ± 0.5	3.4 ± 0.6	3.0 ± 0.5
Mod 64 n=4	4.0 ± 0.8	0	0	0	5.7 ± 0.7	4.9 ± 2.2
Sleep dep. n=2	4.3 ± 0.8	2.6 ± 0.4	3.4 ± 0.6	3.1 ± 0.4	3.6 ± 0.6	2.6 ± 0.5
PS						
amph	2.2 ± 0.5	0	0	0	1.9 ± 0.5	3.2 ± 0.3
mod 64	2.9 ± 0.7	2.0 ± 0.8	2.0 ± 0.7	2.9 ± 0.8	1.7 ± 0.3	2.6 ± 0.5
mod 128	2.0 ± 0.4	1.8 ± 0.6	3.0 ± 0.0	2.7 ± 0.8	1.3 ± 0.3	2.4 ± 0.5
sleep dep	2.4 ± 0.7	0	0	0	2.1 ± 0.4	1.5 ± 0.5
vehicle	2.0 ± 1.0	2.3 ± 0.6	2.2 ± 0.4	1.8 ± 0.3	2.1 ± 0.3	1.8 ± 0.3
W						
amph	3.2 ± 1.7	60.0 ± 0.0	60.0 ± 0.0	5.5 ± 3.2	2.0 ± 0.8	1.7 ± 0.6
mod 64	4.1 ± 1.8	14.9 ± 8.3	3.5 ± 3.5	1.5 ± 0.3	1.4 ± 0.5	1.0 ± 0.4
mod 128	5.6 ± 2.6	11.0 ± 4.4	3.6 ± 0.9	1.8 ± 0.4	1.9 ± 0.6	1.3 ± 0.2
sleep dep	2.9 ± 1.2	60.0 ± 0.0	60.0 ± 0.0	60.0 ± 0.0	3.0 ± 2.2	6.9 ± 6.1
vehicle	3.8 ± 1.2	2.9 ± 0.7	1.6 ± 0.4	1.4 ± 0.4	1.8 ± 0.5	1.9 ± 0.7

Table 3. Duration of waking, rebound of ripple occurrence and its recovery time.

	waking, min	*ripples rebound, %*	*recovery time, min*
Vehicle n=6	13.2 ± 2.3	35.0 ± 8.9	11.5 ± 5.6
Amph n=5	167.3 ± 13.2	110.9 ± 33.5	154.5 ± 35.6
Mod 128 n=6	78.9 ± 21.7	36.8 ± 14.7	18.8 ± 7.8
Mod 64 n=4	55.8 ± 9.8	44.6 ± 13.8	44.2 ± 18.6
Sleep dep. n=2	180.0 ± 0.0	103.00 ± 16.00	108.0 ± 9.0

Table 4. Intraripple frequency in a sequence of SWS episodes (pre – pre-treatment, 1-4 – post-treatment).

	Intraripple frequency (Hz) in SWS episode				
	pre	1	2	3	4
Vehicle n=6	155.9 ± 2.5	164.7 ± 2.3	164.3 ± 2.5	164.5 ± 2.1	162.6 ± 2.6
Amph n=5	158.2 ± 1.2	162.7 ± 0.9	162.5 ± 1.6	158.8 ± 1.1	158.8 ± 1.2
Mod 128 n=6	158.7 ± 1.7	159.6 ± 1.8	159.6 ± 2.0	158.2 ± 2.2	158.2 ± 1.9
Mod 64 n=4	157.4 ± 2.6	164.7 ± 2.6	161.7 ± 1.6	157.1 ± 2.2	159.5 ± 2.1
Sleep dep. n=2	157.3 ± 1.7	177.0 ± 2.2	172.1 ± 2.7	172.6 ± 2.4	170.2 ± 1.6

Table 5. Amplitude and duration of ripple oscillations. Mean amplitude and duration (± SE) of ripples (>140 Hz) are given for pre- and post-treatment SWS episodes (separated by slash).

	Amplitude, mV	*Duration, ms*
Vehicle n=6	1.38 ± 0.10 /1.39 ± 0.07	63.6 ± 2.0 / 62.3 ± 1.8
Amph n=5	1.08 ± 0.03 / 1.25 ± 0.02	67.4 ± 1.6 / 68.6 ± 1.0
Mod 128 n=6	1.16 ± 0.04 / 1.21 ± 0.04	61.0 ± 2.0 / 63.1 ± 2.2
Mod 64 n=4	0.85 ± 0.06 / 0.86 ± 0.04	62.2 ± 2.0 / 66.6 ± 2.3
Sleep dep. n=2	1.35 ± 0.06 / 1.31 ± 0.03	63.8 ± 2.1 / 64.3 ± 1.7

Table 6. Decay of ripple occurrence during SWS episodes preceded by waking or PS.

	Decay of ripple occurrence during SWS preceded by PS, %	*Decay of ripple occurrence during SWS preceded by waking, %*
Vehicle n=6	4.9 ± 3.1	18.3 ± 3.1
Amph n=5	26.5 ± 10.2	19.8 ± 13.1
Mod 128 n=6	4.0 ± 1.6	14.5 ± 3.4
Mod 64 n=4	8.4 ± 5.9	17.6 ± 4.4
Sleep dep. n=2	28.3 ± 19.8	20.4 ± 21.0

Table 7. Ripple occurrence in sets of SWS episodes separated by PS (SWS1-PS-SWS2 sequences). PS negatively modulated ripple occurrence in set A and positively in set B.

	SWS 1 (onset)	*SWS 1 (offset)*	*SWS 2 (onset)*	*SWS 2 (offset)*
Set A (n=12)	158.2 ± 29.5	136.7 ± 22.6	110.3 ± 16.3	112.4 ± 19.0
Set B (n=22)	137.8 ± 16.8	97.1 ± 12.6	133.1 ± 18.0	92.2 ± 12.6

Table 8. Duration of sleep episodes in the two sets of SWS1-PS-SWS2 sequences.

	Sleep episode duration, min Set A	*Sleep episode duration, min Set B*
SWS 1	19.6 ± 5.0	19.4 ± 2.2
PS	3.3 ± 0.3	3.4 ± 0.3
SWS 2	10.2 ± 3.1	16.7 ± 2.7

Table 9. Ripple occurrence following treatment with benzodiazepine site agonist, diazepam.

	Post-treatment ripple occurrence, % to baseline					
	10'	*20'*	*30'*	*40'*	*50'*	*60'*
Saline n=5	94.2 ± 4.3	101.3 ± 4.9	99.6 ± 3.3	102.6 ± 3.8	81.7 ± 13.6	101.8 ± 3.4
Diazepam 1 n=5	22.3 ± 4.9	36.2 ± 6.0	54.4 ± 8.1	80.0 ± 11.1	88.8 ± 9.4	96.9 ± 6.8
Diazepam 0.1 n=4	89.8 ± 4.4	99.9 ± 6.7	86.3 ± 12.7	98.3 ± 2.1	98.8 ± 9.8	106.0 ± 4.2

Table 10. Ripple occurrence following treatment with benzodiazepine site agonist, zolpidem, and antagonist, flumazenil.

	Post-treatment ripple occurrence, % to baseline					
	10'	*20'*	*30'*	*40'*	*50'*	*60'*
Saline n=5	84.6 ± 4.4	99.5 ± 4.0	104.0 ± 5.3	96.0 ± 3.7	97.3 ± 5.6	94.2 ± 1.8
Zolpidem 10 n=5	77.5 ±11.5	59.6 ± 5.9	37.2 ± 4.2	55.0 ± 7.3	60.3 ± 7.9	82.3 ± 10.9
Flumazenil 10 n=5	78.9 ± 8.9	78.6 ± 7.9	68.6 ± 6.2	67.5 ± 4.8	73.7 ± 5.5	76.5 ± 5.4

Table 11. Parameters of ripple structure following treatment with benzodiazepine site agonists and antagonist.

	Amplitude. mV		*Duration. ms*		*Frequency. Hz*	
	Baseline	Post-treat.	Baseline	Post-treat.	Baseline	Post-treat.
Saline n=3721	1.8 ± 0.0	1.8 ± 0.0	85.7 ± 0.5	86.1 ± 0.8	158.5 ± 0.4	158.2 ± 0.3
Diazepam 1 n=1769	1.9 ± 0.0	1.5± 0.0	81.4 ± 1.2	72.8 ± 1.0	157.3 ± 0.7	152.5 ± 0.7
Diazepam 0.1 n=1450	1.8 ± 0.0	1.9± 0.0	78.2 ± 3.9	73.3 ± 2.1	159.9 ± 1.5	156.6 ± 1.2
Zolpidem 10 n=2555	1.5 ± 0.0	1.3 ± 0.0	92.2 ± 0.9	109.7 ± 1.5	157.4 ± 0.4	146.3 ± 0.4
Flumazenil 10 n=2206	1.2 ± 0.0	1.2 ± 0.0	87.1 ± 1.9	79 ± 1.2	183.3 ± 1.1	184.1 ± 1.4

Table 12. Ripple occurrence following treatment with histamine receptor antagonists.

	Post-treatment ripple occurrence, % to baseline					
	10'	*20'*	*30'*	*40'*	*50'*	*60'*
Saline N=4	83.7 ± 2.9	108.7 ± 6.1	101.9 ± 7.1	97.0 ± 6.8	97.3 ± 5.6	94.2 ± 1.9
Pyrilamine 5 N=5	126.8 ± 8.7	153.6 ± 14.6	183.8 ± 29.3	167.0 ± 22.5	141.9 ± 22.2	82.7 ± 12.8
Zolantidine 10 N=5	89.8 ± 12.7	85.7 ± 11.3	99.4 ± 4.4	96.9 ± 9.6	124.1 ± 5.8	87.9 ± 11.2
Thioperamide 5 N=5	54.1 ± 6.1	90.5 ± 11.6	94.9 ± 10.1	102.9 ± 5.5	99.2 ± 7.3	105.0 ± 9.6

Table 13. Neuronal firing patterns in the EPN and BL in different vigilance states.

	SWS	*PS*	*W*
EPN units. Hz n=24	0.59 ± 0.03	0.41 ± 0.20	0.43 ± 0.11
EPN units. low/burst firing ratio	7.72 ± 2.30	15.84 ± 9.73	13.85 ± 2.09
BL bursting units. Hz n=29	0.74 ± 0.11	0.65 ± 0.20	0.38 ± 0.06
BL bursting units. low/burst firing ratio	13.25 ± 5.19	24.40 ± 4.66	20.09 ± 5.31